THE UNIVERSITY OF CALGARY

NMR studies of the Na^+/K^+ pump and cellular energetics in the rat heart

by

Clinton Ho

A THESIS

SUBMITTED TO THE FACULTY OF GRADUATE STUDIES

IN PARTIAL FULFILLMENT OF THE REQUIREMENTS

FOR THE DEGREE OF MASTER OF SCIENCE

UNIVERSITY BIOCHEMISTRY GROUP

CALGARY, ALBERTA

AUGUST, 1991

ISBN 0-315-75219-X

The University of Calgary

Faculty of Graduate Studies

The undersigned certify that they have read, and recommend to the Faculty of Graduate Studies for acceptance, a thesis entitled, "NMR studies of the Na^+/K^+ pump and cellular energetics in the rat heart" submitted by Clinton Ho in partial fulfillment of the requirements for the degree of Master of Science.

Supervisor
H.J. Vogel, University Biochemistry Group

C.E. Hill, Department of Biological Science

D. Severson, University Biochemistry Group

H.E.D.J. ter Keurs,
Department of Medical Physiology

16 August, 1991

Abstract:

We have systematically characterized a number of commonly used aqueous shift reagents with respect to their ability to induce chemical shifts and enhance relaxation of various monovalent cations. Ions with larger hydrated radius such as Li^+ and Na^+ were shifted to the greatest extent by $Dy(TPP)_{2.5}$ (prepared using Na^+ as the counterion) whereas smaller hydrated ions like Rb^+ and Cs^+ were shifted most extensively by $Tm(TPP)_{2.5}$. Both K^+ and NH_4^+ were shifted to a similar degree by $Dy(TPP)_{2.5}$ and $Tm(TPP)_{2.5}$; however, induced linebroadening was generally smaller with $Tm(TPP)_{2.5}$ for all nuclei tested. Contributions of the complex formation shift to the total shift reagent induced shift was found to be significant in smaller ions such as Rb^+ and Cs^+ which explains the larger induced downfield shift of these ions by $Tm(TPP)_{2.5}$. Both DyTTHA and TmTTHA induced smaller shifts than their TPP derivatives but are useful in physiological studies where competing divalent cations are present in large amounts. Cs^+ turned out to be the most suitable cation for our intended study of the Na^+/K^+ pump in vivo. Cesium-133 has high NMR-senstivity, small natural linewidth but most importantly, does not require the use of a potentially toxic shift reagent to separate intra- and extracellular signals because of its sensitivity to its chemical environment.

In the perfused rat heart, we found that the uptake of Cs^+ was inhibited by ouabain in a dose-dependent manner which confirmed that the Na^+/K^+ pump was the main mechanism responsible for Cs^+ entry into the cell. After a 75 minute washout period, the intracellular Cs^+ decreased by only 20 % which confirmed that Cs^+ was a blocker of various K^+ channels and allowed us to use the changes in the Cs^+ integral as a reflection of the Na^+/K^+ pump activity. Energy metabolism and intracellular pH were not affected by cesium perfusion but spontaneous heart rate was reduced by an average of 70 %. Our results provided no support for a functional compartmentation of ATP in the rat heart.

Oxidatively generated ATP was found to be as effective to support Na^+/K^+ pump activity as hearts that had both functional glycolysis and oxidative phosphorylation. Furthermore, hearts that had only glycolytically generated ATP showed a reduced Na^+/K^+ pump activity. These results are not consistent with the hypothesis that glycolytic ATP fuels the pump. The accumulation of inorganic phosphate as a secondary effect of cyanide poisoning, observed by ^{31}P NMR, may have complicated the situation because it is known that Pi has an inhibitory effect on the Na^+/K^+ pump and the contractile process. Upon onset of ischemia, the uptake of Cs^+ was found to cease immmediately in all groups tested. We believe that this represents an inactivation of the Na^+/K^+ pump by factors brought on by ischemia other than the lack of ATP as substrate. We have shown by ^{31}P NMR that the ATP level at the onset of the inactivation was near normal and thus cannot be the cause of the inhibition. The exact cause of the inactivation of the Na^+/K^+ pump is unknown but may involve changes in membrane fluidity or production of endogeneous inhibitors. During reperfusion, only the pyruvate perfused hearts showed consistent mechanical and Na^+/K^+ pump functional recovery. In comparison with the glucose perfused group which showed no recovery in mechanical and Na^+/K^+ pump functions, we concluded that one of the protective effects of pyruvate against ischemic damage in the rat heart is the preservation of the Na^+/K^+ pump function after an ischemic period.

In the studies of cyclosporin-A treated hearts, we confirmed previous observations that CsA treated rat hearts developed lower systolic pressure than controls at any diastolic pressure tested. This functional impairment is not a result of abnormal energy metabolism, intracellular pH or free magnesium level as determined by ^{31}P NMR. Furthermore, from Cs^+ uptake studies, the function of the Na^+/K^+ pump in the CsA treated hearts was also judged to be normal. Thus, the functional impairment must be related to other factors such as altered calcium metabolism.

Acknowledgements

Firstly, I would like to thank Dr Peter Lundberg for teaching me to operate the NMR spectrometer and for introducing me to the Macintosh computer. I would also like to thank Dr Eef Harmsen for constructing the perfusion system and for showing me the technique of heart perfusion. I also appreciate Dr G. Robillard's help in arranging my stay in Groningen where I learned alot. Thanks also go to the members of my supervisory committee, Drs Severson and ter Keurs for many helpful discussions. I wish to thank Dr Hill for agreeing to serve on my thesis defence committee. Dr Leen Paul also deserves many thanks for his help in the Cyclosporin-A work. Thanks also go to Dr Liz Dixon for her continued support throughout my studies. Finally, I would like to show my appreciation to Dr Hans Vogel for the financial assistance and guidance he provided for the past few years. Without all these people this work would not have been possible.

Table of Contents

List of Tables

List of Figures

List of abbreviations

ADP	adenosine diphosphate
AMP	adenosine monophosphate
ATP	adenosine triphosphate
au	arbitrary units
BPM	beat per minute
CN	cyanide
CsA	cyclosporin-A
downfield	upfrequency
DyTPP, $Dy(TPP)_{2.5}$	dysprosium (tripolyphosphate)2.5
DyTTHA	dysprosium triethylenetetraminehexaacetic acid
gdw	gram dry weight
glc	glucose
glu	glutamate
HR	heart rate
Hz	hertz
IAc	iodoacetate
LuTPP	lutetium (tripolyphosphate)2.5
LuTTHA	lutetium triethylenetetraminehexaacetic acid
MDP	methylenediphosphonic acid
NMR	nuclear magnetic resonance
NOE	nuclear Overhauser effect
PCr	phosphocreatine
P_{dia}	diastolic pressure
Pi	inorganic phosphate
PME	phosphomonoester
ppm	parts per million
P_{sys}	systolic pressure
pyr	pyruvate
RBC	red blood cells
RPP	rate pressure product
SE, SEM	standard error of the mean
SR	shift reagent

TmTPP, $Tm(TPP)_{2.5}$	thulium $(tripolyphosphate)_{2.5}$
TmTTHA	thulium triethylenetetraminehexaacetic acid
upfield	downfrequency

Chapter 1

General Introduction

Introduction

The cessation of coronary flow leads to a rapid deterioration of cardiac function. The systolic pressure drops very quickly to zero and the diastolic pressure decreases at first but increases as the ischemic period is prolonged. This is accompanied by a rapid loss of high energy phosphates and equilibration of ionic gradients across the cell membrane. The level of phosphocreatine drops quickly after flow occlusion and the ATP level also decreases but at a slower rate. Accumulation of potentially toxic metabolites like inorganic phosphate, lactate and H^+ is also dramatic. At the same time the concentration gradient of ions such as Na^+ and K^+ across the membrane collapses probably as a result of decreased Na^+/K^+ pump activity and increased membrane permeability. If, however, reperfusion takes place shortly after ischemia, near complete recovery of cardiac functions and metabolism is possible. Prolonged ischemia will give rise to irreversible damage typified by low mechanical output and substantial loss of high energy phosphates. Various hypotheses have been put forward to account for the cause of the irreversible damage (for reviews see 1-4). All have received experimental support, thus reflecting the possibility that multiple events are taking place during ischemia and reperfusion that give rise to the irreversible damage in combination . In this thesis, we have used multinuclear NMR to study the contribution of the changes in the Na^+/K^+ pump activity to myocardial recovery after an ischemic period in the Langendorff perfused rat heart. The study of the Na^+/K^+ pump activity was facilitated by studying the uptake of a K^+ analogue during perfusion, ischemia and reperfusion. High energy phosphate metabolism in the heart was monitored by ^{31}P NMR and cardiac output was measured by a balloon inserted into the left ventricle. In-vitro studies were completed first to identify optimal conditions for the study of cation

fluxes across the cell membrane (chapter 2). We then applied those conditions to the perfused rat heart to study the Na^+/K^+ pump activity during perfusion, ischemia and reperfusion and its relation to cell energy status (chapter 3). Lastly, the Na^+/K^+ pump activity and energy status of cyclosporin A treated rat hearts was studied in a similar way to investigate the possibility of abnormal cation metabolism in these hearts during normoxic conditions (chapter 4).

The advantages of using NMR for the study of biological matter are well known. The non-destructive nature of this technique allows multiple studies (eg ^{133}Cs, ^{31}P NMR, flow studies and cardiac function) to be carried out on the same sample while the structural integrity of the sample is maintained. Furthermore, almost all of the elements of the periodic table can be studied by NMR which provides NMR spectroscopists with many opportunities in experimental design. A list of the various possibilities for monovalent cations is shown in Table 1.1. Generally, one chooses the study of nuclei with the highest sensitivity, natural abundance and resonance frequency, as this will give the greatest detectability. The use of ^{31}P NMR is very common in the study of living matter because of its high NMR sensitivity and the vast amount of information that it can provide (for review see 5-8). The natural abundance of the ^{31}P isotope is 100% and because of its relatively large magnetogyric ratio, phosphorus-containing compounds can be readily detected in living matter. A typical ^{31}P NMR spectrum of human red blood cells is shown in figure 1.1. The prominent peaks under those experimental conditions are those of 2,3-diphosphoglycerate and the three peaks of ATP. Since the area of the peaks in the spectrum is proportional to intracellular concentrations, quantitive measurements are also possible with the NMR technique. Other phosphorus-containing compounds that can be detected by NMR in muscle tissues are shown in Table 1.2. In addition to the detection of the various metabolites, ^{31}P NMR can also provide information on intracellular pH and

free magnesium concentration from the chemical shift of the inorganic phosphate peak and the ATP peaks respectively.

In order to study ion fluxes in intact cells by NMR, a shift reagent (SR) must be used. This is because the NMR signals for the cation inside and outside of the cell are generally isochronous and hence aqueous shift reagents need to be added to shift away the resonance for the extracellular signals. In separate studies, we have found that the resolution given by a particular shift reagent is not the same for all cations (figures 1.2a,b). One of the reasons is that the natural linewidth of the ions in a NMR spectrum differ and that the physiological concentration of the various ions are not the same. For example, the natural linewidth of Rb^+ in ^{87}Rb NMR spectra is much broader than that of K^+ (see chapter 2); therefore, at the same concentration of shift reagent, the resolution of the K^+ peaks in a ^{39}K NMR spectrum would be better. Since good resolution between the intra/extracellular peaks is required for quantitive studies, we will need to identify optimal conditions for this type of NMR study. In chapter 2 of this thesis, in-vitro studies are described aimed at accomplishing just this. The ions of the alkali metal family were systematically titrated with various commonly used shift reagents to characterize their shift and relaxation enhancement behavior. According to the theoretical analysis of Inagaki et al. (9), complexes of dysprosium and thulium should give rise to opposite SR induced shifts that are larger than those induced by other lanthanides (figure 1.3a). In the present study, tripolyphosphate and triethylenetetraminehexaacetate complexes of dysprosium and thulium were used for this reason. Furthermore, if pseudocontact shift is the dominant mechanism responsible for the SR induced shift then the ratio of dysprosium to thulim induced shift should theoretically be -1.9 (figure 1.3a). Putative structures of the two complexes are shown in figure 1.3b. It is believed that the monovalent ions bind weakly to the outside of these reagents, probably in their hydrated state.

The study of the alkali metal family is of importance because Na^+ and K^+ have pivotal roles in physiological functions, Li^+ is known to have therapeutic effects against manic depression possibly by inhibition of the inositol phosphate metabolism in the brain (10), Rb^+ and Cs^+ can be used as K^+ analogues (figure 1.4), furthermore NH_4^+ is added to the list because it can also act as a K^+ analogue (11).

^{23}Na NMR spectra of living tissues are relatively easy to obtain. The natural abundance of the ^{23}Na is 100%. Furthermore, because of its fast relaxation properties, ^{23}Na NMR spectra of living tissues can be obtained within minutes. While ^{39}K combines a favorable high natural abundance (93%) with an unfavorable low sensitivity and resonance frequency, it can still be studied with relative ease, because its intracellular concentration is high and it relaxes rapidly. Consequently, many studies have been done using ^{23}Na and ^{39}K NMR to observe changes in the steady state concentrations of these ions in cells after applying some sort of intervention (12-15). However, only the steady state concentration of the ions is measured and this is a balance between uptake and release, hence no conclusion can be made on the actual cation fluxes. This problem can be solved, however, by using an isotope of K^+ that is also NMR sensitive. By adding enriched ^{41}K to the medium, the uptake or the release of K^+ can be studied separately by NMR. The main disadvantage with this type of studies is the cost: 1 mg of ^{41}KCl costs about $10 US (Oakridge National Lab., 1989). In addition, ^{41}K NMR has very poor NMR characteristics. The use of K^+ analogues such as Rb^+ and Cs^+ in combination with the sensitive ^{87}Rb and ^{133}Cs NMR can be another way to circumvent this problem. Rb^+ has been a commonly used K^+ analogue to study the activity of the Na^+/K^+ pump in many types of tissue (16-18). The only disadvantage from an NMR point of view is the broad natural linewidth of ^{87}Rb, which is about 20 times greater than that of Na^+. As a result, high concentrations of shift reagent is needed to give good separation of the

intra/extracellular peaks (see chapter 2). On the other hand, Cs^+ is beginning to gain popularity as a K^+ analogue in biological studies (19,20). In studies of ionic channels, Cs^+ is often used as a K^+ channel blocker to isolate membrane currents and in the heart Cs^+ has also been found to block many of the K^+ channels (21,22). Thus, the accumulation of Cs^+ by the heart can be seen as a reflection of the uptake process. The NMR sensitivity of ^{133}Cs is good and nice narrow peaks can be obtained even in the inhomogeneous beating heart. However, the biggest advantage of ^{133}Cs-NMR over the other nuclei in NMR studies is that its chemical shift is very sensitive to the chemical environment. As Cs^+ is taken up by the cells, the difference between the intra- and extracellular milieu is sufficient to shift the intracellular Cs^+ peak from the extracellular one. Consequently, no potentially toxic shift reagent is required to separate the peaks. In figures 1.5(a,b,c,d), the profile of the ^{133}Cs spectra with or without shift reagent in human red blood cells are shown. It should be remembered however that in spite of its advantages, Cs^+ is not a physiological ion and is known to alter cardiac functions (19). Nitrogen-14 is a relatively difficult nucleus to study by NMR because of its relatively poor sensitivity and low resonance frequency. Typical changes in the ^{14}N spectrum of post-mortem rat muscle and ischemic rat heart are shown in figure 1.6a; a ^{14}N spectrum of the muscle extract is shown in 1.6b. Broad and poorly resolved peaks in the spectrum of intact tissue is usually the norm but sharper lines can be obtained from extracts and from symmetrical molecules such as NH_4^+. The inherent broadness of the lines in the ^{14}N spectrum makes quantitation studies difficult even with the use of line-simulation programs. Even though NH_4^+ can mimic K^+ in activating the Na^+/K^+ATPase (11), one serious disadvantage is that it can cross the membrane passively as NH_3. In figure 1.7(a,b), it is shown that intracellular NH_4^+ is rapidly equilibrated with extracellular NH_4^+ and that the intracellular signal is directly proportional to the amount of red blood

cells (hematocrit). This diminishes the usefulness of NH_4^+ as a K^+-analogue to study pump activity but it may be effective as an intracellular volume marker in those NMR studies where an accurate measure of the amount of cells that is being detected is required. The results of these in vitro studies described here and in chapter 2 were then used as a guideline in the subsequent perfused heart studies.

In chapters 3 and 4, studies were carried out using isolated rat hearts that were Langendorff-perfused through the aorta using the apparatus shown in figure 1.8. Briefly, two vessels were equipped on the perfusion system to facilitate buffer changes during the experiment (not shown in diagram). A latex balloon containing a reference compound was inserted through the left atrium into the left ventricle to measure cardiac function and to act as a NMR standard in quantitative ^{31}P studies. The balloon was connected to a pressure transducer positioned at the same level as where the heart would be inside the magnet. The transducer was connected to a chart recorder which has been calibrated to give the developed pressure and heart rate continuously. Effluent from the heart was pumped out via a tube placed ~ 3 cm above the heart inside the NMR tube. Coronary flow was measured by collecting the outflow from the pump placed far away from the magnet. The 20 mm NMR tube containing the isolated heart was then inserted into the magnet. The water signal was used to shim the magnet until a water linewidth of about 30-40 Hz was obtained (in the 20 mm probe). More detailed description of the experimental protocols can be found in chapters 3 and 4.

The quantitation of the resonance for the phosphorylated metabolites in the heart was accomplished by comparing the integral of the methylenediphosphonate peak in the ^{31}P spectrum after an known amount of MDP had been added to the balloon with the integral prior to the addition; the difference in peak area was proportional to the added amount of MDP and could be used to calculate the amount of phosphorylated metabolites

present in the heart. The quantitation of Cs^+ uptake is more difficult because of the fact that cesium is a quadrupolar nucleus with a nuclear spin of 7/2 and because of this the NMR visibility of intracellular Cs^+ may deviate from 100 %. That is, it is possible that only a portion of the intracellular Cs^+ can be detected by NMR (23). In order to quantitate the uptake of Cs^+ by NMR we need to have a knowledge of its visibility in the heart or we can assume a visibility factor as others have done (19). Another problem, that makes it often difficult to obtain quantitative results directly from NMR, is the T1 relaxation process. Since the NMR experiment is based on repetitive radio frequency pulsing, if after excitation, one does not allow sufficient time for all nuclei to return to their original state, one will obtain a lower intensity. Since the T1 generally varies between the metabolites, this can attenuate their intensities to different extend. A slower pulse rate would alleviate this, but often leads to unacceptably long spectral acquisition times, thus giving poor time resolution in the physiological studies. Thus one often uses overpulsed spectra and corrects peak intensities afterward.

Upon perfusion with a Cs^+ containing buffer, the systolic pressure of the heart decreased quite rapidly to ~ 50% of normal but recovered to normal values after about 10 minutes. By the end of the 60 minute perfusion period, the developed pressure of the heart was comparable to that during pre-Cs^+ conditions but the heart rate was about 70% of normal (figure 1.9). Typical force tracings obtained with a pyruvate perfused heart during normoxia, ischemia and reperfusion are shown in figure 1.10.

Table 1.1: Properties of NMR isotopes of monovalent cations.

Cation	NMR Nucleus	Spin	Natural Abundance (%)	Resonance# Frequency at 9.4 T (MHz)	Sensitivity relative to ^{1}H (%)
Li^+	^{6}Li	1	7.42	58.9	0.8
	^{7}Li	3/2	92.58	155.5	2.9
NH_4^+	^{14}N	1	99.63	28.9	0.1
	^{15}N	-1/2	0.37	40.5	0.1
Na^+	^{23}Na	3/2	100	105.8	9.3
K^+	^{39}K	3/2	93.1	18.7	0.051
	^{41}K	3/2	6.88	10.2	0.0084
Rb^+	^{86}Rb	5/2	72.2	38.6	1.1
	^{87}Rb	3/2	27.85	130.9	17.5
Cs^+	^{133}Cs	7/2	100	52.5	4.7
*	^{31}P	1/2	100	162	6.6

Corresponding ^{1}H NMR frequency is 400 MHz.
* ^{31}P is shown here for comparison

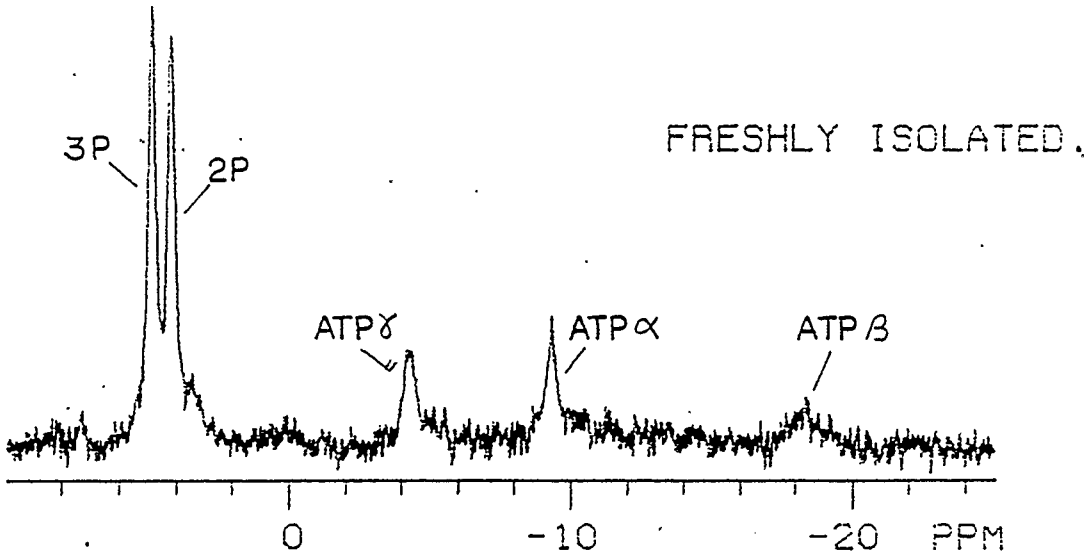

Figure 1.1: Typical ^{31}P NMR spectrum of freshly drawn human red blood cells. Peaks assignment are from left to right: the two peaks of 2,3-diphosphoglycerate and the three peaks of ATP. The chemical shift of the resonances for the various metabolites is presented in units of ppm which was calculated by the computer {=(resonance frequency-carrier frequency)/carrier frequency * 10^6} to facilitate comparison with studies done at other magnetic field strengths.

Table 1.2: Some phosphorus-containing metabolites detectable by NMR in muscles at neutral pH#$.

Compounds		Chemical shift (ppm)*
Glucose-6-phosphate		6.91
Mannose-6-phosphate		6.91
Fructose-1,6-disphosphate		6.52
Fructose-1,6-disphosphate		6.29
3-phosphoglycerate		6.57
AMP		6.35
Glucose-1-phosphate		4.99
Inorganic phosphate		4.93
ATP-Mg^{2+}	α	-7.57
	β	-16.1
	γ	-2.47
ADP-Mg^{2+}	α	-7.01
	β	-2.99

* Chemical shift are referenced to PCr set at 0 ppm.

Table adapted from Lundberg, 1989 (24).

$ For a more complete listing of phosphorus containing metabolites see reference 25.

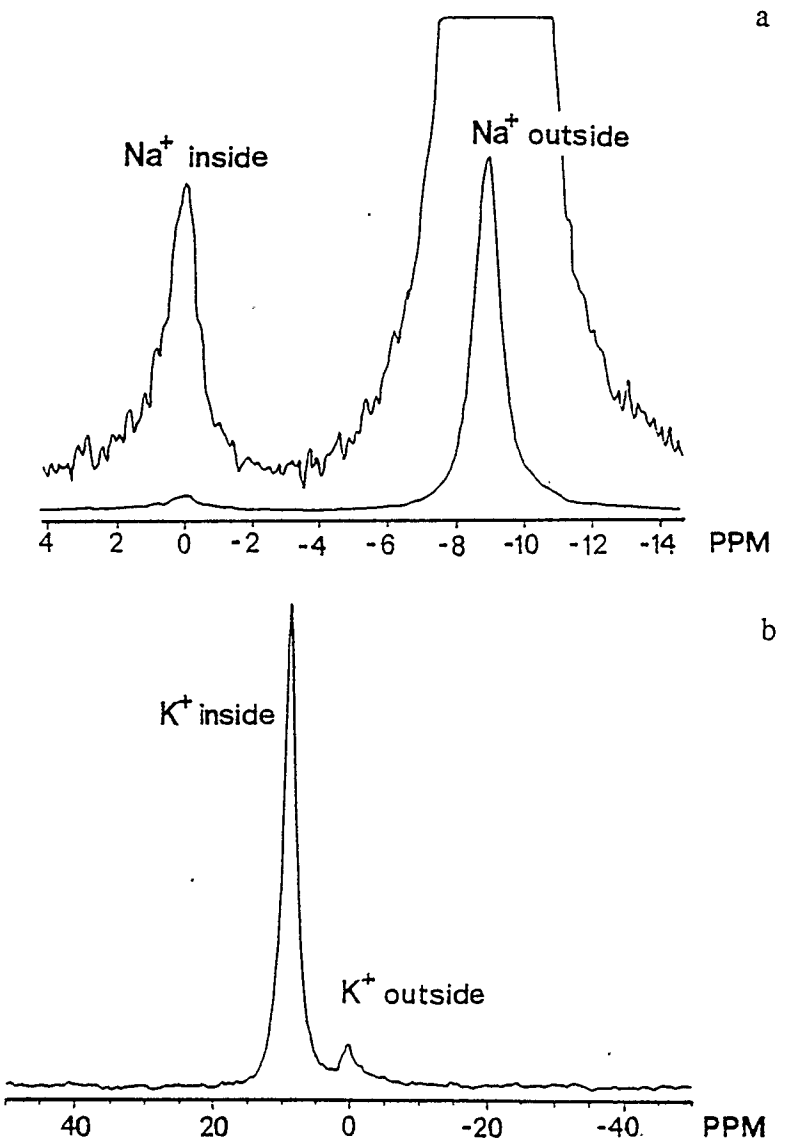

Figure 1.2: a) Typical ^{23}Na NMR spectrum of human red blood cells in the presence of the shift reagent $DyTPP_{2.5}$ (top). b) a ^{39}K spectrum of the same sample as above is shown (bottom). Clearly in fresh samples, the intracellular K^+ level is high, while that of Na^+ is low illustration the action of the Na^+/K^+ ATPase.

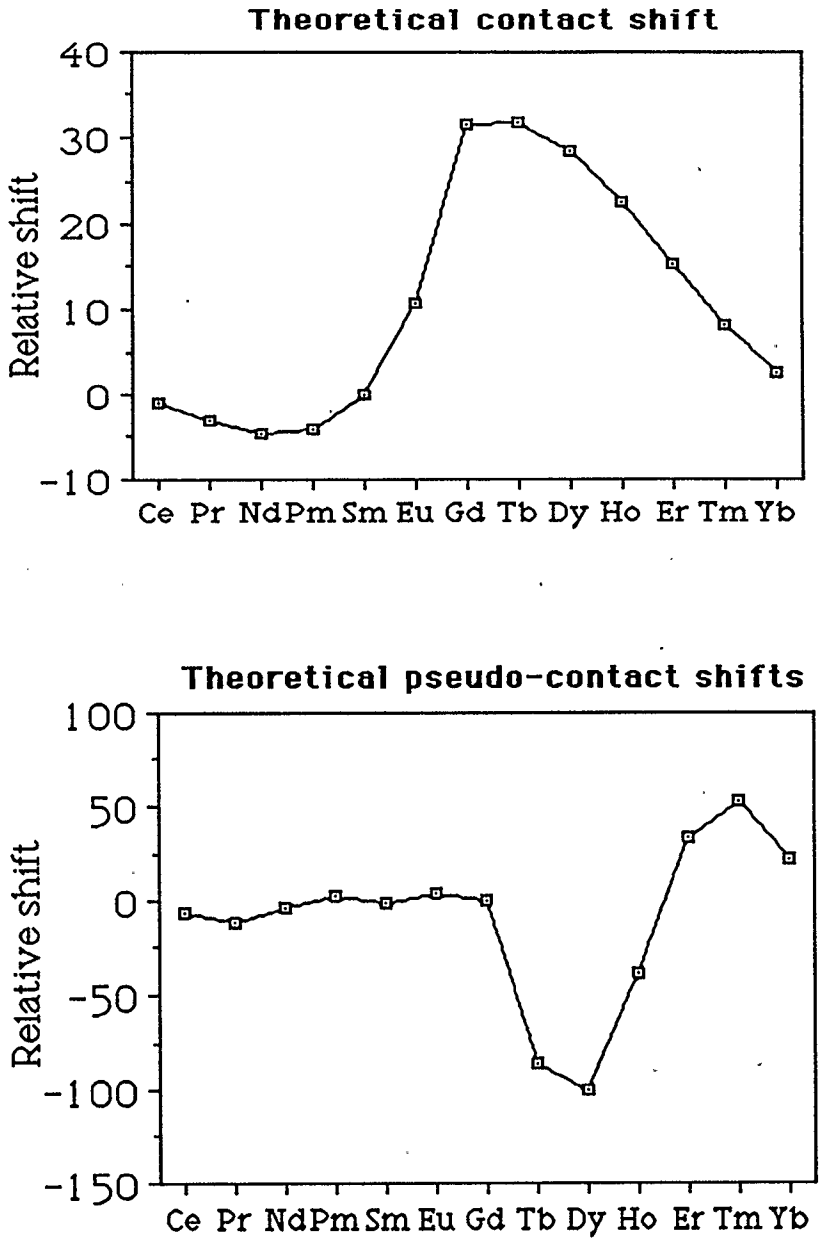

Figure 1.3a: Theoretical analysis of the contribution of the contact and pseudo-contact mechanisms to the shift reagent induced shift by ions of the lanthanide family. Adapted from Inagaki et al. (9).

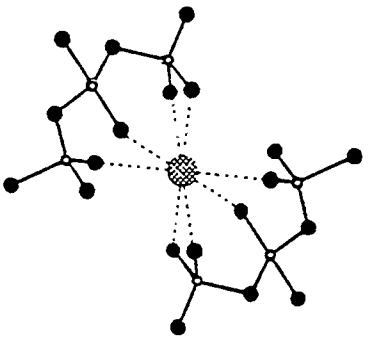

$Ln(TPP)_2^{7-}$

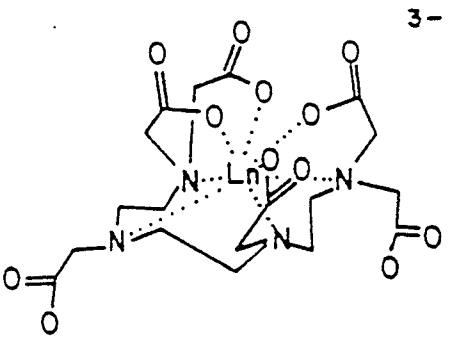

$LnTTHA^{3-}$

Figure 1.3b: Hypothetical structure of $Ln(TPP)_2^{7-}$ and $LnTTHA^{3-}$. Adapted from Chu et al. (26).

Cations	ATPase activity	
	V_m %	$K_{0.5}$ (mM)
K^+	100	0.8
Rb^+	90	1.13
Cs^+	80	7
Li^+	36	20
Tl^+	96	0.25
NH_4^+	100	4

Figure 1.4: Comparison of the characteristics of various K^+ analogues in activating the axonal Na^+/K^+ ATPase. Adapted from Gache et al. (11).

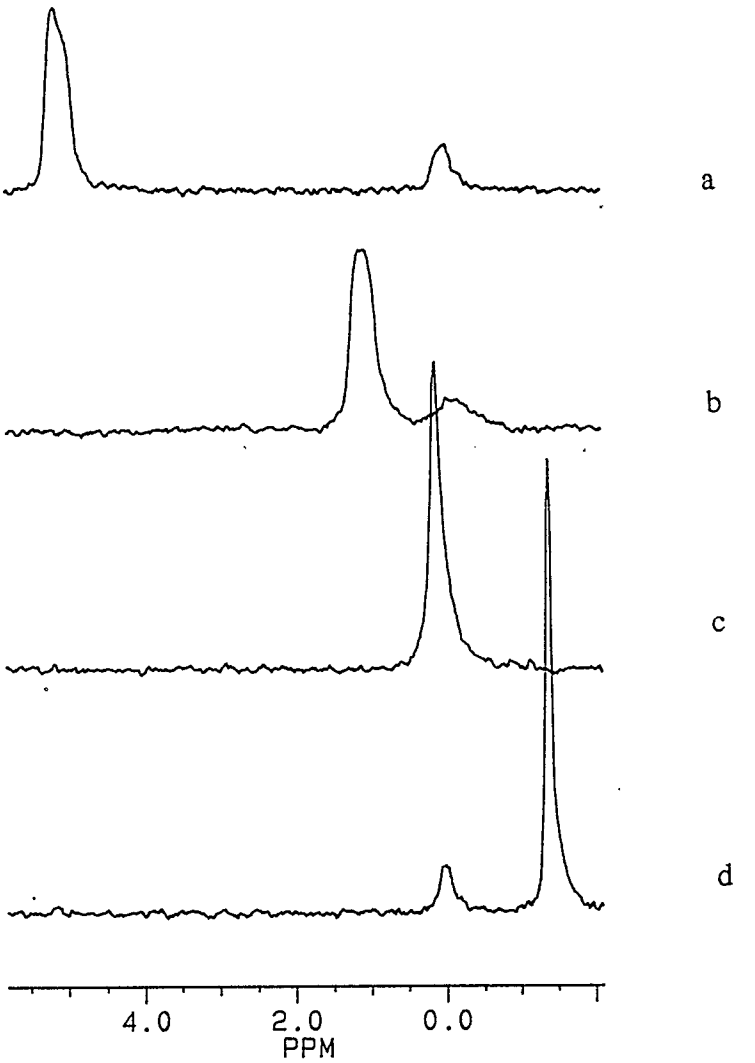

Figure 1.5: ^{133}Cs NMR spectra of human red blood cells incubated in glucose buffer containing 10mM of CsCl. In 3a (bottom), spectrum was obtained with no shift reagent added; 3b, 3mM of DyTPP had been added; 3c, 3mM of DyTTHA had been added and 3d (top), 3mM of TmTPP had been added. The chemical shift of the intracellular Cs^+ was not affected by the presence of the shift reagents and was assigned as 0 ppm. The chemical shift of the extracellular Cs^+ changed in relation to the shift reagent used. The uptake rate of Cs^+ determined under these four conditions was identical (data not shown), showing that the shift reagents do not interfere with the uptake of Cs^+ ion.

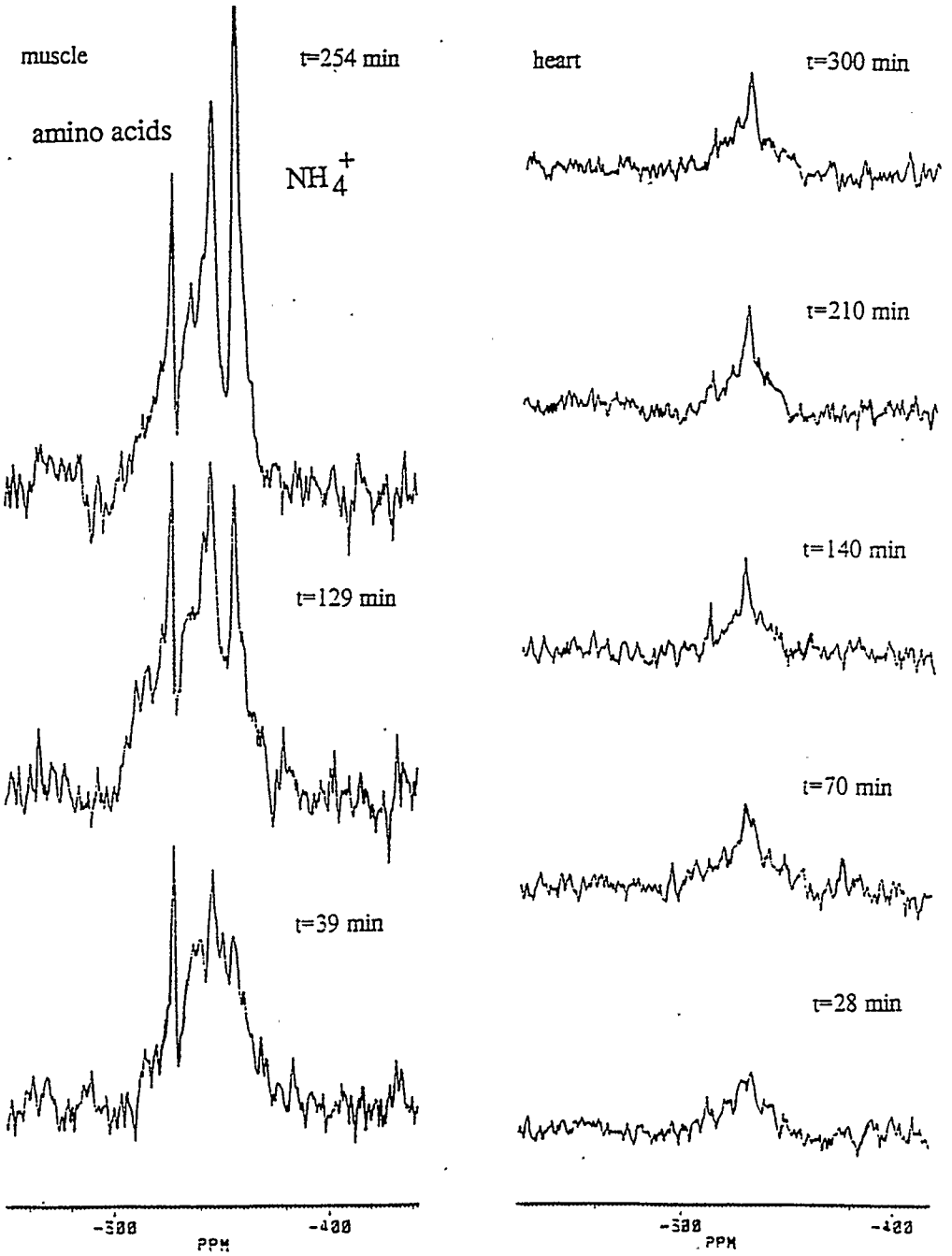

Figure 1.6a: Typical 1 hour ^{14}N spectra of post-mortem rat muscle and ischemic heart. The number in each spectrum refers to the amount of time elapsed after the extraction of muscle or the onset of ischemia for the heart. For peaks assignment see figure 6b.

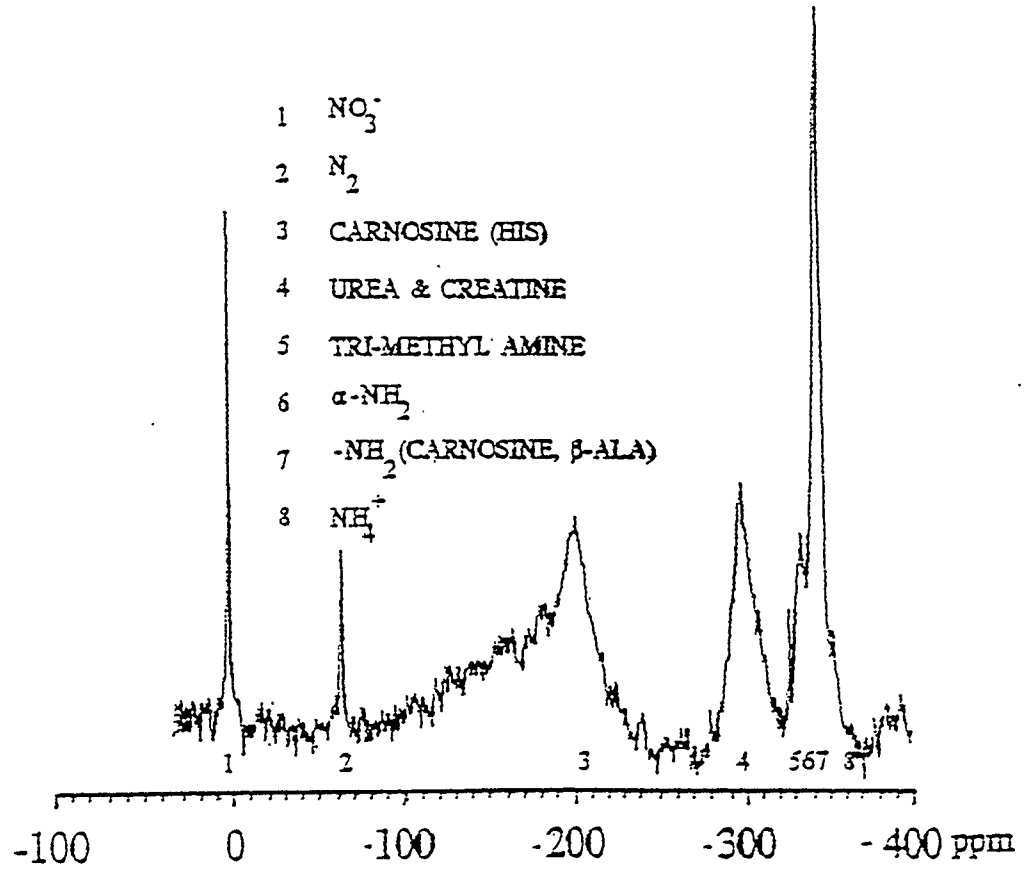

Figure 1.6b: A typical ^{14}N NMR spectrum of rat muscle extract. Peaks are assigned with respect to the reference, KNO_3.

a

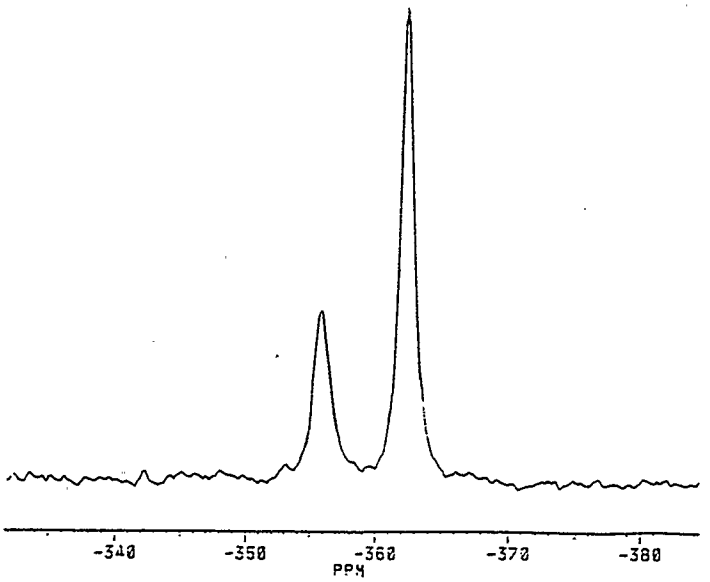

b

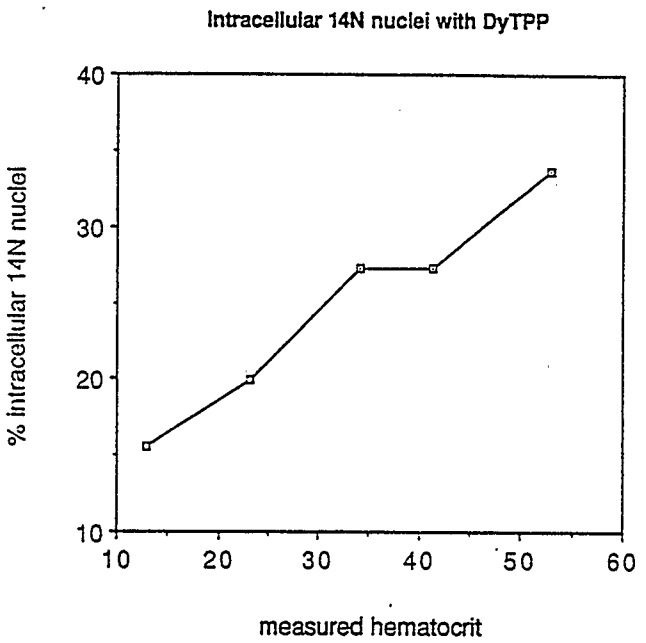

Figure 1.7: a) Typical ^{14}N NMR spectrum of RBC bathed in glucose buffer containing 40 mM NH_4^+. Spectrum taker ~ 20 min after addition of NH_4^+. b) The uptake of NH_4^+ by human red blood cells in relation to the measured hematocrit (%) as observed by ^{14}N NMR using the shift reagents, Dy(TPP)2.5.

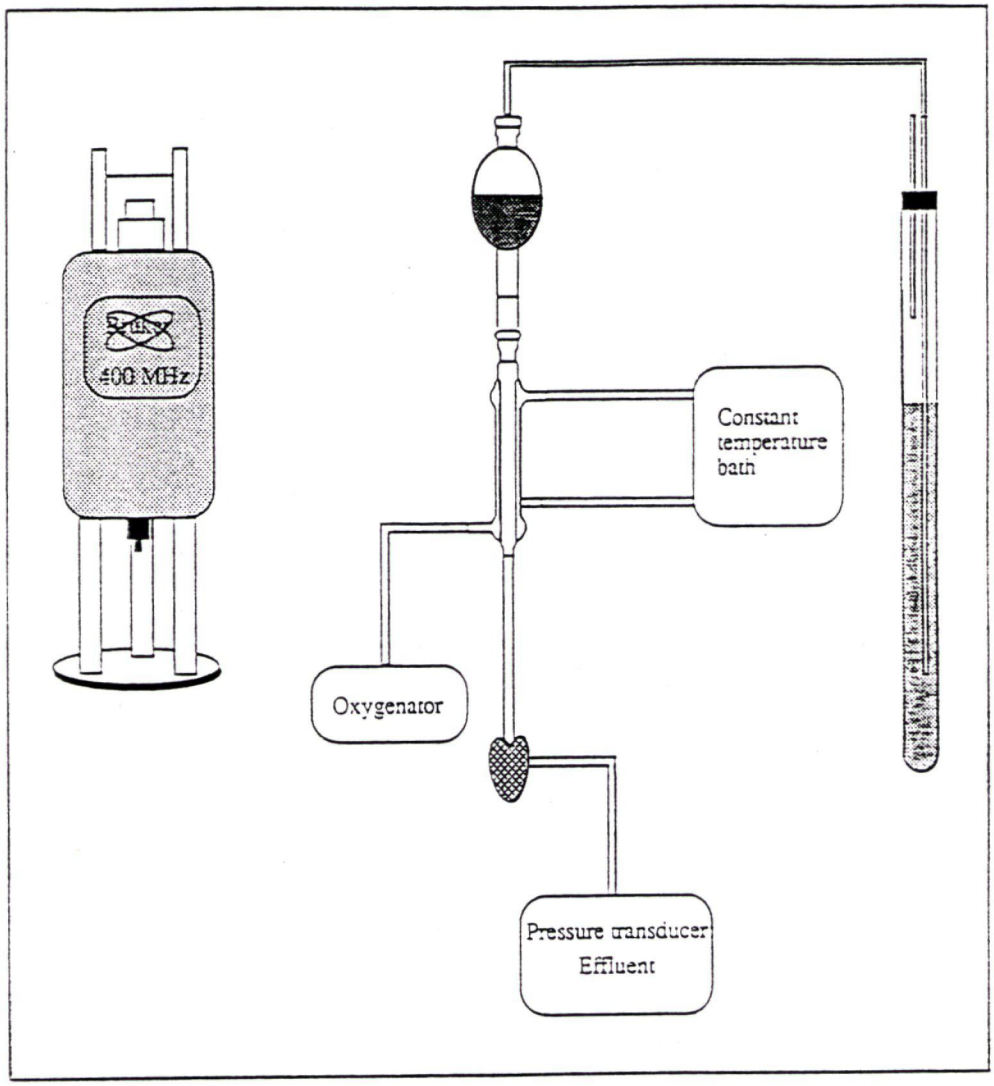

Figure 1.8: A schematic diagram of the perfusion rig.

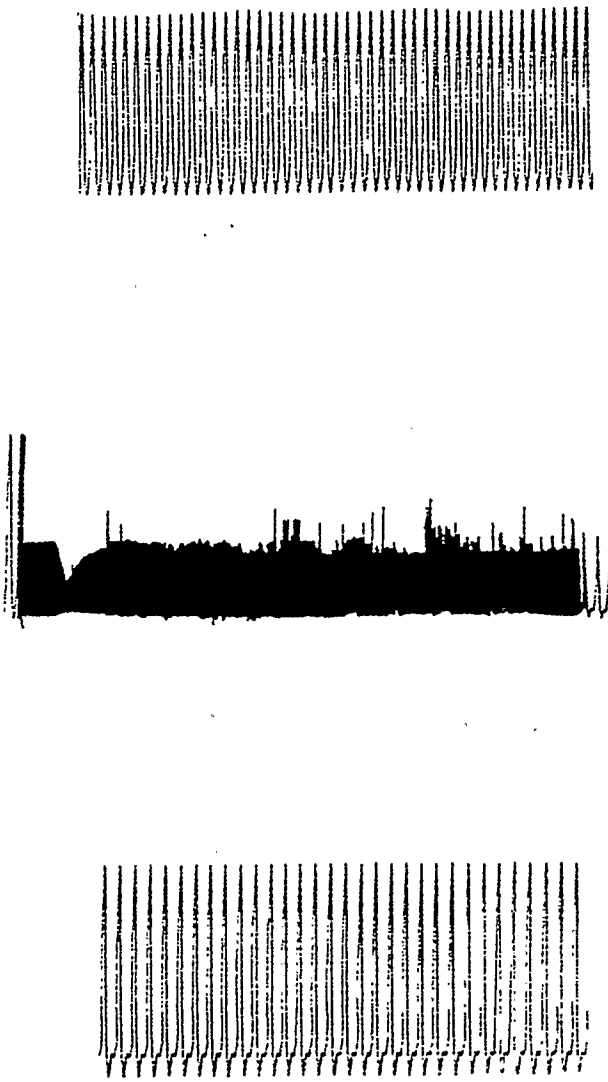

Figure 1.9: Typical force tracing of a heart perfused with glucose buffer with or without cesium added. In period 1, the heart was perfused with a normal glucose buffer (full scale). During period 2, the perfusion medium was switched to one containing 2.95 mM CsCl (half scale). In period 3, after 60 min of perfusion with the glucose-cesium buffer, the systolic pressure returned to normal but the heart rate was ~ 70 % of normal (full scale).

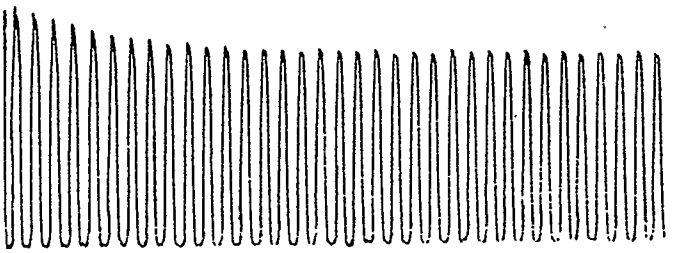

a

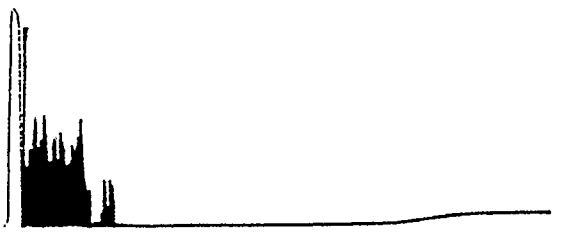

b

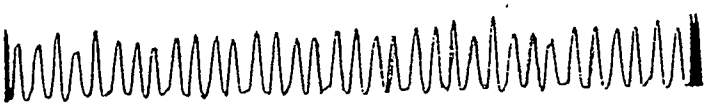

c

Figure 1.10: Typical force tracings of a pyruvate-cesium perfused heart. a) Tracing obtained after 60 min of perfusion with the pyruvate-cesium buffer. b) Tracing of heart function during global ischemia. c) Functional recovery of heart after 20 min of reperfusion with the pyruvate-cesium buffer.

Chapter 2

Characterization of various aqueous shift reagents.

Introduction

Membrane ionic gradients are of great importance to living cells. Biological processes such as excitation-contraction, secretion, cell proliferation, and active transport of various metabolites are all dependent either directly or indirectly on the ionic gradients. The asymmetrical distribution of ions across the cell membrane is generally created by the ion-pumps and acts as a storage of energy. As a result, there is considerable interest in the studies of ion metabolism in vivo. Prior to the advent of suitable NMR methods (27-30), classical techniques requiring ion-selective electrodes or chemical analysis were exclusively used; however, the problem of cell-invasiveness is clear. NMR spectroscopy of cations gives the advantages of being non-invasive; moreover it measures the concentration of the free aqueous species of the monovalent cations in cells rather than the total concentration. In addition, the multinuclear capabilities of modern spectrometers allow the study of various ions in the same sample with ease. One disadvantage of NMR studies of ion gradients is that extracellular and intracellular ions have the same resonance frequency; therefore, they can only be differentiated by using suitable shift reagents (SRs). The most commonly used shift reagents in biological system are compounds composed of a paramagnetic lanthanide ion (eg Dy^{3+}, Tm^{3+}) and a chelating agent (eg TPP^{5-} (29), $TTHA^{6-}$ (30)). Because of their negative charges the paramagnetic shift reagents interact with monovalent and divalent (27-31) cations, which induces a change in the local magnetic field of these bound nuclei. As a result, the resonance frequency of these nuclei is shifted. The applicability of shift reagents lies in the fact that they cannot penetrate across the cell

membrane. Consequently, only the signals for the extracellular nuclei are shifted, while those for the intracellular ones remain at their original resonance position.

To date a fairly large number of biological studies have used the SR-NMR techniques to study cation gradients and fluxes (for reviews see for example 32-36). The shift induced by the shift reagents can be the sum of 3 different mechanisms, namely the complex formation shift, the contact shift and the pseudo-contact shift (37). Briefly, the complex formation shift arises from the disruption of the electron cloud of the substrate upon binding to the shift reagent. Contact shifts arise from the induced unpaired electron spin of the nuclei by the unpaired electron of the lanthanide. Therefore, depending on the magnitude of the hyperfine coupling between the shift reagent and the substrate, the amount of contact shift will vary. The pseudo-contact shift, on the other hand, arises from the local magnetic field induced by the magnetic moment of the lanthanide ion. Upon complexation, the electrostatic potential of the chelating agent affects the 4f electrons of the lanthanide ion in a way such that a net magnetic field in the shift reagent complex is generated. The strength of this local magnetic field is dependent on the distance between the substrate and the shift reagent complex. It has been demonstrated that the magnitude of the pseudo-contact shift is proportional to the inverse third power of the distance and the complexing angle between the lanthanide and the substrate (37). Finally, the chemical exchange rate has a large effect on the observed shift. Since only the bound substrates exhibits a shift, and the exchange rate is considered fast on the NMR time scale, the observed chemical shift is an average of the bound and unbound states. Substrates with higher affinity for the shift reagent are therefore expected to experience larger shifts. In addition to inducing chemical shifts, shift reagents can also broaden the linewidth of the NMR peaks as a result of enhanced relaxation rate. In general, the transverse relaxation rate ($1/T_2$) of magnetic

nuclei in paramagnetic complexes is inversely proportional to the sixth power of the distances between the paramagnetic lanthanide and the magnetic nuclei.

In this paper, we have systematically characterized a number of commonly used shift reagents with respect to their ability to alter the chemical shift and to enhance the relaxation rate of various monovalent cations of the alkaline earth family. Since good resolution between the intra/extracellular signals is needed for quantification of the ion content inside the cells, we have attempted to identify those shift reagents which induce the largest degree of shift without excessive linebroadening. These results have also allowed us to differentiate between the three different mechanisms that can contribute to the SR-induced chemical shift change.

Materials & Methods:

All NMR spectra were recorded on a Bruker AM 400 spectrometer using a broadband 10 mm probe at 25°C. ^{7}Li spectra were observed at 155.5 MHz with a spectral width (SW) of 5376 Hz. ^{23}Na spectra were observed at 105.8 MHz, SW of 2358 Hz. ^{39}K spectra were observed at 18.7 MHz and SW of 747 Hz. ^{87}Rb spectra were observed at 130.9 MHz and SW of 9803 Hz. ^{14}N spectra were observed at 28.9 MHz and SW of 20000 Hz. ^{133}Cs spectra were observed at 52.5 MHz and SW of 1577.3 Hz. In all cases 90° pulses, 4 K data points and 96 number of scans were used (512 scans was used for the ^{14}N NMR study of NH_4^+).

The solutions used in the experiments contained 40 mM of the chloride salt of the respective observed nuclei at natural abundance and 20% D_2O for frequency locking during the experiments. The deuterium field frequency lock normally eliminates any contributions to the observed chemical shift from bulk magnetic susceptibility changes (30,31,38). Stock solutions of shift reagents (100 mM) were prepared by adding the respective chloride hexahydrates (Aldrich Chemical Company Inc.) of dysprosium (Dy), thulium (Tm), or the diamagnetic lutetium (Lu) to the pentasodium salt of tripolyphosphate (TPP) or triethylenetetraminehexaacetic acid (TTHA), obtained from Sigma. A ratio of 1:2.5 of lanthanide to tripolyphosphate and a ratio of 1:1 for lanthanide to TTHA were used. We have mainly used $Dy(TPP)_{2.5}$ because it has been reported to give rise to larger Na^+ and K^+ shifts than $Dy(TPP)_2$ (39). However, results obtained with $Dy(TPP)_2$ showed identical trends as seen with $Dy(TPP)_{2.5}$ (data not shown). The pH of the shift reagent was adjusted to about 7.3 with HCl in the case of tripolyphosphate and NaOH in the case

of TTHA. Thus the counterion in all cases was Na^+. The original salt solution was used to set the chemical shift reference and induced shifts were measured after each addition of SR. Upon addition of the TPP-derivatives, the pH of the solutions rapidly rose to about pH 8; no further pH adjustment were made unless otherwise stated. With the TTHA complexes the pH remained constant during the titration. In competition studies, chemical shifts were recorded after a competiting cation was added to the samples which contained a constant amount of a given cation and a SR. Spectra were transformed with 2 Hz line-broadening and linewidths were measured at half height. All data shown are the results of 2 or more independently repeated experiments.

Results:

In figure 2.1a, it is shown that all nuclei tested were shifted by DyTPP in a concentration dependent manner. With the exception of Cs^+, upfield shifts were observed as has been reported previously (30). Clearly, at any concentration of DyTPP, Na^+ was shifted to a greater extent than the other nuclei. The large Na^+ shift could perhaps be accounted for by the fact that sodium-tripolyphosphate salt was used to prepare the shift reagent. As a result, whenever SR was added to the samples, Na^+ was also added which would compete with other ions for binding to the shift reagent. We corrected for the added Na^+ by taking a ratio between the amount of shift reagent added and the total amount of monovalent cations that is in solution and can bind to the SR,

$$\text{ie. } \frac{\text{mol SR}}{\text{mol } (Na^+ + X)} ,$$

where Na^+ is the amount of sodium ion added along with the SR and X is the amount of the nuclei of interest. The above equation can be simplified to give directly the ratio of nuclei to SR:

$$\frac{1}{(Y + \frac{X}{SR})} ,$$

where Y is the proportionality constant between the amount of SR present and the inherent sodium ion plus all other cations (except the ion of interest) that can bind to the reagent. Under the present conditions, Y is equal to 12.5 when pentasodium-tripolyphosphate at a 2.5 ratio was used and is 6 (the actual measured value in the titration was 5.6 corresponding to the amount of NaOH needed to titrate the solution to pH 7.3) when TTHA was used. When we replotted the shift data using the above equation, the curved

lines of figure 2.1a became linear (figure 2.1b) with Cs^+ being the exception. This confirms the idea that sodium ion acts like a competitor and that most cations bind to the same site(s) on the SR. The magnitude of shift induced by DyTPP was greatest for Na^+, followed by Li^+, K^+, NH_4^+ and Rb^+. Cesium was different in that it shifted downfield in contrast to the other ions and the shift-curve showed a shallow slope initially but rose rapidly as more SR was added (figure 2.1b). This suggests that Cs^+ interacts with DyTPP in an usual manner. The slope of the curves shown in figure 2.1b are given in Table 2.1. During the titration the pH of the solutions rose to ~ pH 8 upon addition of DyTPP and remained at ~ pH 8.2 at the end of the experiment. In a separate experiment, when we maintained the pH at 7.3 by adding HCl after each addition of DyTPP, the chemical shift of the nuclei followed the same trend as shown in figure 2.1b (data not shown). This is in agreement with results obtained by Chu et. al. where they observed a negligable decrease in Na^+ shift when a solution of DyTPP and Na^+ was adjusted from pH 8 to 7 (30).

Similar shift experiments were carried out using TmTPP, DyTTHA and TmTTHA as shift reagents. In the case of TmTPP (figure 2.2a), all nuclei were shifted downfield, the opposite to what was observed with DyTPP. This outcome is expected if the dipolar shift mechanism dominates (37,40). Na^+ and Cs^+ were shifted by the greatest amount, followed by Rb^+, K^+, NH4$^+$ and Li^+. The general trend of the slopes was: $Cs^+ > Na^+ > Rb^+ > K^+ > NH_4^+ > Li^+$ (Table 2.1). As expected the use of DyTTHA and TmTTHA gave rise to opposite shifts for all the nuclei tested, with the largest shift being caused by DyTTHA (figure 2.3a). The magnitude of shift induced by these shift reagents were much lower than their respective TPP derivatives (Table 2.1). From Table 2.1, the order of the magnitude of the shift was: $Cs^+ > K^+ > Na^+ > NH_4^+ > Rb^+ > Li^+$ for DyTTHA, and $Na^+ > K^+ > NH_4^+ > Rb^+ > Li^+ > Cs^+$ for TmTTHA. Finally, the ^{14}N resonance of

tetramethylammonium was not shifted by DyTPP, TmTPP nor the TTHA derivatives to any great extent (data not shown).

In order to investigate the contribution of the complex formation shift induced by the above shift reagents, we performed titration experiments with the diamagnetic lanthanide lutetium. This was selected over lanthanum because of its closer similarity in ionic radius, compared to the paramagnetic Dy and Tm. Since all the 4f electrons of lutetium are paired, no contact and pseudo-contact induced shift are possible. Both LuTPP and LuTTHA had little effects on the larger hydrated cations such as Li^+, Na^+, K^+ and NH_4^+ (figure 2.2b, 2.3b). The chemical shift and the linewidth of these ions stayed relatively constant during the addition of the shift reagent. On the other hand, Cs^+ and Rb^+ were shifted downfield, both by LuTPP and LuTTHA in a concentration dependent manner with the former being more effective. The downfield shift of Cs^+ was greater than that of Rb^+ regardless of whether the TPP or TTHA derivative was used. The susceptibility of Cs^+ to large complex formation shifts may explain its abnormal shifts in the presence of various shift reagents. The line width of Cs^+ was not affected by these shift reagents, but the Rb^+ line width was broadened to a considerable extent.

The relaxation enhancement effects of the shift reagents are shown in figures 2.4 and 2.5. It can be seen that although Na^+ is shifted most effectively by DyTPP, it is also broadened to the largest extent. Li^+ and K^+ were broadened to a similar degree, and the linewidth of NH_4^+ and Cs^+ remained relatively unaffected. The natural linewidth of Rb^+ is much greater than that of the other ions and by the end of the titration the Rb^+ peak was broadened almost beyond detection(figure 2.4). With respect to TmTPP (figure 2.5), the broadening was smaller but the order of broadening was the same as observed for DyTPP ie. $Rb^+ > Na^+ > K^+ > Li^+ > NH_4^+ > Cs^+$. It has been noted before that TmTPP causes

less of a broadening than DyTPP for certain cations (30,31). Both DyTPP and TmTPP broadened the Rb^+ linewidth to the same degree even though TmTPP induced greater shifts than DyTPP (compare figures 2.1b & 2.2a).

In competition studies where KCl was used to displace bound ion from the SR complex, it could be seen that the affinity of the SR for the various nuclei was different. Lithium, sodium and ammonium ions all were displaced from DyTPP by K^+ in a concentration dependent manner (see figure 2.6a,b,c). As more KCl was added, the Dy/(X+Na+K) ratio decreased, and the chemical shift of the ions returned to their original value. The co-linearity of the shift and competition curves suggests a quite similar affinity of these cations for DyTPP. On the other hand, the competition curves of Rb^+ and Cs^+ displayed a more unusual character (see figure 2.7). Upon addition of KCl, the chemical shift of Rb^+ returned quite fast to zero, suggesting that K^+ binds more tightly than Rb^+ (figure 2.7A). However, the Cs^+ shift increased further upon adding KCl or NaCl (figure 2.7b). It has been reported that the chemical shift of Cs^+ is very sensitive to environmental factors such as anion concentration, the nature of the anion and temperature (41). Therefore, we reasoned that the unexpected downfield shift of Cs^+ in the presence of KCl could be the result of the anions present in the competitor solution. By using sodium acetate instead of KCl to compete against Cs^+ binding to DyTPP, the chemical shift of Cs^+ did not increase further as the competitor was added (figure 2.7b). This indicates that the increase in chloride ions causes a further Cs^+ shift. The unusual Cs^+ shift in the presence of DyTPP could also be the result of a distinct binding site on the SR that is different from that for the other ions. However, CsCl acted as a competitor and could displaced Na^+ from DyTPP indicating a common binding site on DyTPP (figure 2.8).

Discussions:

NMR studies of monovalent cation gradients across the cell membrane have been performed during the last decade in a variety of living systems (for reviews see 32-36). While attention originally was mainly focused on the highly sensitive ^{23}Na NMR to study Na^+ influx (28,29,43), as well as the study of the high intracellular levels of K^+ by ^{39}K NMR (39,44), later ^{7}Li NMR was utilized to study the gradients and uptake of Li^+ into cells (45,46). More recently, the uptake of the K^+ analogues, Rb^+ and Cs^+ have been studied by ^{87}Rb (47-49) and ^{133}Cs (50,51) NMR. The latter two K^+ analogues have the advantage that they allow for a direct measurement of cation fluxes, rather than measuring changes between steady-state cation gradients that one obtains by ^{39}K NMR. It has also been possible to study the uptake of $NH4^+$ into plant cells with the help of shift reagents by ^{14}N NMR (52). Here we have systematically studied the shift and line-broadening of the two most commonly used shift reagents based on TPP and TTHA.

In the present study, we have found that TPP containing SRs induced much larger shifts than the TTHA species for each of the cations we have tested. Several previous studies have shown that TPP containing shift reagents induced much larger shifts than their respective TTHA derivatives (30,31,42). The higher negatively charged TPP complex can bind more cations or bind them more tightly and this would lead to higher shifts. Nevertheless, the usefulness of TTHA derivatives lie in the fact that they give a lower line-broadening, have less pH dependency and that they have a lower affinity for divalent cations such as calcium and magnesium than the TPP containing shift reagents. In studies where high levels of divalent cations in the extracellular medium are required, such as in excitable tissue studies, the TTHA derivatives are therefore a better choice (53). We have

also found that while DyTPP induced larger shift changes for ions with larger hydrated radius like Li^+ and Na^+ than TmTPP, the reverse was true for smaller ions such as Rb^+ and Cs^+. The large downfield shift of these two ions induced by TmTPP is probably the result of a contribution of the complex formation shift; in titrations with the diamagnetic LuTPP, only Rb^+ and Cs^+ showed an appreciable amount of downfield shift. This downfield complex formation shift added to the TmTPP induced paramagnetic shift but subtracted from that induced by DyTPP. The extent of line-broadening was consistently greater when DyTPP was used than when TmTPP was used. In view of the fact that TmTPP induced larger shifts without excessive broadening for rubidium and cesium NMR signals, it is probably a better choice for a shift reagent in the studies of these ions. The use of DyTTHA always induced larger shifts of the cations than TmTTHA at all concentrations tested. Both SRs shifted smaller ions like K^+ to a greater extent than a larger ion such as Li^+. Titrations with LuTTHA showed that again only Rb^+ and Cs^+ displayed some complex formation shift. The line broadening characteristics of these SRs were similar with DyTTHA producing somewhat more line-broadening. However, the induced broadening was always less than that observed with DyTPP.

It has generally been accepted that the major shift mechanism induced by the lanthanides is due to the pseudo-contact term (30,31,40). Since the unpaired 4f electrons of the lanthanides are shielded by the 5s and 5p electrons, the hyperfine coupling constant is expected to be small and, as a result, the contact shift would be small (37). All the lanthanides are chemically similar, therefore, the lanthanides are believed to form isomorphous complexes with the chelates. Consequently, the ratio method (see below) can be used to give an empirical measure of the relative contributions of pseudo-contact and contact shifts given by a particular shift reagent (30,31). Assuming that the binding

constants of analogous complexes of Dy^{3+} and Tm^{3+} for a given cation are similar, then the ratio between the dysprosium and thulium induced shift should theoretically be -1.9 if the pseudocontact shift is dominant (37). We applied the ratio method to estimate the pseudocontact contribution by dividing the slope of the DyTPP shifts by the TmTPP slopes (Table 2.1). In the case of the TPP derivatives, it was found that the ratios of the slopes did not give rise to the theoretical ratio of -1.9 but varied linearly with the radius of the ions. Bigger hydrated ions like Li^+ and Na^+ gave rise to a Dy/Tm ratio close to -1.9, but those of K^+, Rb^+, NH_4^+ and Cs^+ did not. Attempts to correct for the contribution of the complex formation shift by adding or subtracting LuTPP slopes accordingly from the DyTPP and TmTPP slopes before division did not give the theoretical ratio. The simplest explanation for this observation is that the DyTPP and TmTPP complexes are not isomorphous. Potassium and ammonium ions, which have similar hydrated radii, gave rise to comparable ratios, attesting to the accuracy of the measurements. Rubidium and cesium ions have the smallest hydrated radii and their ratios were far from the theoretical value even after the complex formation shift contributions had been corrected for. It is possible that the size of these substrates had an effect on DyTPP-substrate complex that is different from the TmTPP complex (54) which led to some form of contact shift contribution. Better results were obtained with the TTHA-derivatives, in that all of the ions except Rb^+ and Cs^+ gave rise to a ratio close to -1.9 indicating that the Dy and TmTTHA are isomorphous complexes. The Rb^+ and Cs^+ ratios are probably the result of downfield shifts induced by various mechanisms. All of the Dy/Tm ratios were negative which suggested that the pseudo-contact shift mechanism was involved.

From the competition studies, it is evident that all of the smaller ions tested bind to DyTPP in an analogous manner. The co-linearity observed in the shift and competition

curves (Figure 2.6) is indicative of a similar affinity of these ions for DyTPP and suggests a common binding site for these ions.

The anomalous Cs^+ shift observed with DyTPP is likely attributable to the binding of anions, contributions of the complex formation shift and possibly contact shift. The chemical shift of Cs^+ has been reported to be very sensitive to its chemical environment (41). We have observed downfield shift of Cs^+ by simply adding NaCl or KCl to the solution. When Na-acetate was used instead of NaCl to displace Cs^+ from DyTPP, the Cs^+ shift did not increase but stayed relatively constant. This indicates that Cl^- was responsible for causing the downfield shifts in the competition experiment with NaCl and KCl. However the linewidth of Cs^+ decreased toward its natural linewidth upon addition of either KCl or Na-acetate as competitor, suggesting that K^+ or Na^+ must have displaced Cs^+ from DyTPP, thus reducing the paramagnetic line-broadening effect. The unusual DyTPP induced Cs^+ shift is unlikely a result of a different binding site for cesium ion, since Cs^+ can displace Na^+ from DyTPP indicating common binding site(s) for both ions. The diamagnetic LuTPP shifted Cs^+ more downfield than DyTPP; the combination of the complex formation shift and the anions inherent in the LuTPP solution is evidently more positive than the DyTPP paramagnetic induced upfield shift. It is noteworthy that the sensitivity of Cs^+ to its ionic environment allows the separation of intra- and extra-cellular resonances without a shift reagent in certain situations, thus circumventing the need for the use of an SR with this cation (50,51).

In summary, DyTPP induced a much bigger shift change for the larger hydrated such as Na^+ and Li^+ than TmTPP. On the other hand, TmTPP shifted the resonances for the smaller Rb^+ and Cs^+ ions to the largest degree with similar line-broadening as DyTPP. Both TmTPP and DyTPP shifted K^+ and NH_4^+ to about the same degree, but TmTPP

induced somewhat less line-broadening, again indicating that it is the preferred shift reagent over DyTPP, for these two cations. While the TPP derivatives consistently gave larger shifts than the TTHA derivatives, their greater linebroadening (30,31), susceptibility to pH changes (30,31) and their toxicity (55,56) and hydrolyzability by extracellular phosphatases (57), make them often not the SR of choice. Thus, the TTHA derivatives are useful in experiments where the concentration of divalent cations must be kept constant (53), where extracellular phosphatases are present, or where measurements at lower pH (<7) need to be done.

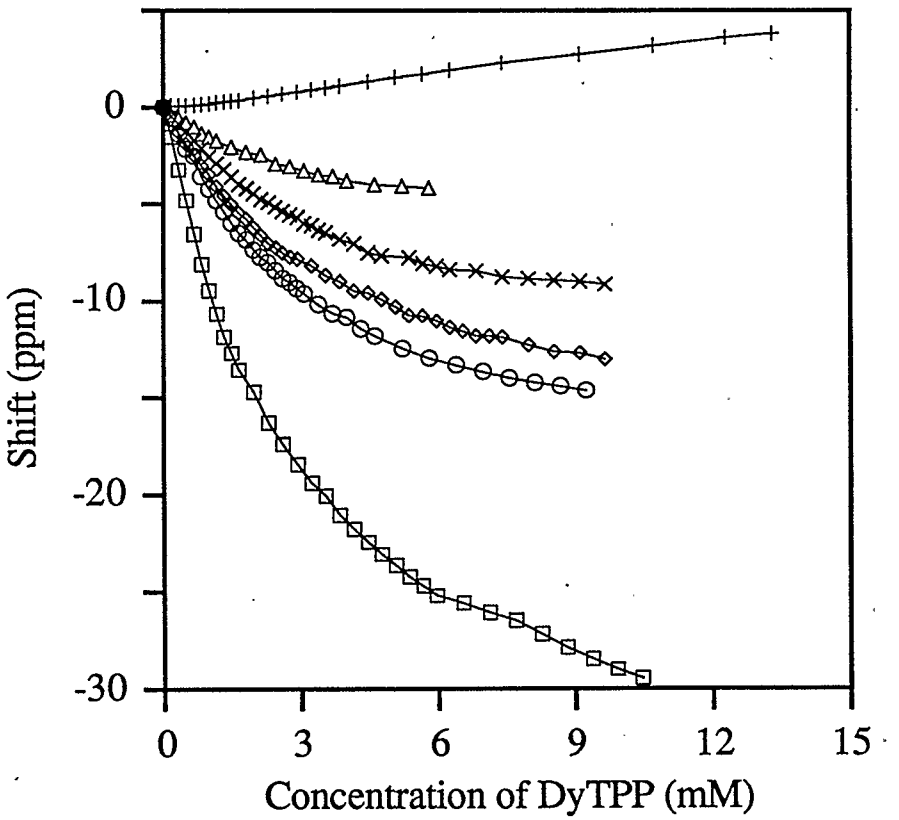

Figure 2.1a: Chemical shifts of various monovalent cations titrated with the shift reagent, $Dy(TPP)_{2.5}$. The symbols are: Li^+ (○), Na^+ (□), K^+ (◇), NH_4^+ (×), Rb^+ (△), Cs^+ (+).

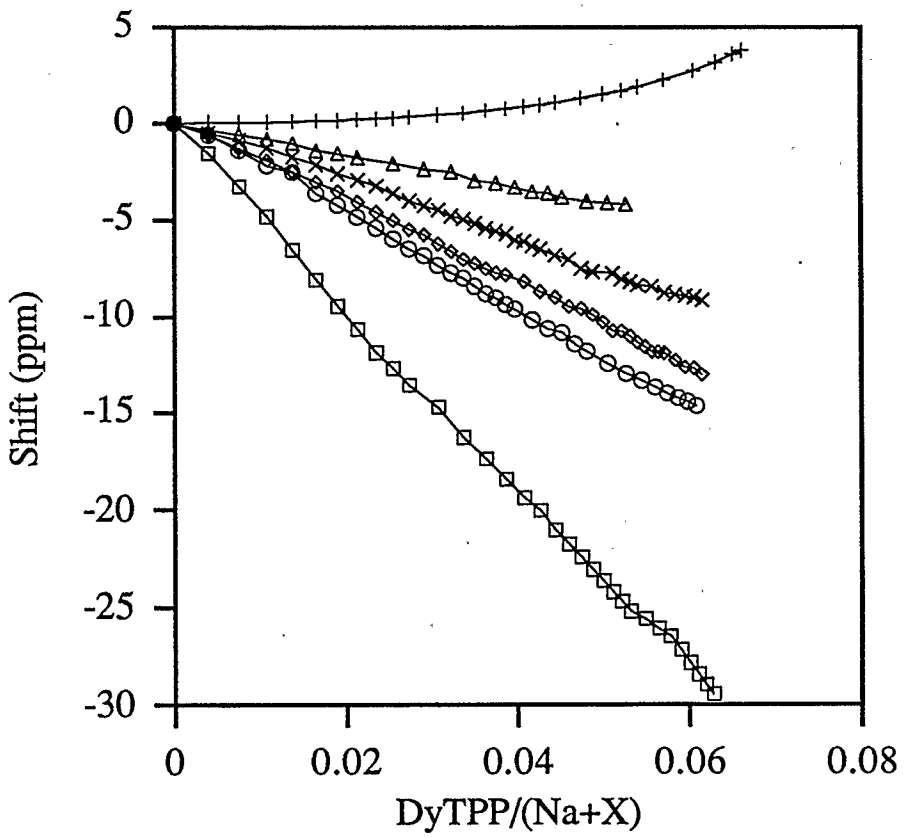

Figure 2.1b: The data presented in figure 1a is replotted to account for the Na^+ added as a counterion. The symbols are: Li^+ (○), Na^+ (□), K^+ (◇), NH_4^+ (×), Rb^+ (△), Cs^+ (+).

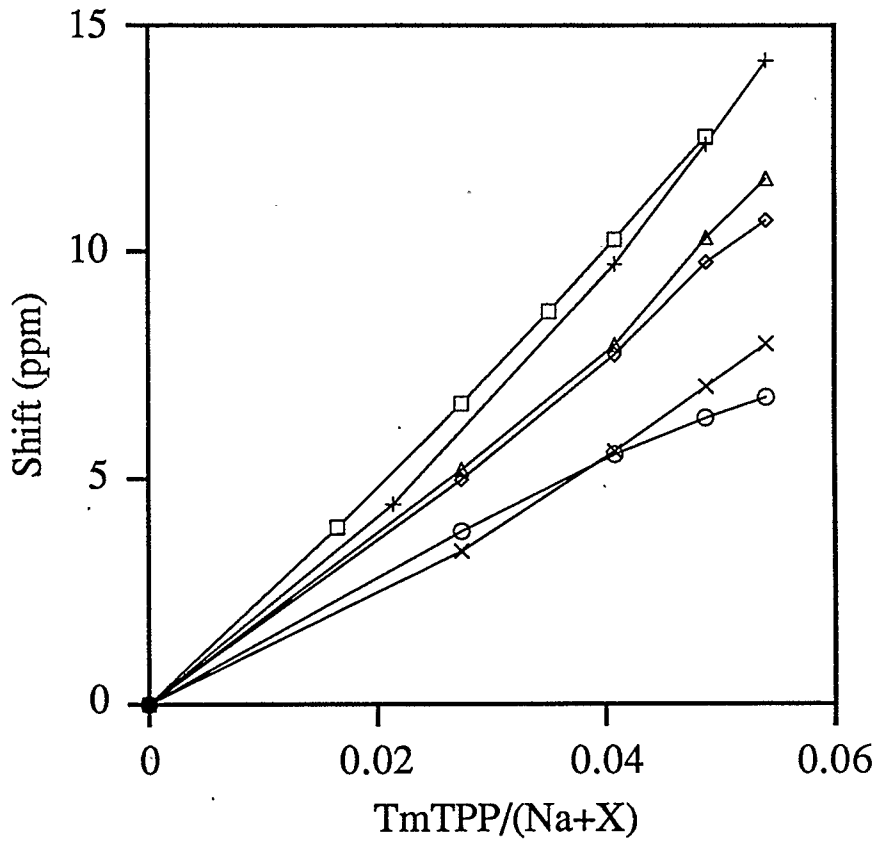

Figure 2.2a: Chemical shifts of various monovalent cations titrated with the shift reagent, $Tm(TPP)_{2.5}$. The symbols are: Li^+ (○), Na^+ (□), K^+ (◇), NH_4^+ (×), Rb^+ (△), Cs^+ (+).

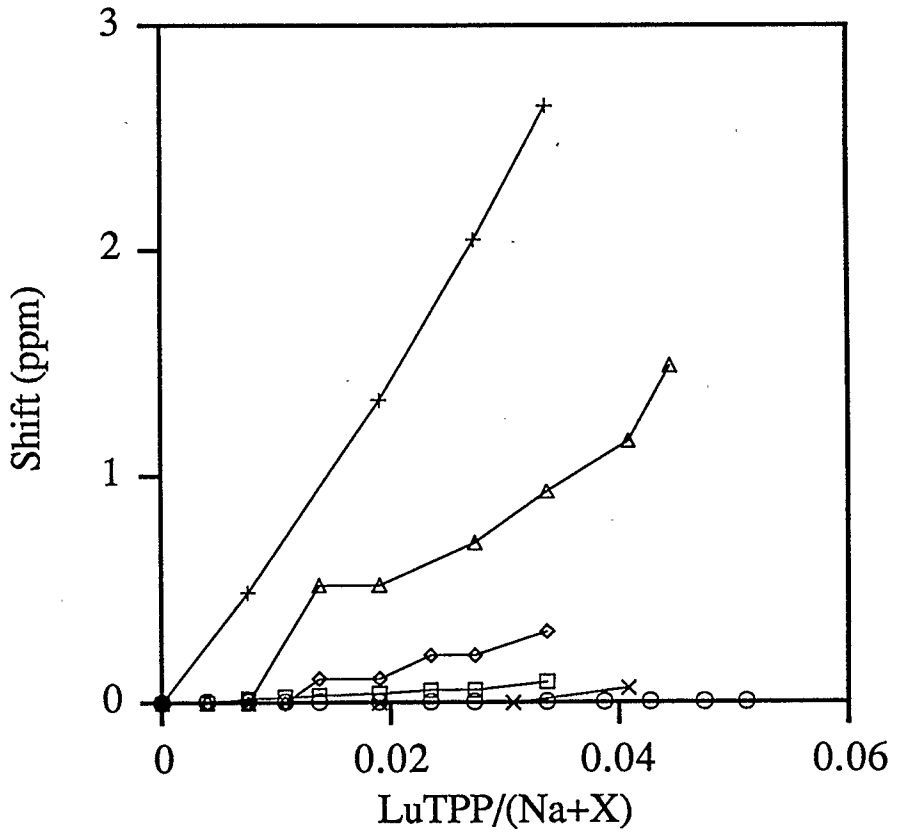

Figure 2.2b: Chemical shifts of various monovalent cations titrated with the diamagnetic shift reagent, Lu(TPP)2.5. The symbols are: Li^+ (○), Na^+ (□), K^+ (◇), $NH4^+$ (×), Rb^+ (△), Cs^+ (+).

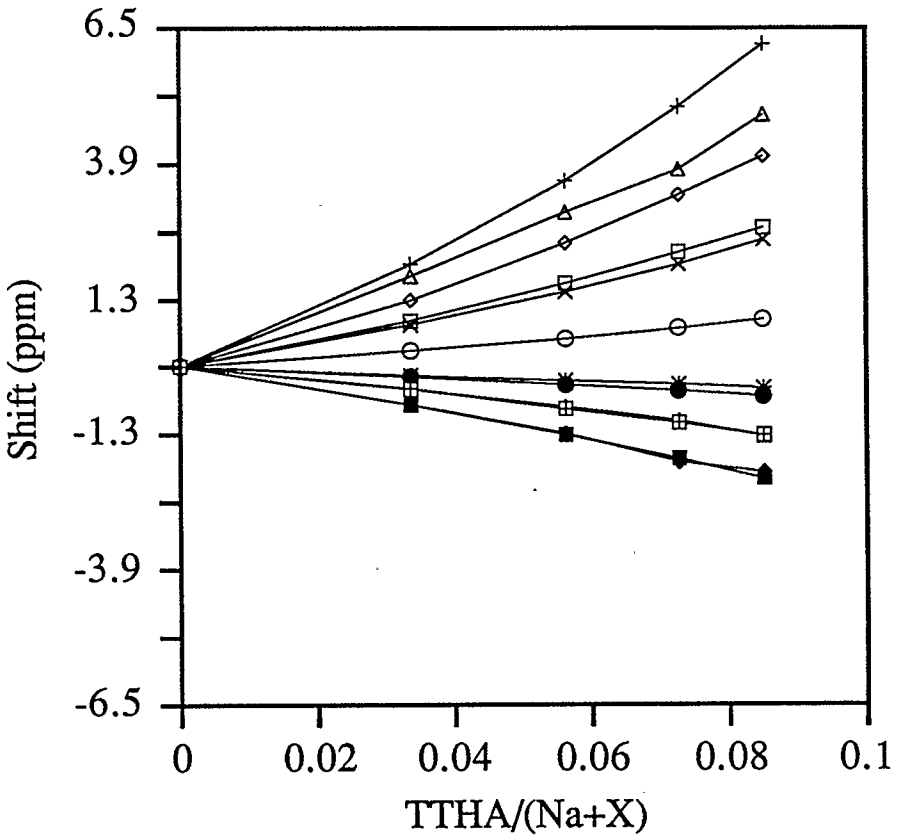

Figure 2.3a: Chemical shifts of various monovalent cations titrated with the shift reagents, DyTTHA and TmTTHA. The symbols for DyTTHA and TmTTHA are respectively: Li^+ (○,●), Na^+ (□,■), K^+ (◇,◆), $NH4^+$ (×,⊞), Rb^+ (△,▲), Cs^+ (+,✳).

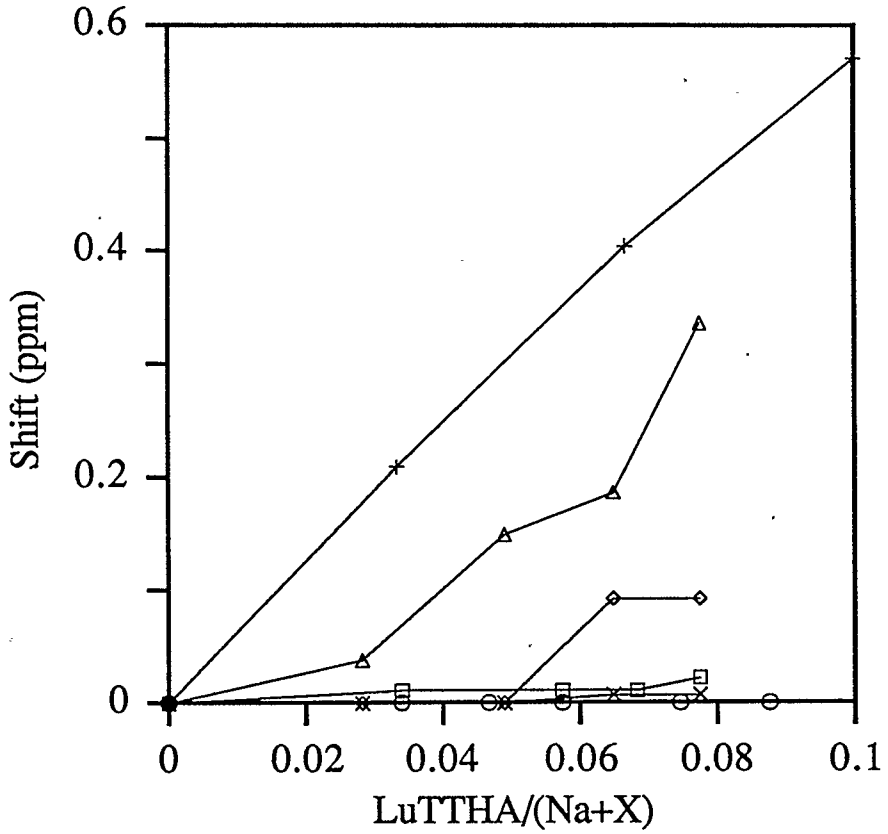

Figure 2.3b: Chemical shifts of various monovalent cations titrated with the diamagnetic shift reagent, LuTTHA. The symbols are: Li^+ (○), Na^+ (□), K^+ (◇), NH_4^+ (×), Rb^+ (△), Cs^+ (+).

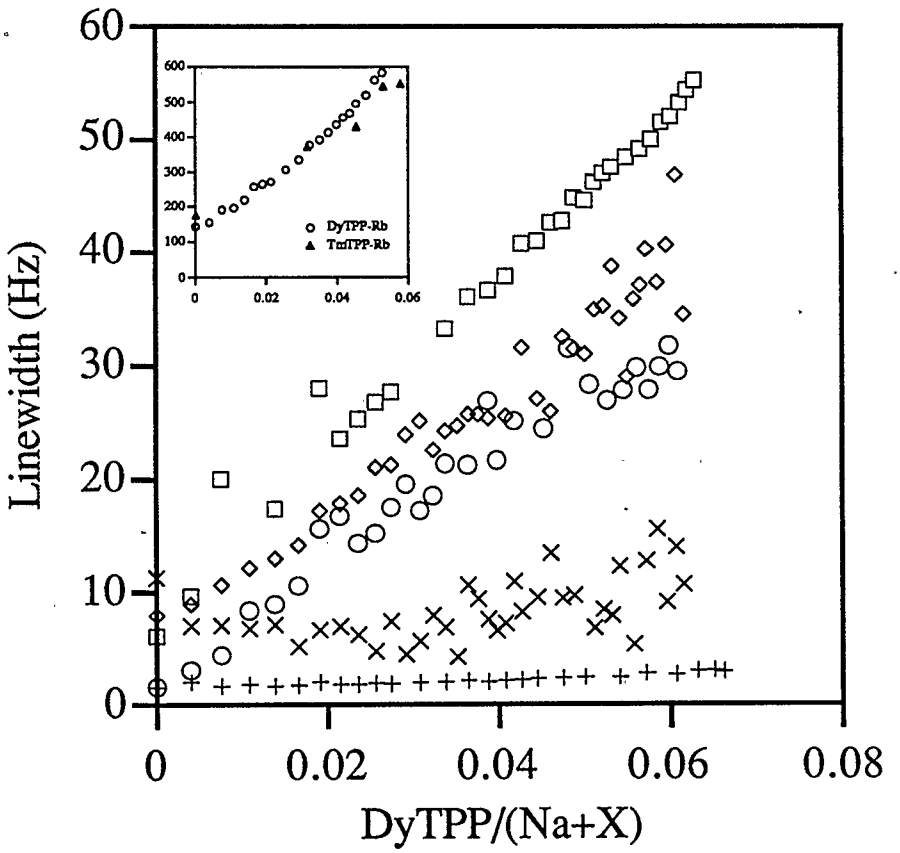

Figure 2.4: The line-broadening effect of $Dy(TPP)_{2.5}$ on the various monovalent cations. The symbols are: Li^+ (○), Na^+ (□), K^+ (◇), NH_4^+ (×), Cs^+ (+). In the insert, the linebroadening effect of $Dy(TPP)_{2.5}$ and $Tm(TPP)_{2.5}$ on Rb^+ is shown.

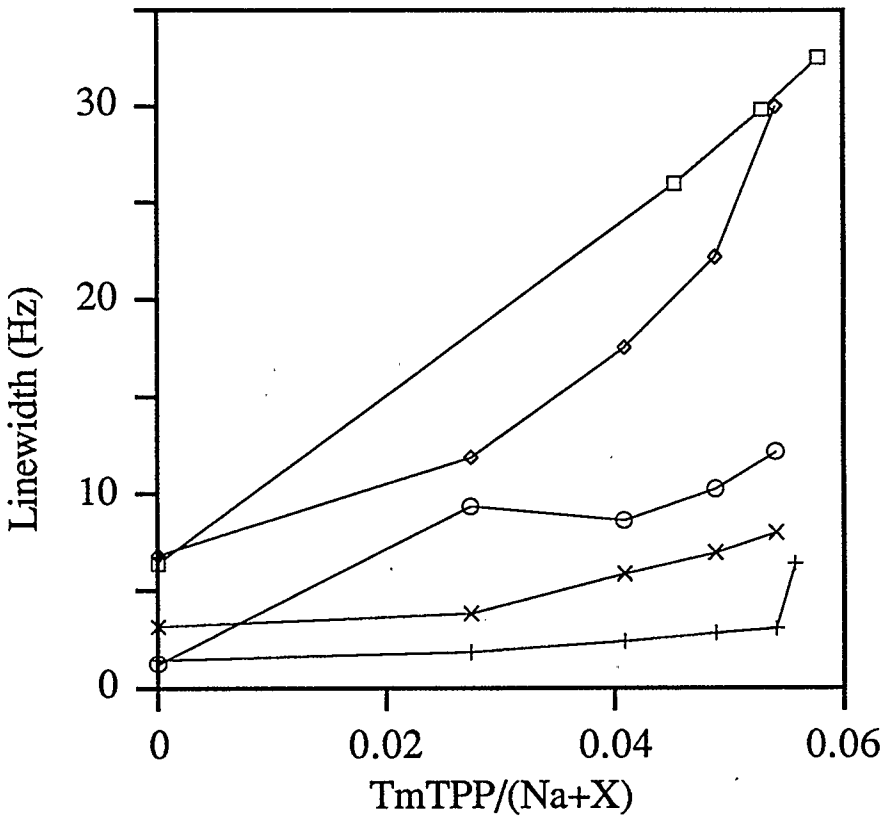

Figure 2.5: The line-broadening effect of $Tm(TPP)_{2.5}$ on the various monovalent cations. The symbols are: Li^+ (○), Na^+ (□), K^+ (◇), NH_4^+ (×), Cs^+ (+).

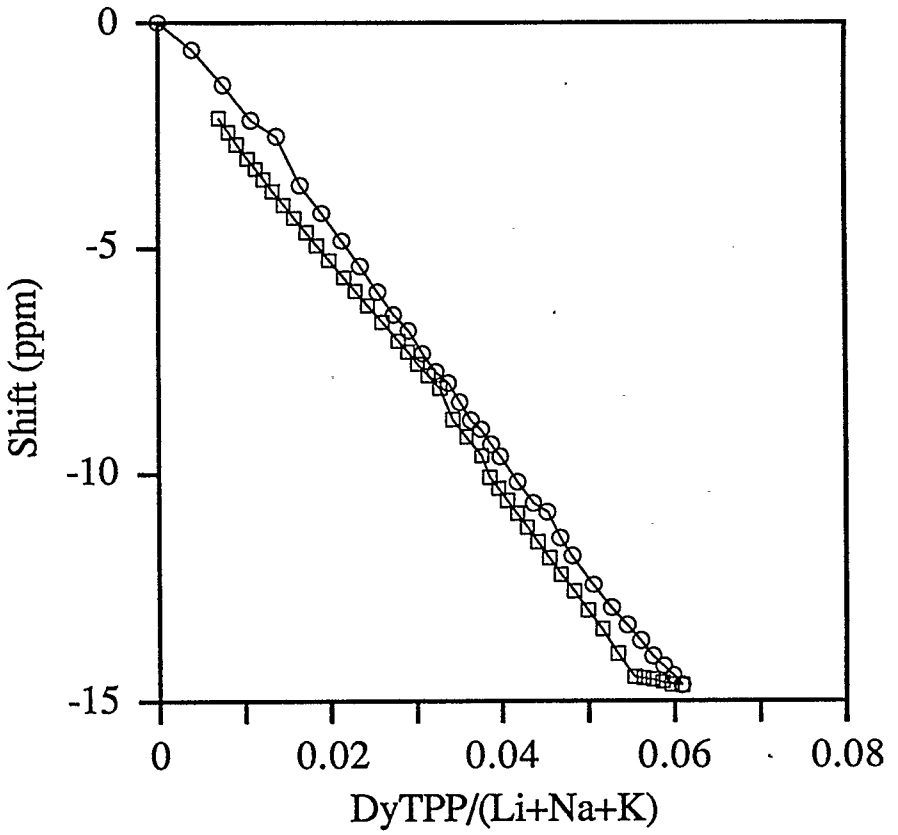

Figure 2.6a: The shifting of the Li^+ resonance (○) by $Dy(TPP)_{2.5}$ is superimposed with the competition curve (□) in which KCl was used as a competitor to displace Li^+ binding from $Dy(TPP)_{2.5}$.

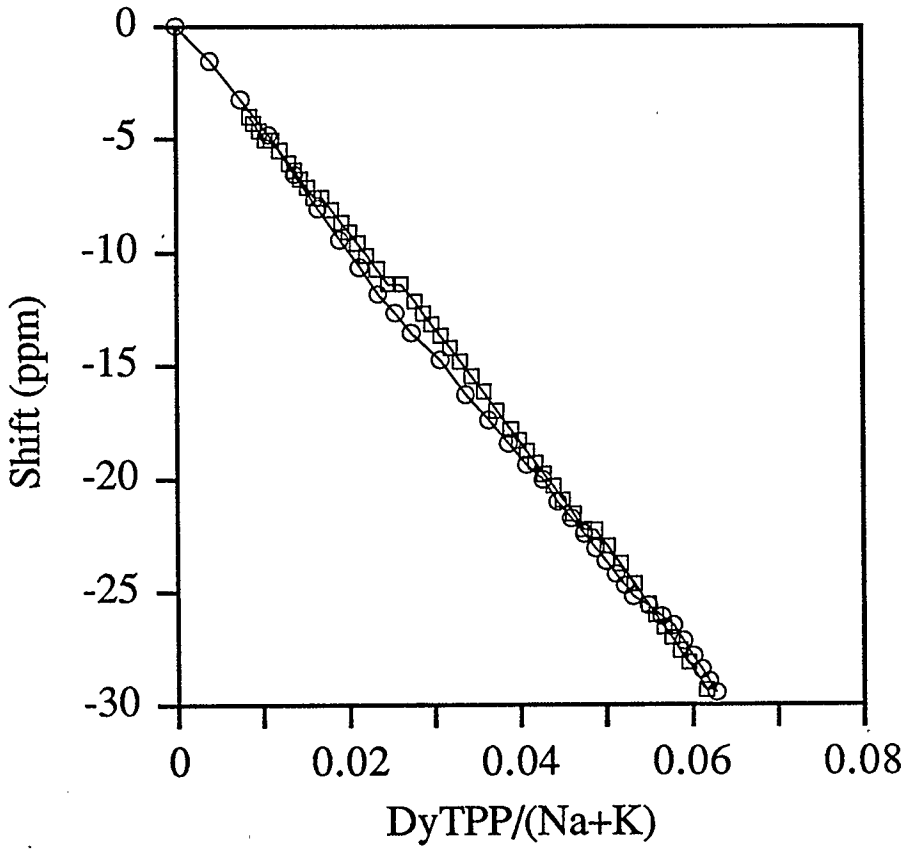

Figure 2.6b: The shifting of the Na^+ resonance (○) by $Dy(TPP)_{2.5}$ is superimposed with the competition curve (□) in which KCl was used as a competitor to displace Na^+ binding from $Dy(TPP)_{2.5}$.

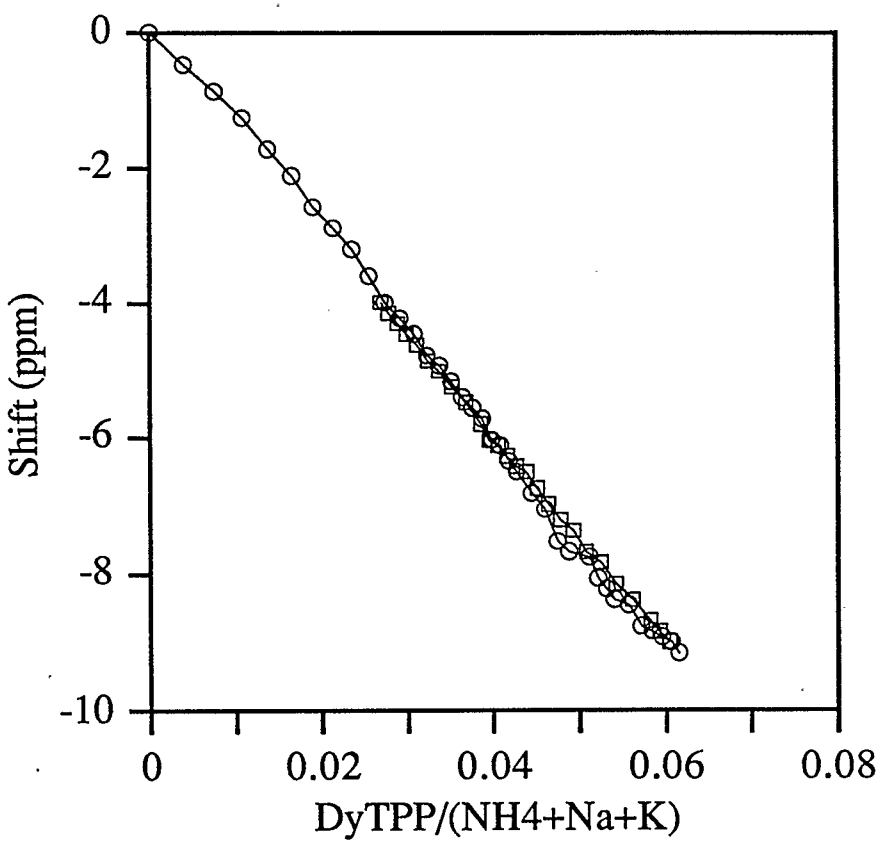

Figure 2.6c: The shifting of the NH_4^+ resonance (○) by $Dy(TPP)_{2.5}$ is superimposed with the competition curve (□) in which KCl was used as a competitor to displace NH_4^+ binding from $Dy(TPP)_{2.5}$.

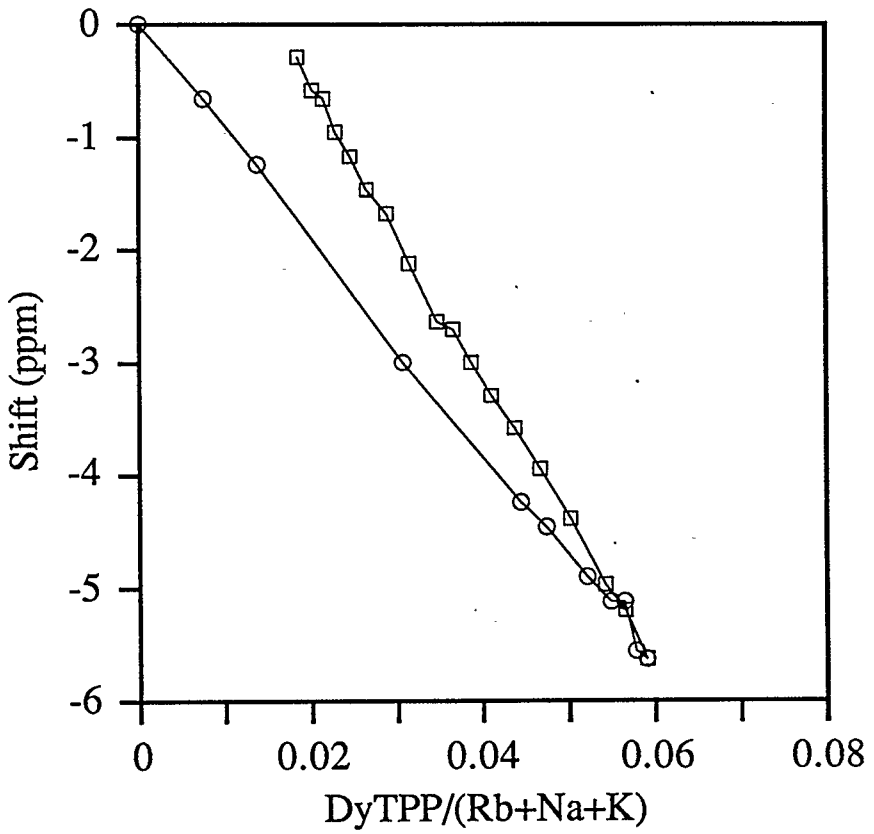

Figure 2.7a: The shifting of the Rb^+ resonance (○) by $Dy(TPP)_{2.5}$ is superimposed with the competition curve (□) in which KCl was used as a competitor to displace Rb^+ binding from $Dy(TPP)_{2.5}$.

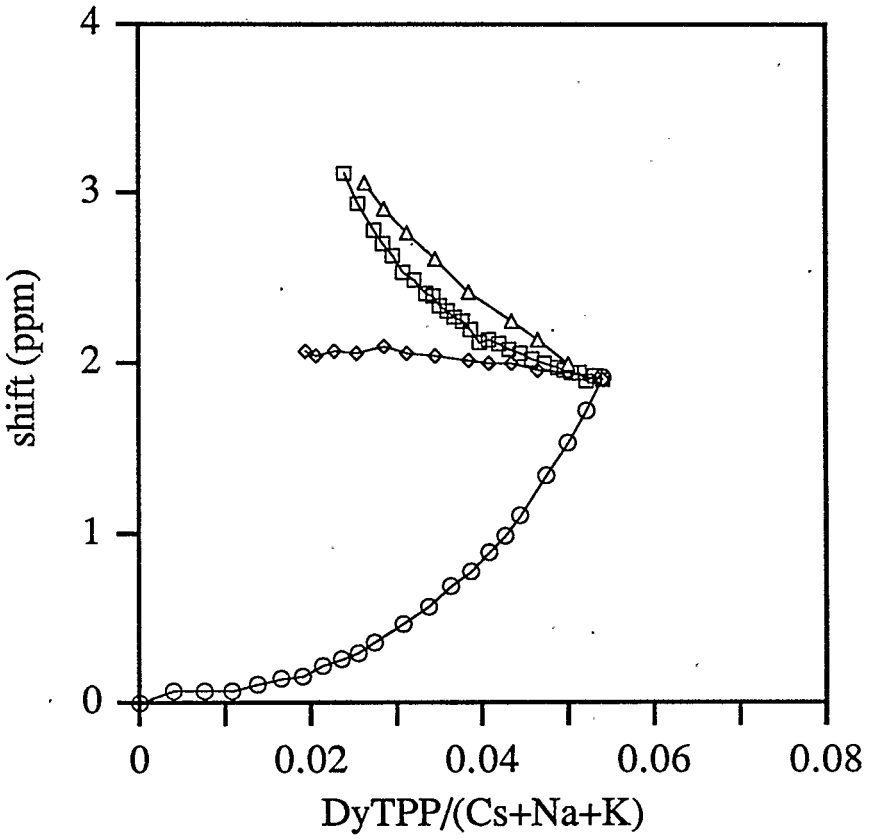

Figure 2.7b: The shifting of the Cs^+ resonance (○) by $Dy(TPP)_{2.5}$ is superimposed with the competition curve in which KCl (□), NaCl (△) or sodium acetate (◇) was used as a competitor to displace Cs^+ binding from $Dy(TPP)_{2.5}$.

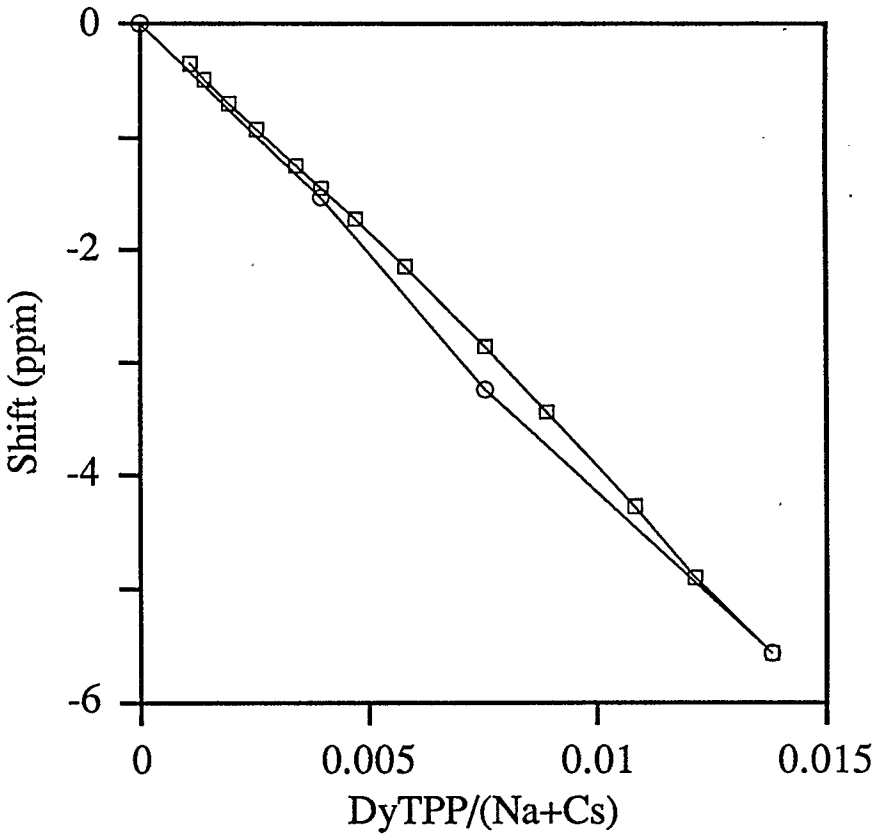

Figure 2.8: The shifting of the Na^+ resonance (○) by $Dy(TPP)_{2.5}$ is superimposed with the competition curve in which CsCl (□) was used as a competitor to displace Na^+ binding from $Dy(TPP)_{2.5}$.

Table 2.1: A summary of the slope of the SR induced shift for the various cations tested.#

Nuclei	Hydrated $ Radius (Å)	Slope*	Slope**	Slope ratio***
Li^+	3.5	-252.1(-252.1)	112.6(112.6)	-2.2(-2.2)
Na^+	3.3	-463.4(-465.9)	260.3(257.4)	-1.8(-1.8)
K^+	3.15	-215.9(-225.9)	199.2(189.3)	-1.1(-1.2)
NH_4^+	3.15	-158.1(-159.3)	144.7(143.7)	-1.1(-1.1)
Rb^+	3.0	-82.4(-115.4)	215.1(182.1)	-0.4(-0.6)
Cs^+	2.8	13.4(-64.8)	283.5(205.3)	0.05(-0.3)

$ Data obtained from reference 58.
* Slopes of the DyTPP induced shift calculated from figure 2.1b.
** Slopes of the TmTPP induced shift calculated from figure 2.2a.
*** Ratio of the DyTPP slope and the TmTPP slope.
# Numbers in brackets represent the slope after it has been corrected for the complex formation shift.

Nuclei	Ionic Radius (Å)	Slope^	Slope^^	Slope ratio^^^
Li^+ #	0.68	10.6(10.6)	-6.8(-6.80)	-1.6(-1.6)
Na^+	0.97	31.6(31.4)	-25.8(-26.0)	-1.2(-1.2)
K^+	1.3	47.5(46.2)	-25.1(-26.4)	-1.9(-1.8)
NH_4^+	1.4	28.7(28.6)	-15.8(-15.9)	-1.8(-1.8)
Rb^+	1.5	55.5(51.4)	-15.7(-19.8)	-3.5(-2.6)
Cs^+	1.7	72.2(63.4)	-4.9(-13.7)	-14.7(-4.6)

^ Slopes of the DyTTHA induced shift calculated from figure 2.3a.
^^ Slopes of the TmTTHA induced shift calculated from figure 2.3a.
^^^ Ratio of the DyTTHA slope and the TmTTHA slope.
# Number in brackets represents the slope after it has been corrected for the complex formation shift.

Chapter 3

^{31}P and ^{133}Cs NMR studies of the energy status and activity of the Na^+/K^+ pump in the perfused rat heart.

Introduction

The ubiquitous Na^+/K^+ pump is responsible for maintaining ionic gradients across the cell membrane. It couples the free energy of ATP hydrolysis to the active antiport of Na^+ and K^+ across the membrane. The outcome of various studies has suggested that the ATP requirement of the Na^+/K^+ pump is derived preferentially from the glycolytic pathway and that mitochondrial derived ATP is primarily used for other functions such as contractility in muscle tissues (59-62). Thus, it has been hypothesized that there is a functional compartmentation of ATP. In hearts, for example, it has been suggested that energy derived from glycolysis is preferentially used in supporting membrane functions, whereas, oxidatively derived ATP preferentially supports contractile functions (59-62). Similar suggestions have been made for renal cells (63) and smooth muscles (64,65). However, studies which are in apparent conflict with this hypothesis have also been reported. For example, no evidence for the functional coupling between Na^+ pump activity and ATP can be detected in myocardial sarcolemmal vesicles (66). In addition, a linear relationship between the activity of the Na^+/K^+ pump and the amount of mitochondrially generated ATP in renal cells (67,68) and in pancreatic cells (69) have been observed.

In view of this conflicting evidence regarding the possibility of functional compartmentation of cytoplasmic ATP, we have investigate this issue further in the Langendorf-perfused rat heart in the first part of this study. We have used ^{31}P and ^{133}Cs NMR to study both the energy status and the Na^+/K^+ pump activity during various metabolic conditions in the rat heart. The heart was perfused with glucose (glc) or pyruvate

(pyr) buffer with or without various inhibitors added such as iodoacetate (IAc) or cyanide (CN) which are known to block either glycolysis or oxidative phosphorylation respectively. The intracellular levels of free ATP, inorganic phosphate (Pi), phosphocreatine (PCr), and the intracellular pH were followed continuously by ^{31}P NMR. The uptake of Cs^+ from the perfusion medium by the hearts was monitored by ^{133}Cs NMR and serves as a indicator of the Na^+/K^+ pump activity. The use of Cs^+ as a K^+ congener provides certain advantages. First of all, it is a very sensitive NMR nucleus which gives rise to sharp, easily detectable resonances. Secondly, because of the great sensitivity of the Cs^+ chemical shift to its chemical environment (70), intracellular and extracellular signals can be separated without the use of a potentially toxic shift reagent (71-73). Finally, Cs^+ is a well established inhibitor of most inward and outward K^+-channels (74,75) and thus an inward Cs^+ flux would arise almost exclusively from the activity of the Na^+/K^+ pump (76). However, one disadvantage is that since Cs^+ is a K^+-channel blocker, generally a decrease of the spontaneous heart rate and some transient effects on developed pressure are observed (76).

In the second part of this study, we have also investigated the activity of the Na^+/K^+ pump during normoxic, ischemic and reperfusion periods in the rat heart. Alterations in myocardial cation homeostasis during ischemia and reperfusion may account for some of the damage suffered by the heart after an ischemic period. The elevated intracellular level of Na^+, which may result from pump failure, would give rise to increased Ca^{2+} levels via the Na^+-Ca^{2+} exchange mechanism. The elevated Ca^{2+} in turn can lead to irreversible injury such as mechanical contracture and mitochondrial dysfunction during reperfusion (77-79). In the intact cell, the main regulator of the Na^+/K^+ pump activity is believed to be intracellular Na^+. The regulatory role of ATP (K_m=0.1-0.6 mM) is important only during severe ischemia and physiological variations in extracellular K^+

have little effect on pump activity (80). However, it has been shown that intracellular Na^+ increases early after the onset of ischemia even when ATP level is still high in the rat heart (81) and in liver (82). A plausible explanation for this is an inhibition of the Na^+/K^+ pump during ischemia by factors other than the lack of ATP. Various authors have demonstrated a decrease in Na^+/K^+ pump/ATPase activity during ischemia and reperfusion in isolated myocardial sarcolemma (83,84), in perfused rabbit heart (85) and in cultured ventricular cells (86). The cause of this inhibiton is still unknown. Oxygen free radicals have been suggested to be the culprit (87); others have proposed alterations in membrane structural integrity/fluidity during ischemia (88,89). A continuous recording of the Na^+/K^+ pump activity and energy status of the heart during periods of normoxia, ischemia and reperfusion would be helpful in correlating the exact onset of the inhibition of contractility, pump activity, energy depletion and pH decrease.

In this second part of the study, we used a similar protocol as in the initial study. The uptake of Cs^+ was monitored continuously for three 1 hour periods namely, normoxic, ischemic and reperfusion. The rate of Cs^+ accumulation is used as an indicator of the pump activity. The intracellular level of high energy phosphates, inorganic phosphate and the pH are studied with ^{31}P NMR. The rat hearts were perfused under conditions that will facilitate functional recovery during reperfusion in one group (perfusion with glucose+glutamate (90-92) or pyruvate (93,94) as substrate) and non-recovery in the other (glucose as substrate).

Methods and Materials

Heart Perfusion. Male Sprague-Dawley rats (250-330g) were anaesthetized with diethylether just prior to heart excision. After cooling in ice-cold buffer, the excised heart was perfused in the Langendorff mode with a modified Krebs Henseleit buffer (standard buffer) at a perfusion pressure of 100 cm water and allowed to beat spontaneously. A latex balloon containing a solution with a known concentration of methylenediphosphonate (MDP) was inserted into the left ventricle to measure ventricular function and to act as an NMR concentration standard. After a 20 min equilibration period, the content of high-energy phosphate metabolites in the heart was measured by collecting two fully relaxed ^{31}P spectra (one before and one after a known amount of MDP had been added to the latex balloon). The perfusion buffer was then switched to one of the Cs^+-containing buffers (see below) and the heart was perfused for one hour. One hour global ischemia was initiated by clamping off the tubing leading to the heart after the perfusion period. This was followed by a one hour reperfusion period using the same kind of buffer used in the perfusion period. During this 3 hour period, the uptake of Cs^+ or cellular energy status was monitored continuously with ^{133}Cs or ^{31}P (non fully relaxed) NMR, respectively.

Ouabain Studies. After 20 min of equilibration, the heart perfusate was changed from the standard buffer to pyr-Cs buffer for one hour. The uptake of cesium was monitored continuously with ^{133}Cs NMR. A ^{31}P NMR spectrum was collected at the end of this period to assess the energy status of the heart. The perfusion buffer was then changed to a pyr-Cs buffer containing varying concentrations of ouabain-octahydrate for one additional hour. A final ^{31}P NMR spectrum was obtained at the end of the experiment to assess the energy status of the heart. Ouabain inhibition of Cs^+ uptake was calculated

by comparing the ouabain-sensitive uptake rate with the total uptake rate. In separate experiments, the ouabain-sensitive Cs^+ uptake was also measured in potassium-arrested hearts. The basic protocal used was the same, but the arresting buffer contained 24 and 12 mM of KCl and CsCl respectively and a corresponding decrease in NaCl concentration.

Cs^+ washout. After equilibration, the perfusion buffer was switched to glc-Cs buffer to commence Cs^+ uptake for one hour. At the end of this period, washout of Cs^+ was initiated by switching the perfusate back to the standard medium.

Solutions. The standard buffer was prepared as per Choong et al (90) and contained (in mM): 115.0 NaCl, 5.9 KCl, 2.3 $CaCl_2$, 1.2 $MgSO_4$, 25 $NaHCO_3$ and 11 glucose. Glucose plus Cs^+ (glc-Cs) buffer contained: 115.0 NaCl, 2.95 KCl, 2.95 CsCl, 2.3 $CaCl_2$, 1.2 $MgSO_4$, 25 $NaHCO_3$ and 11 glucose. Glucose plus glutamate and Cs^+ (glc-glu-Cs) buffer contained the same ingredients as the glc-Cs buffer except 20 mM L-glutamate (prepared by titrating glutamic acid solution to pH 7.5 with NaOH) was added in place of the same amount of NaCl to maintain consistent osmolarity. Glucose plus iodoacetate and Cs^+ (glc-IAc-Cs) buffer had the same composition as the glc-Cs buffer except that 1 mM iodoacetic acid (sodium salt) was added in place of 1 mM NaCl. Glucose plus cyanide and Cs^+ (glc-CN-Cs) buffer had the same composition as the glc-Cs buffer except 5 mM sodium cyanide solution (titrated to pH 7.5 with HCl) was added in place of the same amount of NaCl. Pyruvate plus Cs^+ (pyr-Cs) buffer contained 11 mM of pyruvate instead of glucose in the glc-Cs buffer. Pyruvate plus iodoacetate and Cs^+ (pyr-IAc-Cs) and pyruvate plus cyanide and Cs^+ (pyr-CN-Cs) buffers was prepared in the same manner as the glc-IAc-Cs and glc-CN-Cs buffers respectively except glucose was replaced by pyruvate. All buffers were gassed with 95% O_2 and 5% CO_2 mixture and temperature was regulated at 30°C. All chemicals were purchased from Sigma Co.

NMR Spectroscopy. All NMR experiments were carried out with a widebore Bruker AM 400 spectrometer equipped with a 9.4 T superconducting magnet. The perfused hearts were placed in a 20 mm tube and inserted into the magnet with the temperature set to 30°C. Fully relaxed ^{31}P (resonance frequency=161 MHz) spectra were collected using 8K data points and composite pulse proton decoupling (2 W) during acquistion only. The time between individual pulses was 17.5 seconds. The number of scans was 64 and 90° pulses were used. Non-fully relaxed spectra were collected with bi-level decoupling (2 W during acquistion, 0.5W otherwise), a cycling time time of 3.5 seconds, 64 scans and a pulse angle of 75°. All chemical shift were referenced with respect to phosphocreatine which was assigned a shift of 0 ppm. The intracellular pH was measured from the chemical shifts of the inorganic phosphate using an appropriate standard calibration curve (95). ^{133}Cs (resonance frequency=52 MHz) spectra were collected with a cycling time of 6.5 seconds, 32 scans and a pulse angle of 45°. ^{31}P and ^{133}Cs spectra were Fourier transformed with a line-broadening of 15 and 2 Hz respectively and baseline-corrected before manual integration. Peak integrals were quantitated using standard Bruker integration software.

Data. All experiments were repeated three times unless otherwise stated. Data are reported as mean±SEM.

Results:

A typical fully relaxed ^{31}P NMR spectrum of a heart perfused with the standard buffer is shown in figure 3.1. The average rate pressure products (RPP), which is the product of heart rate and developed pressure, was 30,874±1076 mmHg/min (n=31) and the ^{31}P NMR determined metabolite concentrations were (in umol/gdw, n=24): 8.6±0.8 phosphomonoesters, 9.8±1.2 Pi, 33.3±1.4 PCr and 17.7±0.9 ATP. These values are in good agreement with reported values in similar heart studies (96-98).

In the cesium uptake experiment, the ^{133}Cs NMR spectrum of a heart perfused with pyr-Cs buffer showed two peaks (figure 3.2). The downfield peak was assigned as the intracellular Cs^+ peak and its area was seen to increase linearly with time. After one hour of perfusion, the effect of ouabain on the rate of Cs^+ uptake in the same heart was measured by switching to a pyr-Cs buffer containing ouabain. In the presence of ouabain the slope of uptake showed a definite decrease compared to pre-ouabain conditions (figure 3.3). In the presence of ouabain, the developed pressure and heart rate increased by an average of 23% and 28% respectively. The final ^{31}P NMR spectrum collected after 1 hour of ouabain perfusion revealed that some hearts had an abnormally high amount of Pi after ouabain treatment (particularly at higher concentrations eg 200 uM) and data obtained from these hearts were discarded. In figure 3.4, the % inhibition of Cs^+ uptake rate in relation to ouabain concentration is shown. We have also measured the ouabain inhibition of Cs^+ uptake rate in K^+-arrested hearts. The average % inhibition at 200 uM of ouabain was found to be 56.0±3.3% (n=4). The final ^{31}P NMR spectra of these hearts were comparable to the pre-ouabain ones. Increased extracellular K^+ also led to a decreased Cs^+ uptake (data not shown). All these data confirm that Cs^+ is taken up via the Na^+/K^+ ATPase.

The results of a Cs^+ washout experiment are shown in figure 3.5. After the initial uptake period of one hour, the perfusion buffer was switched back to the standard buffer for washout. The intracellular Cs^+ level was seen to decrease slightly with time and was reduced to about 80% of the initial value after 75 min of washout. The spontaneous heart rate decreased to an average of 70% of pre-Cs^+ value after one hour of perfusion with the glc-Cs buffer and returned to an average of 87% of normal during the washout period. On the other hand, the developed pressure of the hearts was similar during the three periods.

In titration experiments where solutions of phosphocreatine, fructose-1,6-diphosphate, glucose-6-phosphate and ATP were added to a Cs^+-buffer containing (in mM): 5 $MgCl_2$, 130 KCl, 10 Pi and 2.95 CsCl at pH 6.5 to mimic physiological conditions, the Cs^+ resonance was observed to shift downfield while its integral was relatively unaffected (data not shown).

In order to investigate the possible functional compartmentation of ATP in the rat heart, we assessed the effects of different carbon sources and inhibitors on Cs^+ uptake. A representation of the uptakes is shown in figure 3.6a,b. No significant difference in the rate of uptake was seen between the glc-Cs, glc-glu-Cs and pyr-Cs perfused hearts (Table 3.1). The glc-CN-Cs and pyr-CN-Cs perfused hearts exhibited similar but reduced rates when compared to the groups above and the glc-IAc-Cs perfused group showed the slowest rate. Unexpectedly, the pyr-IAc-Cs group displayed the highest uptake rate amongst all experimental groups. The rate-pressure products of these hearts after one hour of Cs^+ perfusion are also shown in Table 3.1. No obvious correlation existed between the RPP and Cs^+ uptake rate.

Typical ^{31}P NMR spectra of hearts perfused for one hour with the various Cs^+-containing buffers are shown in figure 3.7a. The glc-Cs and glc-glu-Cs perfused hearts showed a similar ^{31}P NMR profile in that all the phosphoryl metabolites were present at

comparable amounts. The pyr-Cs group showed lower amounts of inorganic phosphate and slightly higher PCr levels than the glc-Cs hearts. Large amounts of phosphomonoesters (eg glucose-6-P, fructose-1,6-diphosphate) were seen in the glc-IAc-Cs and pyr-IAc-Cs groups as a result of the inhibition of glycolysis. The content of PCr and ATP was undetectable in the glc-IAc-Cs hearts but was present at lower levels in the pyr-IAc-Cs hearts. Both the glc-CN-Cs and pyr-CN-Cs groups were able to maintain some, albeit smaller, levels of PCr and ATP while Pi was present in relatively high amounts. The glc-CN-Cs group also showed an accumulation of phosphomonoesters probably a result of an activation of the phosphofructokinase enzyme by increased levels of ADP and an inhibition of glyceraldehyde-3-phosphate dehydrogenase by the elevated levels of NADH. From the chemical shift of the inorganic phosphate, we found that the intracellular pH of the hearts was maintained at pH 7.07 throughout the perfusion period except for the glc-IAc group (figure 3.8). Upon perfusing with the glc-IAc-Cs buffer, the intracellular pH dropped rapidly from normal to 6.74 followed by a slow recovery back to the initial pH. The inorganic phosphate concentration also remained relatively constant throughout the perfusion period for the glc-Cs, glc-glu-Cs, glc-IAc-Cs, pyr-Cs and the pyr-IAc-Cs groups with the former three groups having higher levels (figure 3.9). The Pi content of the glc-CN-Cs group did rise throughout most of the perfusion period but dropped to a lower level just prior to ischemia. The pyr-CN-Cs group also showed rapid Pi accumulation which remained elevated throughout the perfusion. The level of intracellular PCr of these hearts showed considerable changes during the perfusions (figure 3.10). The glc-Cs and glc-glu-Cs groups maintained a steady level of PCr during the perfusion period as expected. The pyr-Cs perfused group showed a strong increase in PCr level initially but decreased slowly back toward the glc-Cs level just prior to ischemia. Similarly, the pyr-IAc-Cs group showed elevated level of PCr in the beginning but dropped

rapidly to about to a third of the original content at the end of the 60 minute period. The PCr content of the glc-IAc-Cs, glc-CN-Cs and pyr-CN-Cs groups dropped rapidly with only small recoveries at the end of the period. The ATP content of the hearts, except for the glc-IAc-Cs group, was surprisingly very similiar despite the difference in PCr (figure 3.11). A relatively constant level of ATP was seen irrespective to the perfusion buffer used (although the pyr-IAc-Cs group showed lower amount near the end of the perfusion period). A clear difference was seen however in the glc-IAc-Cs group. The ATP level of this group dropped almost immediately after the onset of perfusion and continued to decrease during the rest of the one hour period.

Cs^+ uptake stopped almost immediately upon the onset of ischemia (figure 3.6). All hearts showed Cs^+ loss during this period (Table 3.1). Despite more scattering, the data clearly showed an inactivation of the Na^+/K^+ pump activity upon ischemia. In the reperfusion period, only the pyr-Cs group showed strong recovery of pump activity. The glc-glu-Cs group showed some recovery of pump activity (figure 3.6); however, the correlation coefficient of the slope was small. All of the other groups showed a negative Cs^+ uptake slope indicating a gradual loss of Cs^+ from the hearts. During ischemia, the cardiac function dropped rapidly to zero for all groups and only the pyr-Cs group showed consistent functional recovery during reperfusion (Table 3.1).

Typical ^{31}P NMR spectra of hearts at the end of a 60 minutes ischemic period and after 20 minutes of reperfusion are shown in figure 3.7b,c respectively. The changes in intracellular pH of the hearts during ischemia varied in relation to the perfusion buffer used. Hearts that were perfused with buffer that inhibited glycolysis (glc-IAc-Cs and pyr-IAc-Cs) or promoted glycogen depletion (pyr-CN-Cs) showed only small changes in pH during ischemia (figure 3.8). Glc-Cs and glc-glu-Cs perfused hearts followed the same trend in intracellular acidification initially, but after 20 minutes, the glc-Cs group dropped to a lower

pH of 5.95. The pyr-Cs and glc-CN-Cs groups followed a slower decrease in pH than the glc-Cs group and reached a minimum pH of 6.04 after about 30 minutes of ischemia. During reperfusion, all pHs returned to normal values. The accumulation of Pi during ischemia followed a similar trend as that of the intracellular proton. Hearts perfused with iodoacetate showed a smaller increase in Pi during ischemia (figure 3.9). The trapping of phosphate in the phosphomonoester form by iodoacetate probably contributed to this. All other hearts showed the similar increase in Pi. During reperfusion, the Pi content of the heart was seen to decrease with time. No difference in the changes of the PCr content was seen during ischemia (figure 3.10). The same dramatic decrease in PCr was seen in all groups within minutes of ischemia and reached the minimum level after 20 minutes. Upon reperfusion, only the glc-Cs, glc-glu-Cs and pyr-Cs groups resumed the production of PCr. The PCr level in the pyr-Cs perfused hearts was consistently higher than the glc-Cs and glc-glu-Cs groups. The decline of ATP level during ischemia is shown in figure 11. The glc-Cs, glc-CN-Cs, and pyr-Cs groups showed similar time dependent loss of ATP. Hearts that were perfused with inhibitor displayed more rapid loss of ATP. Reperfusion brought about some ATP recovery for some groups, particularly those without inhibitors; however, the differences were small.

Discussion:

The results of the ouabain inhibition study clearly demonstrated that the uptake of Cs^+ by the rat heart was ouabain sensitive. The dose-response curve showed a linear relationship between ouabain concentration and inhibition of Cs^+ uptake by the rat heart. At 150 uM ouabain, there was a ~ 70% inhibition of uptake; these values are in reasonable agreement with earlier reported values. Akera et al. (99) found that 50 uM ouabain inhibited the Na^+/K^+ ATPase activity by 50% in rat heart homogenates. Likewise, Vemuri et al. (100) reported that 100 uM ouabain inhibited the Na^+/K^+ ATPase by 45%. At the various concentrations of ouabain tested, the developed pressure increased by an average of 20% which is in agreement with Akera et al. (99) who found similar increases in ventricular muscle developed tension. Since it is known that ADP and Pi are inhibitors of the Na^+/K^+ ATPase in reconstituted enzyme preparations (101) and in red blood cells (102,103), we performed our ouabain inhibition studies with pyr-Cs perfused hearts to keep the ATP level high and the Pi level low. However, at ouabain concentrations greater than 150 uM, we consistently observed an abnormally high amount of Pi in comparison to PCr after one hour of perfusion. The resulting inhibition by Pi of the Na^+/K^+ pump at high ouabain concentrations could cause increases in cellular Ca^{2+} level, via the Na^+/Ca^{2+} exchanger, which may lead to impaired mitochondrial functions. In order to study higher concentrations of ouabain without greatly increasing the Pi level, we made use of K^+-arrested hearts. Hearts were K^+-arrested by perfusing with a modified glc-Cs buffer that contained higher concentrations of KCl and CsCl. In the arrested hearts, 200 uM ouabain inhibited the pump activity by 56% without greatly affecting the phosphoryl metabolites

concentration. It is known that high K^+ concentrations can inhibit ouabain binding (80,99); the drop in % inhibition at 200 uM ouabain can be due to this effect.

In the washout experiment, we verified that Cs^+ was relatively impermeable to the cell membrane. After a 75 minute washout period, the intracellular Cs^+ level decreased by only 20% (figure 3.5). We can therefore be relatively confident that the increase in intracellular Cs^+ level observed is mainly a result of changes in the Na^+/K^+ ATPase pump activity. Furthermore, the efflux of Cs^+ seen here could account for the reduced rate of Cs^+ uptake during the second hour in heart when no ouabain was added (figure 3.4). It is known that Cs^+ is a blocker of a number of K^+ channels, including the one responsible for pace-maker activity (74,75); therefore it is not surprising to see a 30% decrease in spontaneous heart rate and occasional arrhythmias in glc-Cs perfused hearts as compared to standard buffer perfused hearts. The coronary flow of the glc-Cs group measured by collecting the outflow from the heart was also the same as the standard buffer perfused hearts (data not shown) which suggests that cesium has little effects on the smooth muscles lining the vessels. Upon switching back to standard buffer perfusion, ie washout experiment, the heart rate returned to 87% of normal which illustrated the reversibility of the Cs^+ effect on heart rate. The energetics of the glc-Cs perfused hearts observed by ^{31}P NMR was also judged to be unaffected by Cs^+. The level of PCr, ATP and Pi was constant throughout the perfusion period and their changes during ischemia were also comparable to literature data (81,104,105).

In the functional ATP compartmentation study, we perfused hearts with glucose or pyruvate in combination with iodoacetate or cyanide to give either glycolytically or oxidatively generated ATP. The rate of Cs^+ uptake was then correlated to the sources of ATP to investigate the possible functional compartmentation of ATP. Our results show that the concentration of inhibitors used in this study (and others, see ref 61) was effective

enough to alter the energy metabolism of the hearts dramatically. Iodoacetate is a non-specific sulfhydryl group inhibitor that acts on glyceraldehyde-3-phosphate dehydrogenase to block glycolysis; cyanide is an inhibitor of the cytochrome-a complex to block oxidative phosphorylation. Even though iodoacetate is a non-specific inhibitor, studies have shown that it has no effect on Na^+/K^+ ATPase activity directly (106-108). Within minutes of perfusion with the inhibitors, substantial changes were seen in the cell content of PCr and Pi (figures 3.9, 3.10). In experiments with hearts that were designed to give only oxidatively derived ATP (eg, glc-IAc-Cs and pyr-IAc-Cs), a steady state level of PCr could not be maintained but Pi content was kept to a low amount. Endogeneous free fatty acids and exogeneous pyruvate, respectively, should have been able to maintain mitochondrial activity, however, this was not seen. Similar results had been observed with hearts perfused with deoxyglucose and acetate to inhibit glycolysis (109). Hoerter et al. suggested that the trapping of phosphate in the phosphomonoester form may have depleted the available Pi destined for PCr synthesis and thus caused a dramatic decrease in PCr level. Despite the rapid loss of PCr, the level of ATP was maintained near normal in the pyr-IAc-Cs group (figure 3.11). On the other hand, the glc-IAc-Cs group experienced large losses of ATP. The Cs^+ uptake rate was surprisingly high for the pyr-IAc-Cs group and is comparable to groups that had both functional glycolysis and oxidative phosphorylation (ie glc-Cs, glc-glu-Cs and pyr-Cs) (figure 3.6). This suggest to us that mitochondrially generated ATP is freely assessible to the Na^+/K^+ pump. No definite conclusion can be made concerning the Cs^+ uptake rate in glc-IAc-Cs group because of the difference in cellular ATP concentration. The glc-CN-Cs and pyr-CN-Cs groups, which do have functional glycolysis, metabolizing exogeneous glucose and endogeneous glycogen respectively, were able to maintain a steady, normal level of ATP throughout the perfusion period (figure 3.7) and about a third of normal amount of PCr (figure 3.10).

Large increases of Pi were observed during the cyanide-perfusion period. The Cs^+ uptake rate of these hearts were similar but low in comparison to the glc-Cs uptake rate. One possible explanation is that the increase in Pi content brings about an increase in ADP concentration because of the equilibrium conditions of the creatine kinase reaction. Since the Na^+/K^+ ATPase is inhibited by ADP and Pi (101-103), the rate of uptake in these hearts may be reduced as a result. Even though the ADP concentration was not measured in this study, Weiss et al. reported a doubling of ADP concentration in hearts after 10 minutes of hypoxic perfusion (61).

In this part of the study, we found that mitochondrially generated ATP is freely assessible to the Na^+/K^+ pump located in the plasma membrane of the rat heart. Various authors have also observed a close relationship between mitochondrial ATP and Na^+/K^+ pump activity. Graded manipulation of cellular ATP content by the use of mitochondrial inhibitors was seen to correlate directly with the uptake of K^+ or Rb^+ by intact cells (67-69). In contrast, Weiss et al. have reported that glycolytically generated ATP was more effective in preventing accumulation of extracellular K^+ than oxidatively generated ATP in isolated rabbit heart (61). However, the accumulation of K^+ seen by these authors probably reflected the flux of K^+ through the various K^+ channels and does not necessary contradict our data. Furthermore, our studies with the whole organ preparation is a reflection of the activity all the cell types in the heart and thus may be different from their septal preparation. Even though we did not find any support for the compartmentation of ATP supplied to the Na^+/K^+ pump, it is clear that both glycolysis and oxidative phosphorylation are required to maintain normal mechanical function (Table 3.1). In agreement with some in vitro studies, we found that Pi and ADP may possibly play an important role in the regulation of the Na^+/K^+ pump activity under the present conditions. In hearts that were perfused with cyanide to block oxidative phosphorylation (eg glc-CN-

Cs and pyr-CN-Cs), the low uptake rate is possibly a result of Pi and ADP accumulation. This secondary effect of cyanide intoxication may also explain the substantial loss of contractility in these hearts since Pi is known to reduce force generation in skinned ventricular muscle (110). Finally, we did not find any evidence for the compartmentation of Cs^+ in the rat heart under the present conditions. Only two Cs^+ peaks (intra- and extracellular cesium) were observed after 2 hours of perfusion which contrast with what had been observed in maize root where 3 Cs^+ peaks were seen (111), two representing intracellular compartments with different pH. Our results are also in agreement with Davis et al. who found that the intracellular Cs^+ signal relaxed with a single exponential time constant, again indicating accumulation of Cs^+ into one homogeneous compartment (76).

During ischemia, the uptake of Cs^+ was seen to stop almost immediately in all groups (figure 3.6). For example, in the glc-Cs group, the ATP content was still 75% of the normoxic level when the uptake stopped. Therefore, a shortage of ATP cannot be the cause of the lack of Cs^+ uptake during the first 15 minutes of ischemia. Changes in intracellular pH and Pi content are also unlikely to be the cause because some hearts exhibited only modest changes in pH (eg pyr-IAc-Cs and pyr-CN-Cs) and Pi level (eg pyr-IAc-Cs). This acute absence of pump activity upon ischemia is consistent with data reported by Malloy et al. who found significant increases in cellular Na^+ only a few minutes after the onset of ischemia in isolated rat hearts when the ATP level was still relatively unchanged (81). The exact cause of the inactivation is unknown but, similar results have been obtained in rat liver (82), but not in skeletal muscle (113). The effect of ischemia will be an acute collapse of the vascular and extracellular compartment of the heart. Therefore,the possibility that a depletion of Cs^+ in the extracellular medium upon ischemia may have led to the lack of Cs^+ uptake during ischemia in our experiments cannot be ruled out. Moreover, leakage of K^+ from the cells during ischemia would result in

increased vascular K^+, which can compete effectively with Cs^+ for uptake by the Na^+ pump. Although, extracellular Cs^+ was observed in the NMR spectra throughout the ischemic period, this was mainly in the medium surrounding the heart, from which it is unlikely that much uptake would take place. Tani et al have shown that low flow anoxia with normal buffer prevented Na^+ increase in the heart; in contrast, low flow anoxia with K^+-free buffer resulted in 5 times higher Na^+ content which was even higher than that seen in global ischemic hearts (78). These results suggested that a lack of K^+ in the extracellular medium can play a role in the lack of Cs^+ uptake. However, we would have expected to see a gradual decrease in uptake rate and not an abrupt stop if a depletion of substrate is the culprit. Thus other factors such as endogeneous inhibitor (111) and altered membrane structure (88,89) may play a role as well.

The ischemia induced cessation of the Na^+/K^+ pump activity was found to be reversible upon reperfusion only in the pyr-Cs perfused hearts under our experimental conditions (figure 3.6). The rate of Cs^+ uptake during the reperfusion period was about 80% of the pre-ischemic rate (Table 3.1). All other groups failed to recover pump function significantly or showed a loss of intracellular Cs^+ during reperfusion. The extent of pump function recovery during reperfusion is likely a function of the severity of the ischemic period and is therefore difficult to be compared to other studies; however, Daly et al. reported a 70% recovery of Na^+/K^+ ATPase activity after 60 minutes of ischemia (84). The acute nature of the pump function recovery seen here is supported by a study by Tani et al. who found that intermittent perfusion of the ischemic heart significantly reduced intracellular Na^+ accumulation during ischemia, whereas intermittent perfusion with K^+-free buffer (to prevent Na^+/K^+ pump activity) had little effect (79). It is interesting that the glc-Cs and glc-glu-Cs groups showed no or small pump function recovery (Table 3.1) even though their ATP and PCr content were similar to the pyr-Cs group. Therefore, it is

unlikely that the lack of recovery of pump activity is due to a lack of ATP, as the level of ATP in the pyruvate hearts is not much higher than the other two groups. Furthermore, the restoration of extracellular K^+/Cs^+ levels should have allowed resumption of pump activity if the pump were not damaged. Thus, these data are consistent with other reports that the Na^+/K^+ ATPase is damaged during prolonged ischemia (84-86), presumbly by oxygen radicals (87). The mechanical function recovery after 20 minutes of reperfusion was also poor in the glc-Cs and glc-glu-Cs groups in comparison to 50% in the pyr-Cs group. Since it is possible to dissociate Cs^+ uptake from cardiac functions as seen in the K^+-arrested hearts, we conclude that pyruvate may have a protective effect on the Na^+/K^+ pump during ischemia. It is known that perfusion with pyruvate has a protective effect against ischemic damage in hearts and various protective mechanisms have been proposed including higher phosphorylation potential and decreased Pi level (93,94). In this study, no obvious factor can be singled out to explain the protective effect of pyruvate. All parameters measured showed no difference between the glc-Cs and pyr-Cs groups except for intracellular pH. The glc-Cs group reached a pH 5.95 after 20 minutes of ischemia; whereas the pyr-Cs group reached pH 6.04 after 30 minutes. It is expected that the glc-Cs group would have a larger glycogen store then the pyr-Cs group just prior to ischemia because of the low pyruvate carboxylase activity, which is required for gluconeogenesis, in muscles (114). This difference in glycogen content may explain the pH difference. However, since the glc-glu-Cs group exhibited a similar pH profile as the pyr-Cs group, it is not likely that pH was the only factor that afforded protection. In view of the available data on the dependence of Na^+/K^+ pump activity on membrane fluidity and structure (88,89), it is attractive to propose a role played by pyruvate in the maintainence of membrane integrity, possibly through modification of fatty acid metabolism during ischemia. However, recent data have suggested that this also is unlikely. Suyatna et al.

reported that the lipid composition of the ischemic heart membrane was very similar to normal membrane even though the former had only 70% of control Na^+/K^+ ATPase activity (115).

The fact that the glc-Cs group did not recover any Na^+/K^+ ATPase activity during reperfusion even though ATP was present suggests that the degree of damage suffered by the enzyme is dependent on factors other than a depletion of high energy phosphate (ATP, PCr) and/or an accumulation of inorganic phosphate. The acute nature of the inactivation and recovery of pump function as seen in the pyr-Cs group suggests that membrane fluidity may be involved but other factors like availability of extracellular Cs^+ and endogeneous inhibitor cannot be ruled out.

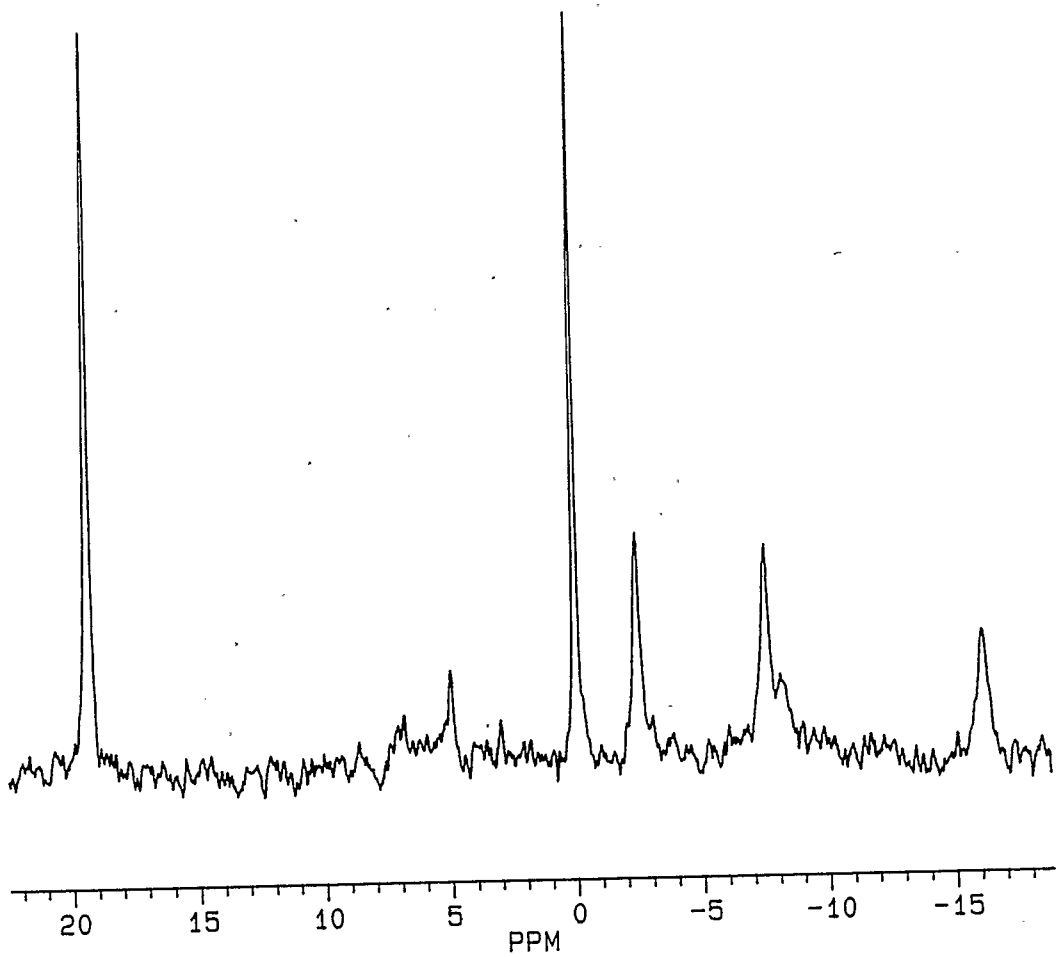

Figure 3.1: Typical fully relaxed ^{31}P NMR spectrum of rat heart perfused with the standard buffer. Peaks assignment are (from left to right): MDP at 19.2 ppm, phosphomonoesters at 6.5 ppm, Pi at 5.0 ppm, PCr at 0 ppm, γ-ATP at -4 ppm, α-ATP at -9 ppm and β-ATP at -16 ppm.

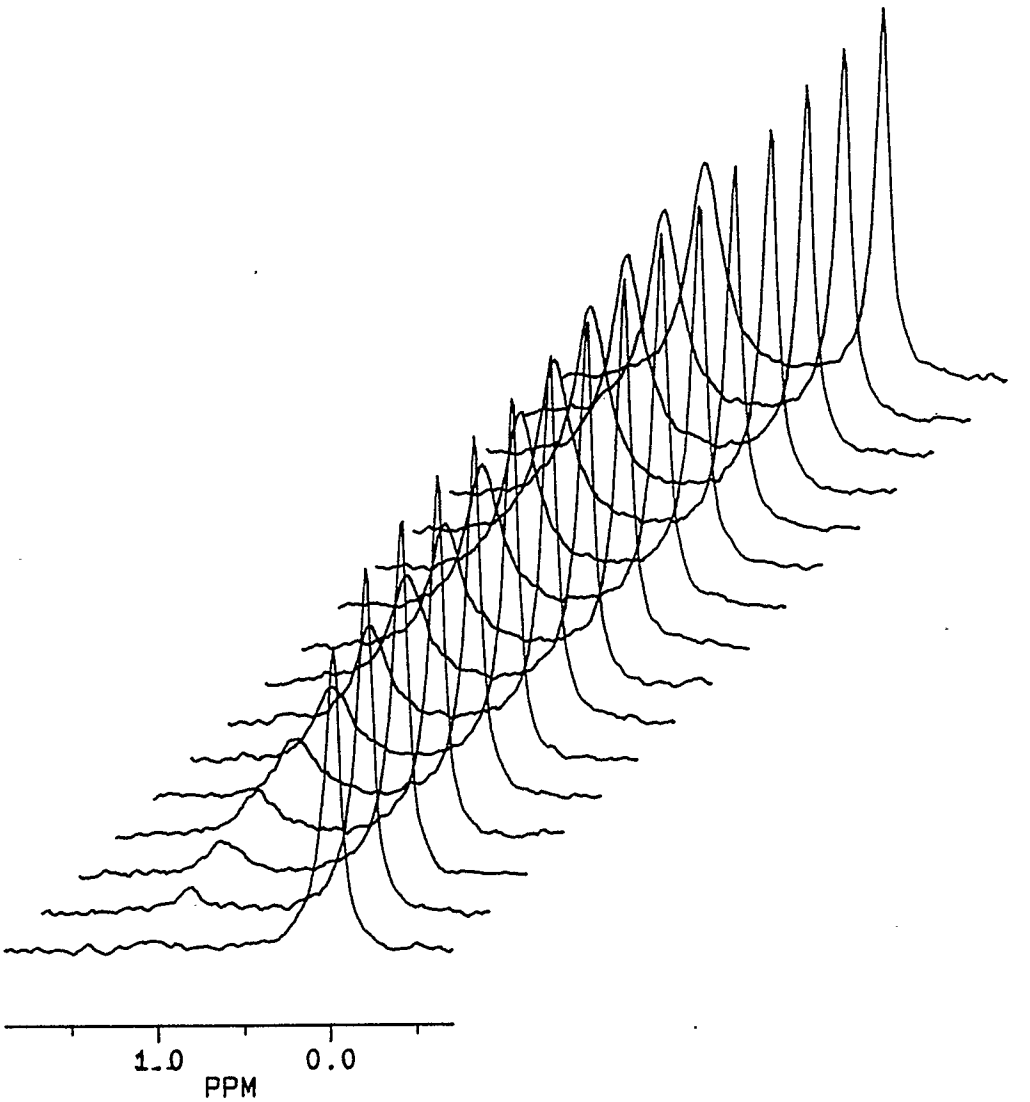

Figure 3.2: Typical ^{133}Cs NMR spectra of Cs^+ uptake in glc-Cs perfused heart. The peak on the left which increases with time is intracellular Cs^+ and the extracellular peak is assigned a chemical shift of 0 ppm.

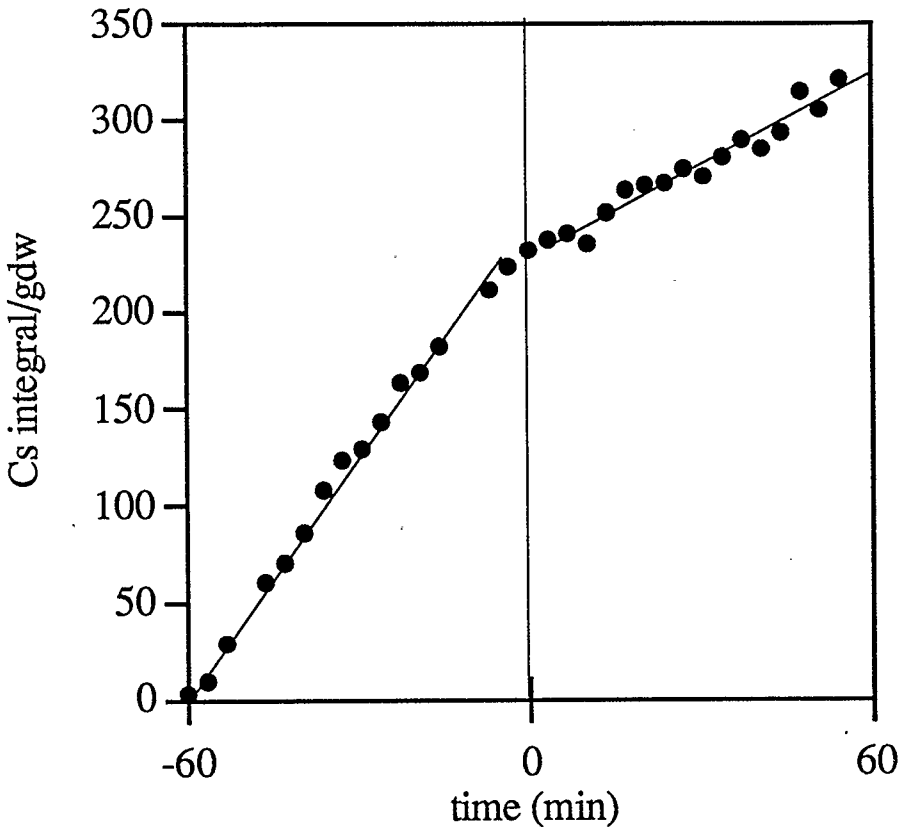

Figure 3.3: Effect of ouabain-perfusion on Cs^+ uptake. The heart was perfused with pyr-Cs buffer for one hour (-60 to 0 min) to allow Cs^+ uptake. The perfusate was then switched to a pyr-Cs buffer containing a certain concentration of ouabain (60 uM in this case) for one additional hour. Ouabain sensitive uptake is defined as the difference between the rate of total uptake and the rate of ouabain insensitive uptake.

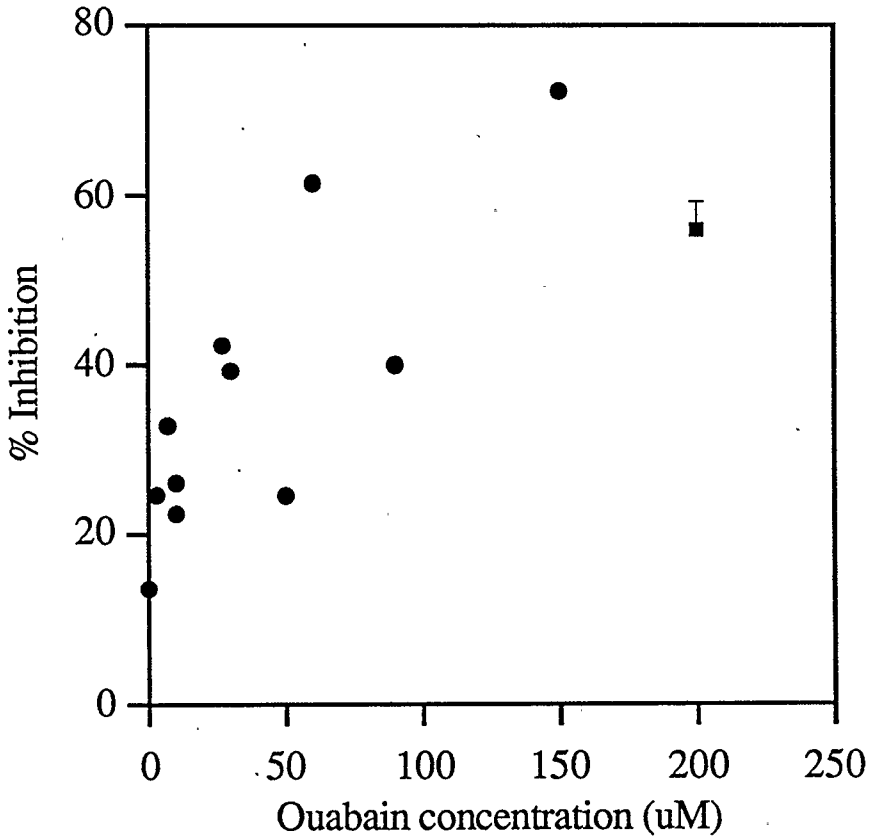

Figure 3.4: Dose-respone curve of the ouabain inhibition on Cs^+ uptake in rat heart. Experiment was performed with hearts perfused with the pyr-Cs buffer (●). Each data point represents one experiment. The effect of perfusion with 200 uM ouabain on Cs^+ uptake in K^+-arrested hearts is also shown (■) (n=4, mean±SE).

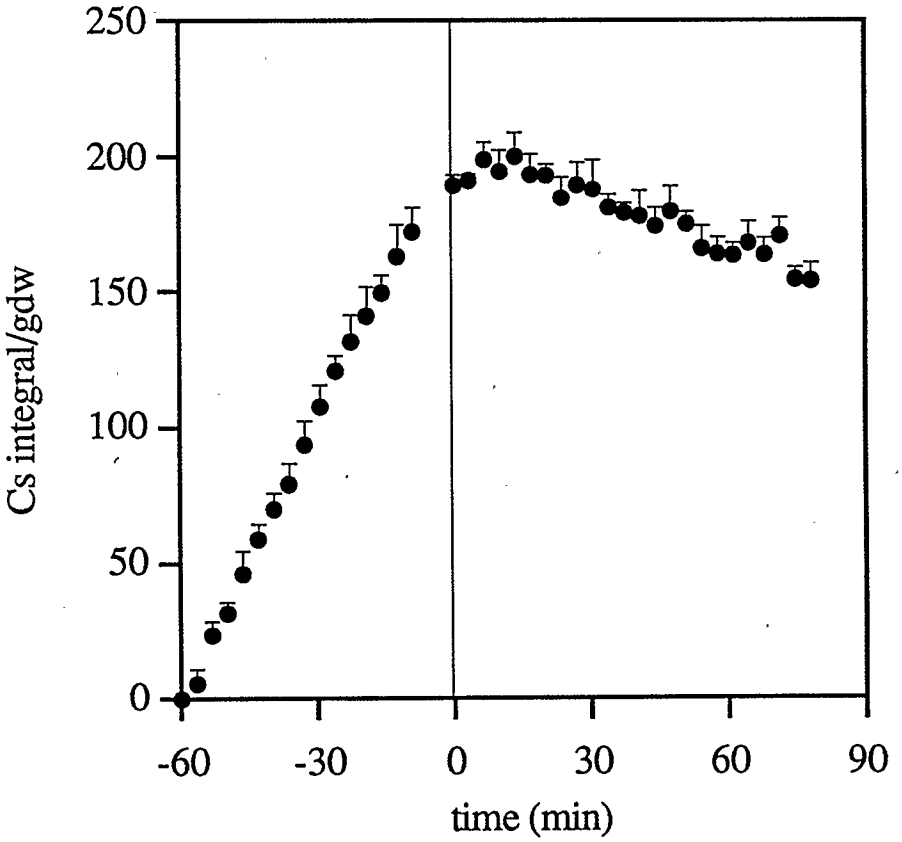

Figure 3.5: Washout of intracellular Cs^+ from perfused rat heart. Initial Cs^+ uptake was accomplished by perfusion with the glc-Cs buffer for one hour. Washout commenced at time=0 by switching the perfusate back to the standard buffer (n=3, mean±SE).

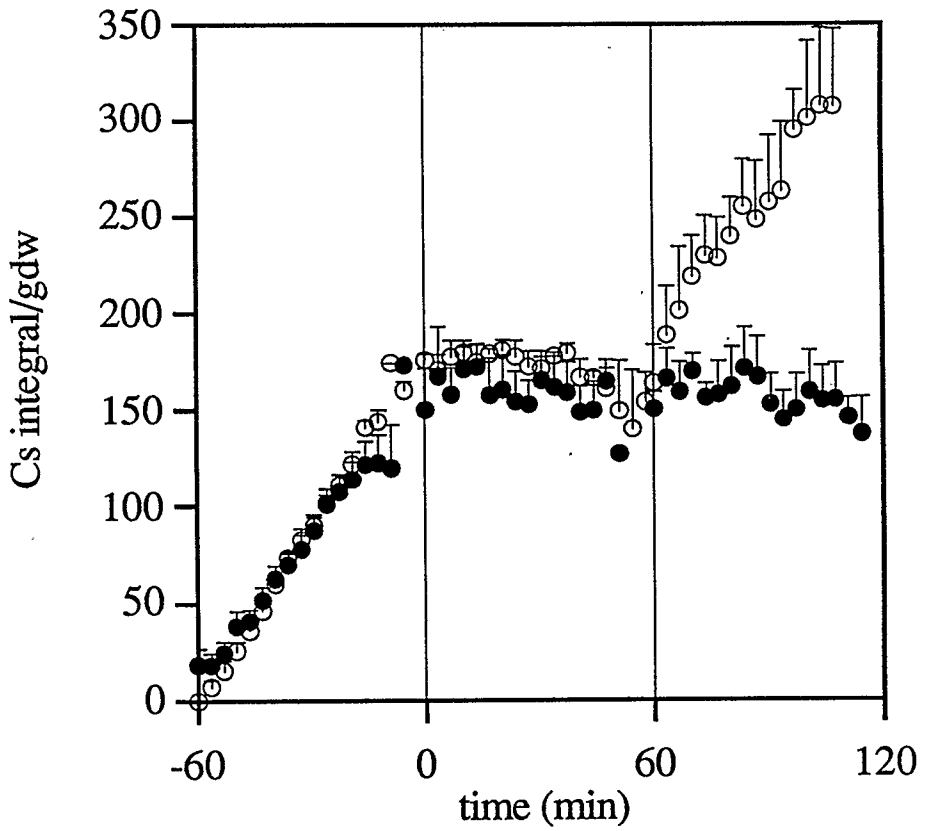

Figure 3.6a: Profile of the changes in cellular Cs^+ content in hearts during periods of perfusion (time -60 to 0), ischemia (time 0 to 60) and reperfusion (time 60 to 120). The glc-Cs (●) and pyr-Cs (○) groups are shown separately to demonstrate the clear difference during reperfusion (n=3).

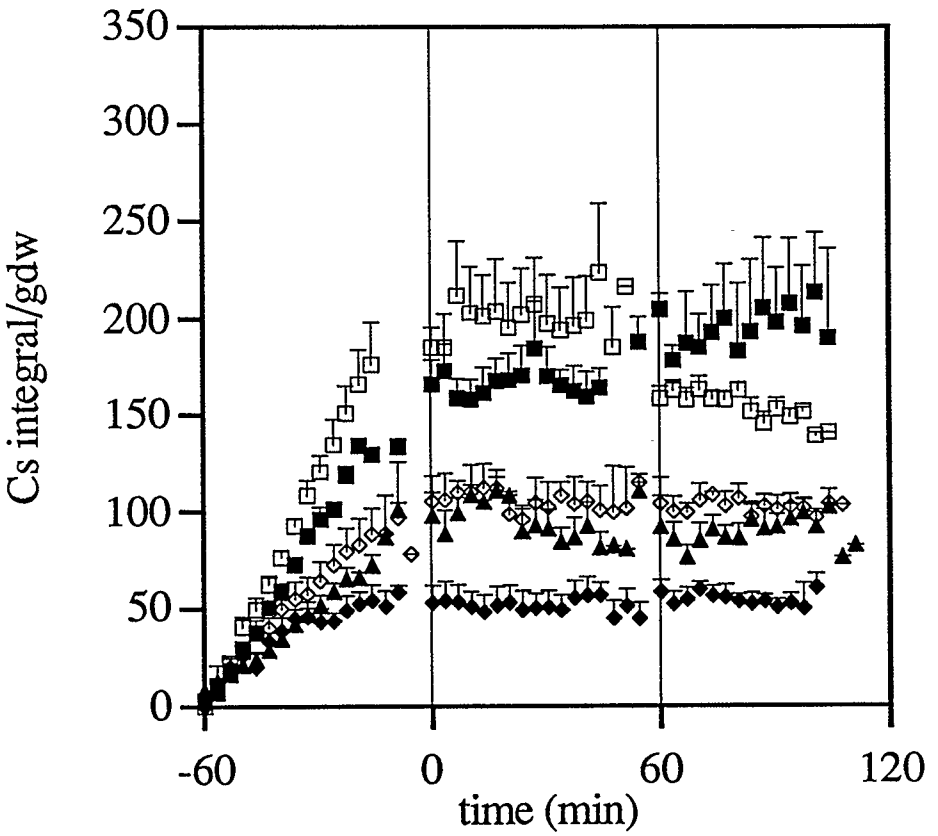

Figure 3.6b: Profile of the changes in cellular Cs^+ content in hearts during periods of perfusion (time -60 to 0), ischemia (time 0 to 60) and reperfusion (time 60 to 120). The glc-glu-Cs (■), glc-IAc-Cs (◆), glc-CN-Cs (▲), pyr-IAc-Cs (□) and pyr-CN-Cs (◇) groups are shown (n=3).

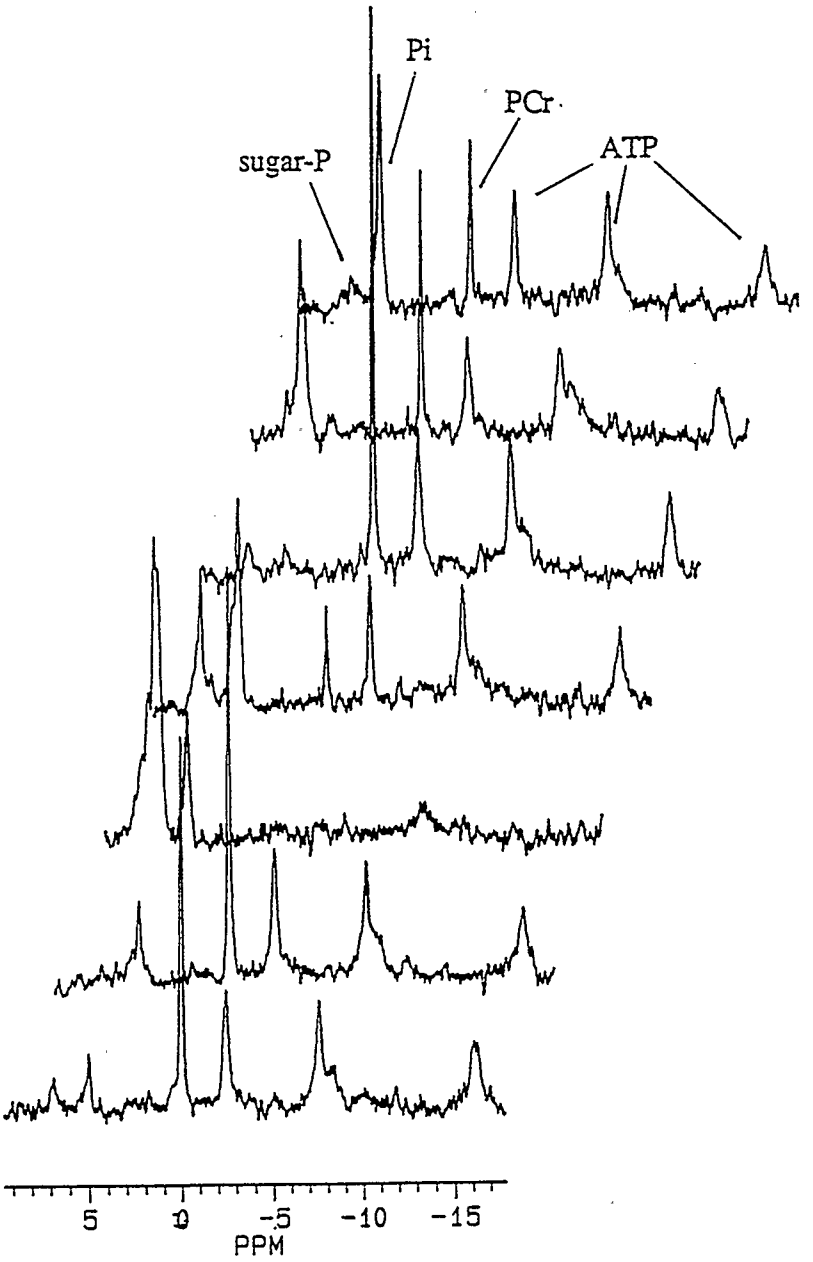

Figure 3.7a: Typical non-fully relaxed ^{31}P NMR spectra of hearts perfused with Cs^+-containing buffer for 1 hour. From botton to top: A) glc-Cs, B) glc-glu-Cs, C) glc-IAc-Cs, D) glc-CN-Cs, E) pyr-Cs, F) pyr-IAc-Cs and G) pyr-CN-Cs. The peaks assignment are indicated in the figure.

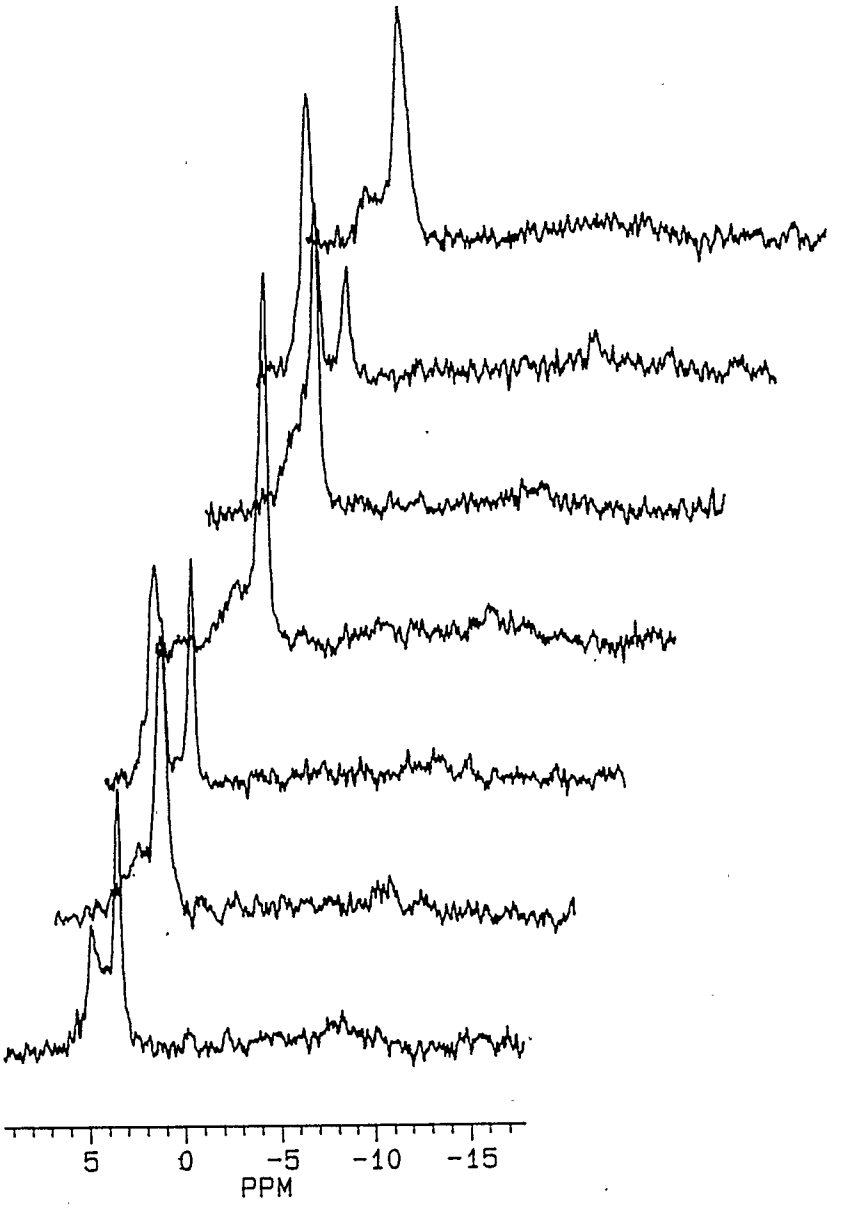

Figure 3.7b: Typical non-fully relaxed ^{31}P NMR spectra of hearts after 60 minutes of no flow ischemia. From botton to top: glc-Cs, glc-glu-Cs, glc-IAc-Cs, glc-CN-Cs, pyr-Cs, pyr-IAc-Cs and pyr-CN-Cs. For peaks assignment see figure 7a.

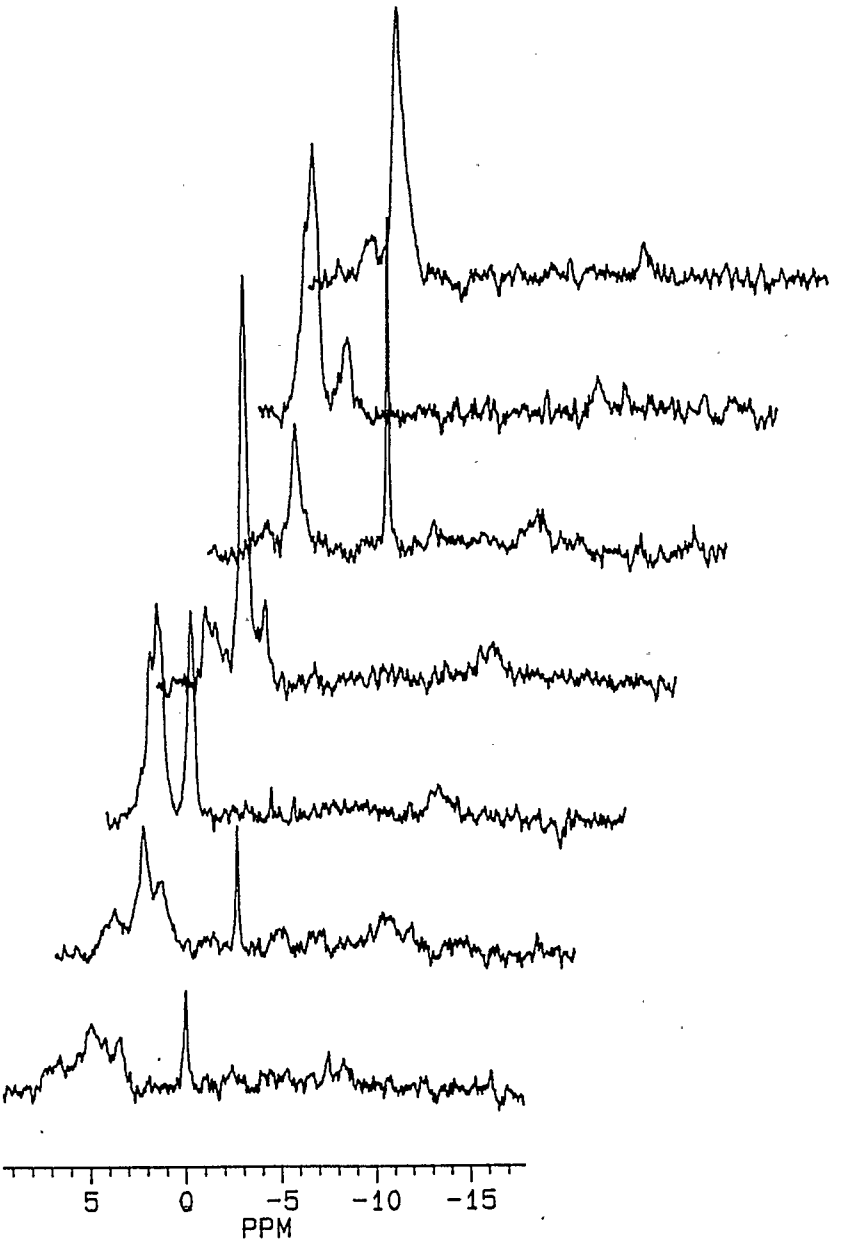

Figure 3.7c: Typical non-fully relaxed ^{31}P NMR spectra of hearts after 20 minutes of reperfusion. From botton to top: glc-Cs, glc-glu-Cs, glc-IAc-Cs, glc-CN-Cs, pyr-Cs, pyr-IAc-Cs and pyr-CN-Cs. For peaks assignment see figure 7a.

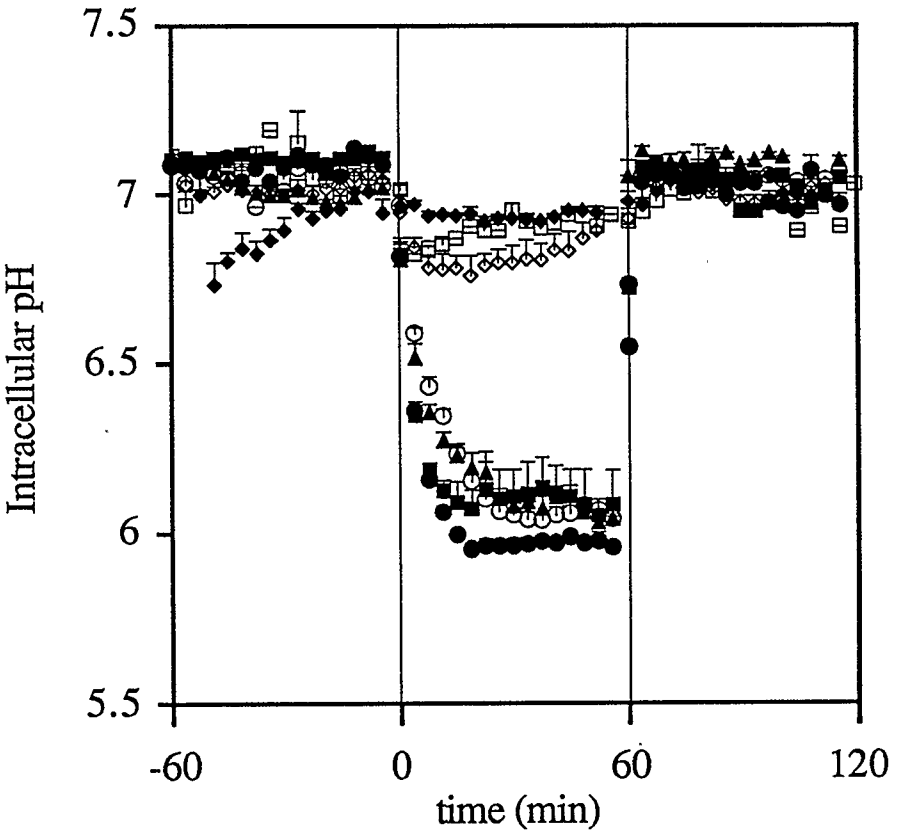

Figure 3.8: Profile of the changes in intracellular pH of hearts during periods of perfusion (time -60 to 0), ischemia (time 0 to 60) and reperfusion (time 60 to 120). The symbols are: glc-Cs (●), glc-glu-Cs (■), glc-IAc-Cs (◆), glc-CN-Cs (▲), pyr-Cs (○), pyr-IAc-Cs (□) and pyr-CN-Cs (◇) (n=3).

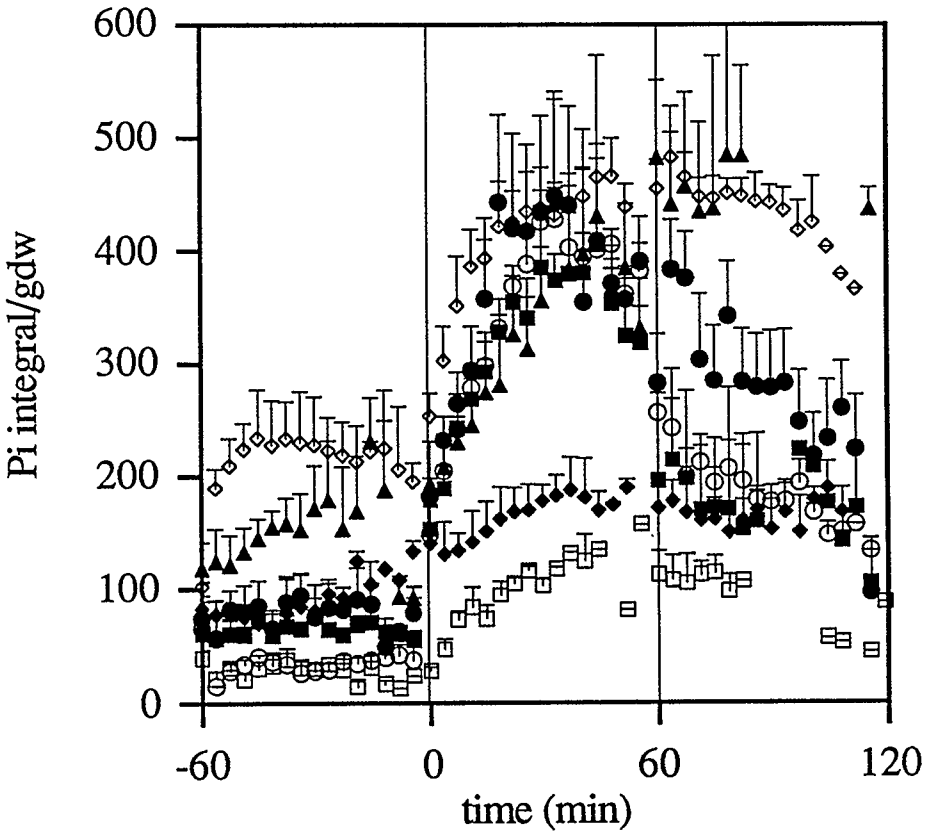

Figure 3.9: Profile of the changes in cellular Pi content in hearts during periods of perfusion (time -60 to 0), ischemia (time 0 to 60) and reperfusion (time 60 to 120). The symbols are: glc-Cs (●), glc-glu-Cs (■), glc-IAc-Cs (◆), glc-CN-Cs (▲), pyr-Cs (○), pyr-IAc-Cs (□) and pyr-CN-Cs (◇) (n=3).

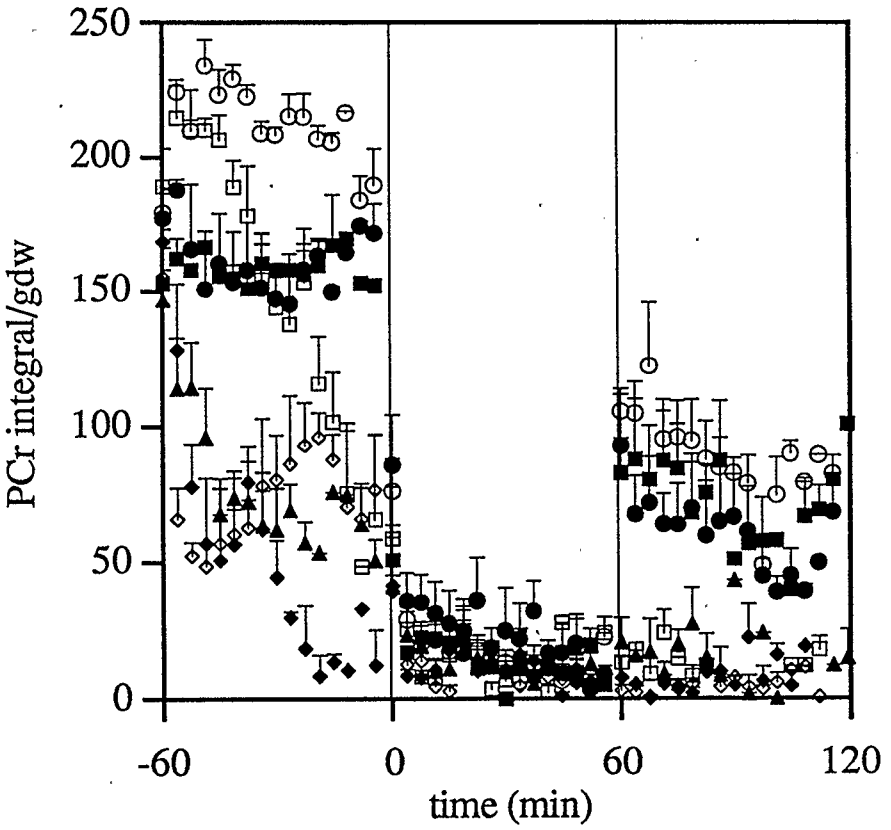

Figure 3.10: Profile of the changes in cellular PCr content in hearts during periods of perfusion (time -60 to 0), ischemia (time 0 to 60) and reperfusion (time 60 to 120). The symbols are: glc-Cs (●), glc-glu-Cs (■), glc-IAc-Cs (◆), glc-CN-Cs (▲), pyr-Cs (○), pyr-IAc-Cs (□) and pyr-CN-Cs (◇) (n=3).

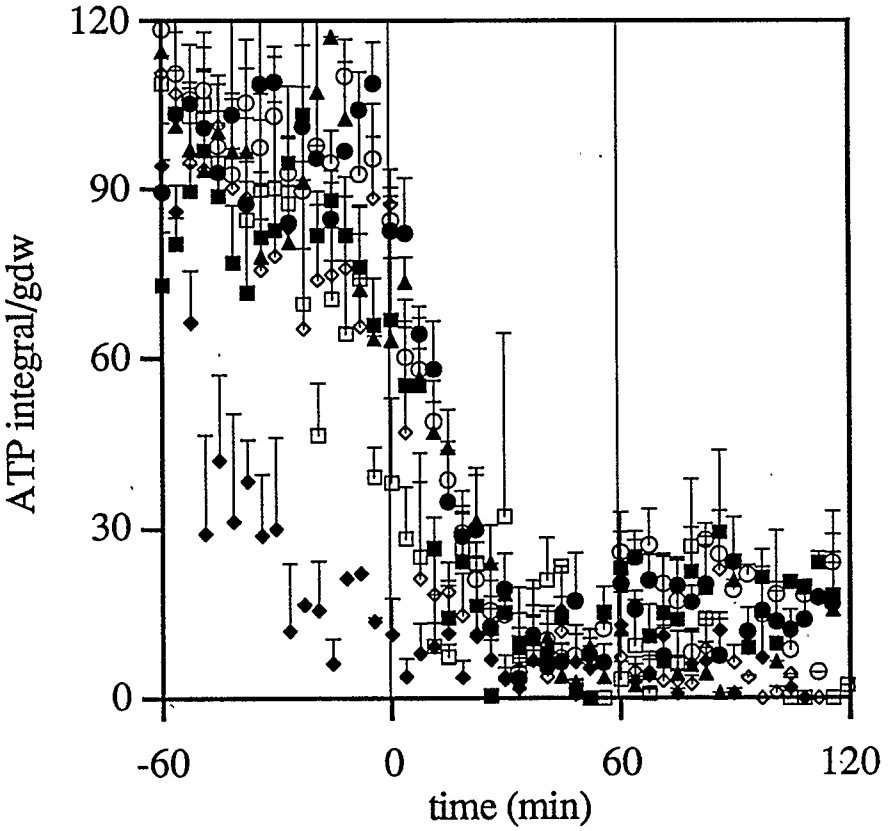

Figure 3.11: Profile of the changes in cellular ATP content in hearts during periods of perfusion (time -60 to 0), ischemia (time 0 to 60) and reperfusion (time 60 to 120). The symbols are: glc-Cs (●), glc-glu-Cs (■), glc-IAc-Cs (◆), glc-CN-Cs (▲), pyr-Cs (○), pyr-IAc-Cs (□) and pyr-CN-Cs (◇) (n=3).

Table 3.1: Summary of heart function and Cs^+ uptake rate during perfusion, ischemia and reperfusion.

Medium	RPP 1[a]	Perfusion[b]	Ischemia[c]	Reperfusion[d]	% functional Recovery[e]
glc-Cs	24,621±890	2.34(0.99)	-0.45(0.61)	-0.41(0.66)	0.67±0.30
glc-glu-Cs	23,955±1400	2.96(0.99)	0.08(0.14)	0.49(0.64)	0.83±0.83
glc-IAc-Cs	0.00	0.97(0.95)	-0.07(0.21)	-0.08(0.29)	-
glc-CN-Cs	2,108±628	1.67(0.99)	-0.49(0.70)	0.13(0.26)	0
pyr-Cs	16,746±2333	3.26(0.99)	-0.38(0.66)	2.67(0.98)	50.0±14
pyr-IAc-Cs	6,127±1620	3.61(0.98)	0.12(0.18)	-0.52(0.86)	0
pyr-CN-Cs	1,548±190	1.65(0.97)	-0.06(0.21)	-0.03(0.15)	0

a. Rate pressure product (mm Hg/min) of hearts after 60 min of perfusion with a Cs^+-containing medium (n=6).

b. Cs^+ uptake rate (au/gdw/min) during the perfusion period (n=3). Number in bracket is the correlation coefficient of the fitted line.

c. Cs^+ uptake rate (au/gdw/min) during the ischemic period (n=3). Number in bracket is the correlation coefficient of the fitted line.

d. Cs^+ uptake rate (au/gdw/min) during the reperfusion period (n=3). Number in bracket is the correlation coefficient of the fitted line.

e. Calculated as the ratio between the RPP after 20 min of reperfusion and RPP 1 above.

Chapter 4

^{31}P and ^{133}Cs NMR studies of Cyclosporin-A treated rat hearts

Introduction:

The immunosuppressive agent Cyclosporine (CsA) has become the drug of choice for the prevention of acute rejection in recipients of solid organ or bone marrow transplants. Despite its beneficial immunosuppressive applications, it has a number of toxic side effects, such as nephrotoxicity, hepatotoxicity and hyperkalemia. Recent evidence also suggest that Cyclosporine may be cardiotoxic (116,117). It has been reported that hearts from CsA treated rats developed 20% lower ventricular pressure than controls at any given preload in vitro (118,119). Papillary muscles and trabeculae prepared from CsA-treated animals showed increased contractile force at low extracellular calcium concentrations while high extracellular calcium concentrations produced decreased force development, suggesting either increased calcium sensitivity or increased intracellular calcium concentration secondary to the use of CsA, as has been shown in isolated cell preparations from various organs, including isolated cardiomyocytes (120-125). Moreover, myocardial calcification and fibrosis associated with elevated tissue calcium has been observed in CsA treated mice (126,127) and tissue magnesium levels in muscle, liver and kidney of CsA treated rats were found to be significantly higher than that in controls (128).

Based on ^{31}P nuclear magnetic resonance study of allogeneic rat heart transplants in recipients treated with CsA, Suzuki et al. concluded that CsA has cardiotoxic side-effects (129). These authors reported abnormally high levels of inorganic phosphate in beating heart transplants in animals that had received CsA. Impaired high-energy phosphate

metabolism may lead to decreased cardiac function and abnormal calcium cycling. Alternatively, impairment of the Na^+/K^+ pump activity may increase intracellular calcium.

In this study, we have investigated CsA treated rat hearts by ^{31}P and ^{133}Cs NMR. This approach should allow us to decide on the possible mechanism(s) that contribute to the observed reduction in ventricular pressure in CsA treated hearts. The intracellular content of inorganic phosphate (Pi), phosphocreatine (PCr), and ATP, as well as the intracellular pH and free magnesium level at various workloads can be studied by ^{31}P NMR. The uptake of Cs^+, an analogue of K^+, by the hearts was studied by ^{133}Cs NMR to assess the activity of the Na^+/K^+ pump (130).

Methods and Materials:

Heart perfusion. Male (LEW x BN) F1 rats were injected subcutaneously with 15mg/kg of CsA dissolved in cremophor EL daily for 3 weeks. Shortly before the NMR experiment, the heart was excised from ether anesthetized rats (control and CsA-treated: body weight =220±15g) and perfused in a Langendorff mode with modified Krebs Henseleit phosphate-free buffer at a perfusion pressure of 100 cm water. The buffer was bubbled with 95% O_2/5% CO_2 and contained (in mM): 120.0 NaCl, 5.0 KCl, 10.0 glucose, 19.0 $NaHCO_3$, 1.5 $CaCl_2$, 1.2 $MgCl_2$ and 1.2 Na_2SO_4. A latex balloon containing a solution with a known concentration of methylenediphosphonate (MDP) was inserted into the left ventricle. This allowed continuous direct measurements of the ventricular function and also provided an NMR concentration standard. After a 20 min equilibration period, the content of high-energy phosphate metabolites in the heart was measured by collecting two fully relaxed ^{31}P NMR spectra -one before and one after a known amount of MDP had been added to the latex balloon. In the second part of the protocol, the mechanical output of the hearts was increased by increasing the preload or diastolic pressure (P_{dia}) by 5 mm Hg increments from 0 to 15 mmHg by adjusting the volume of the balloon. A non-fully relaxed ^{31}P spectrum was collected after each pressure change was introduced and the coronary flow was estimated from the effluent of the heart. Upon completion, the study was repeated once starting at 0 mmHg. In the final part of the protocol, the perfusion buffer was switched to one containing (in mM): 2.9 CsCl, 2.9 KCl, 115.1 NaCl, 2.3 $CaCl_2$, 1.2 $MgSO_4$, 25.0 $NaHCO_3$ and 11.0 glucose to commence the cesium uptake study. The uptake of Cs^+ was monitored continuously by ^{133}Cs NMR for one hour. One final ^{31}P spectrum was collected after the cesium study to ascertain that the

heart was still healthy. In separate studies using K^+-arrested hearts the perfusate contained (in mM): 10 CsCl, 19 KCl, 92 NaCl, 2.3 $CaCl_2$, 1.2 $MgSO_4$, 25.0 $NaHCO_3$ and 11.0 glucose. All hearts were maintained at 37°C throughout the experiment.

NMR Spectroscopy. All NMR experiments were carried out with a widebore Bruker AM 400 spectrometer equipped with a 9.4 T superconducting magnet using a 20 mm broadband probe. The perfused hearts were placed in a 20mm tube and inserted into the magnet with the temperature set to 37°C. Fully relaxed ^{31}P (161 MHz) spectra were collected using 8K data points and composite pulse proton decoupling (2W) during acquistion only. The time between individual pulses was 17.5 seconds, the number of scans was 96 and 90° pulses were used. Non-fully relaxed spectra were collected with bi-level decoupling (2W during acquisition, 0.5W otherwise), a cycling time of 3.5 seconds, 128 scans and a pulse angle of 75°. All chemical shifts were referenced with respect to phosphocreatine which was assigned a shift of 0 ppm. The intracellular pH and the free magnesium concentration were measured from the chemical shifts of the inorganic phosphate and β-peak of ATP respectively using appropriate calibration curves (131). ^{133}Cs (52 MHz) spectra were collected with a cycling time of 6.5 seconds, 32 scans and a pulse angle of 70°. ^{31}P and ^{133}Cs spectra were Fourier transformed with a line-broadening of 15 Hz and 2 Hz respectively and baseline-corrected manually before integration. Peak integrals were quantitated using standard Bruker integration software.

Statistics. All results are reported as mean±SEM. The two tailed student's t test was used to determine if any differences between treated and control groups were significant.

Results:

Typical fully-relaxed ^{31}P NMR spectra of control and CsA treated hearts are shown in figures 4.1a,b. The rate pressure product (RPP), which is the product of the heart rate and developed pressure, was $3.4\pm0.2\times10^4$ mmHg·min^{-1} for the controls (n=5) and $3.0\pm0.3\times10^4$ mmHg·min^{-1} for the CsA treated (n=7) group. The RPP was maintained in this range for the remainder of the study in both groups. There was no difference in the size of the hearts: the dry weight of the hearts was 0.2±0.01g for the control(n=5) as well as for the treated hearts (n=7). The content of high-energy phosphate metabolites in the CsA treated hearts was very similar to that of the controls (Table 4.1). The intracellular concentration of sugar-monophosphates, inorganic phosphate and phosphocreatine were not significantly different between the two groups and are in good agreement with reported values (132,133). However, a relatively large difference ($0.1>p>0.05$) between the two groups was observed in the ATP content with that in CsA treated hearts about 20% lower. The resulting PCr/Pi and PCr/ATP ratios were 2.91 and 1.36 for the controls and 2.45 and 1.59 for the CsA treated group, respectively.

In the second part of the study, we confirmed the previous observation that the systolic pressure of the CsA treated hearts was consistently lower than that of the controls at all the levels of preload or diastolic pressure (P_{dia}) tested (figure 4.2). The difference was much greater at 0 mmHg P_{dia} than at the higher ones. The heart rate and coronary flow were similar and remained constant throughout this part of the study for both groups (Table 4.2a). Typical ^{31}P NMR spectra of the hearts at various diastolic pressures are shown in figure 4.3a,b. No obvious difference was seen in the spectra. From the chemical shift of inorganic phosphate, the intracellular pH of CsA treated hearts was found

to be 0.02 unit more basic than controls (Table 4.2b). The intracellular free magnesium concentration, estimated from the β-ATP chemical shift, was also comparable. Our observed shift is in good agreement with what other authors have reported and corresponds to a free magnesium concentration of 0.6 mM (134,135). The PCr/ATP and the PCr/Pi ratios at various workloads are shown in Table 4.2b. As expected, the ratios remained relatively constant despite the changes in mechanical output in both groups. This suggested that energy production and consumption are in good balance and that the metabolic pathways are functioning normally. It should be noted that we did not correct these numbers for any peak saturation and/or NOE effects inherent under the conditions we ran this part of the NMR experiment. In these experiments we were mainly interested in finding whether the ratios changed in relation to the various workloads. More quantitative determinations would have required excessively long NMR acquisition times (concentrations, are however listed in Table 4.1). The MDP integral which is proportional to the volume of the standard in the balloon in the heart was found to increase linearly with the diastolic pressure (figure 4.4). The integrals did not differ significantly between the two groups and confirmed previous findings that the left ventricular volumes were comparable in both groups (119).

The accumulation of cesium was found to increase linearly with time (figure 4.5) and the slopes of uptake (3.43±0.25 au/gdw/min for the controls (n=3); 3.05±0.21 au/gdw/min for the treated group (n=5)) were virtually the same for both groups (figure 4.6). Near the end of the one hour period, only a slight difference in the cesium integral was seen between the CsA treated and the control group. Although the heart weights were similar between the groups, the average heart rate was about 20% higher in the control group during the cesium perfusion period and may explain the observed difference. When we K^+-arrested the heart by perfusing with a modified KH buffer that contained 19mM

KCl and 10mM CsCl, the rate of uptake was virtually identical. The rates were 1.31±0.16 au/gdw/min (n=3) and 1.42±0.03 au/gdw/min (n=3) for the controls and treated hearts respectively (figure 4.7).

Discussion:

Our data confirm that CsA treatment at a dose of 15 mg/kg/day sc. for 3 weeks caused decreased left ventricular systolic pressure development for any given preload tested. This functional impairment, as compared to controls, is found to be greater at 0 mmHg P_{dia} than at the higher pressures. One possible explanation is that since the systolic pressure was measured about 7 minutes (time required for a ^{31}P spectrum) after the P_{dia} was first adjusted, the hearts might have relaxed somewhat at that time. This practice was done to both groups. The impairment was not associated with detectable differences in high energy phosphate metabolism since the concentration of various phosphoryl metabolites was not significantly different between the treated and control groups except for the ATP content (Table 4.1). A 20 % lower ATP content was found in the CsA treated hearts; however, this difference is probably biologically insignificant since the Km of actomyosin for ATP is in the micromolar range (136). The Pi level is comparable in both groups and is consistent with reported values in high mechanical output Langendorff-perfused hearts (137). We did not observe any abnormality in the level of inorganic phosphate in the treated hearts as described by others (129). Suzuki et al attributed the changes in Pi of the transplanted heart to CsA cardiotoxicity because these hearts continued to beat despite discontinuation of CsA therapy. We feel that the high amount of Pi reported by these authors reflected changes in the heart brought about by graft rejection which is known to give rise to elevate intracellular Pi (140). In addition, overlap of the Pi resonance in the cardiac spectrum with the 2,3-diphosphoglycerate signal of blood could complicate the earlier measurements. Based on our experiments in which rejection did not play a role, we believe that the reported increase in Pi does not reflect cardiotoxicity of CsA treatment.

The PCr/ATP and PCr/Pi ratios remained constant throughout the changes in mechanical output in both groups (Table 4.2b). The coupling between production and utilization of high energy phosphates are therefore judged to be normal in all cases. A statistical significant difference in intracellular pH was observed. The treated hearts were found to be 0.02 pH unit more basic than the controls. Although this difference is statistically significant, it is probably too small to have any biological effects. Moreover, since protons are known to have an inhibitory effect on Ca^{2+} binding by the contractile proteins, a higher pH in the treated group would give rise to a higher calcium sensitivity and therefore greater force production; however, this is in contrast to what we observed. Measurement of the β-ATP chemical shift indicated that the free magnesium concentration was comparable in both groups. We should stress that even though we did not see a difference in free magnesium, it is possible that due to compartmentation we are only observing the cytosolic fraction and therefore our results do not necessarily contradict the total tissue concentration data. However it is unlikely that the functional impairment in the treated hearts is due to the elevated free magnesium concentration.

For a variety of reasons (see also earlier chapters), we chose to use cesium instead of rubidium as a potassium analogue to study the Na^+/K^+ pump activity. One reason is that cesium blocks most of the potassium channels found on the excitable cell membrane. Various authors have also shown that the uptake of cesium is inhibitable by ouabain which infers that the main uptake mechanism is through the Na^+/K^+ pump (130, see also chapter 3). Therefore, we can be confident that the accumulation of this ion in the cells is mainly due to the action of the Na^+/K^+ pump and that leakage through the channels is minimal. We have done washout experiments which showed that after a 75 minute period, the intracelluar cesium integral decreased only ~ 20% (see chapter 3). From an NMR point of view, cesium is a good choice because it does not require a shift reagent to separate the

intra- and extracellular signal (138); in addition cesium-133 NMR has excellent sensitivity and is characterized by narrow lines. It should be noted that in spite of these advantages, cesium is a non-physiological cation and that it caused the heart rate to decrease to about 50% of the pre-cesium level. However, when proper control conditions are maintained, much useful information can be obtained.

The cesium uptake studies suggest that CsA treatment does not impair the Na^+/K^+ pump since virtually identical uptakes rates were found in both groups (figure 4.6). This suggests that the intracellular sodium concentration is also comparable since cellular level of Na^+ is believed to be the main regulator of the Na^+/K^+ pump activity (139). In the K^+-arrested hearts, the functional-independent Cs^+ uptake rate was found to be the same for the controls and the CsA treated group. This substantiates our conclusion that CsA treated hearts have normal Na^+/K^+ pump functioning.

In this study, we have considered a number of possible causes of the functional impairment in the CsA treated hearts. Our data suggest that the changes in CsA treated hearts are not caused by changes in intracellular phosphoryl metabolites level, pH, free Mg^{2+} or malfunctioning of the Na^+/K^+ ATPase. Consequently alternative explanations for the functional impairment have to be considered as more likely. Recent studies suggest that abnormalities in the functioning of the sacroplasmic reticulum may arise from CsA treatment (141). Spontaneous calcium release from the SR could keep the heart in a high tonus state and this would affect systolic pressure development.

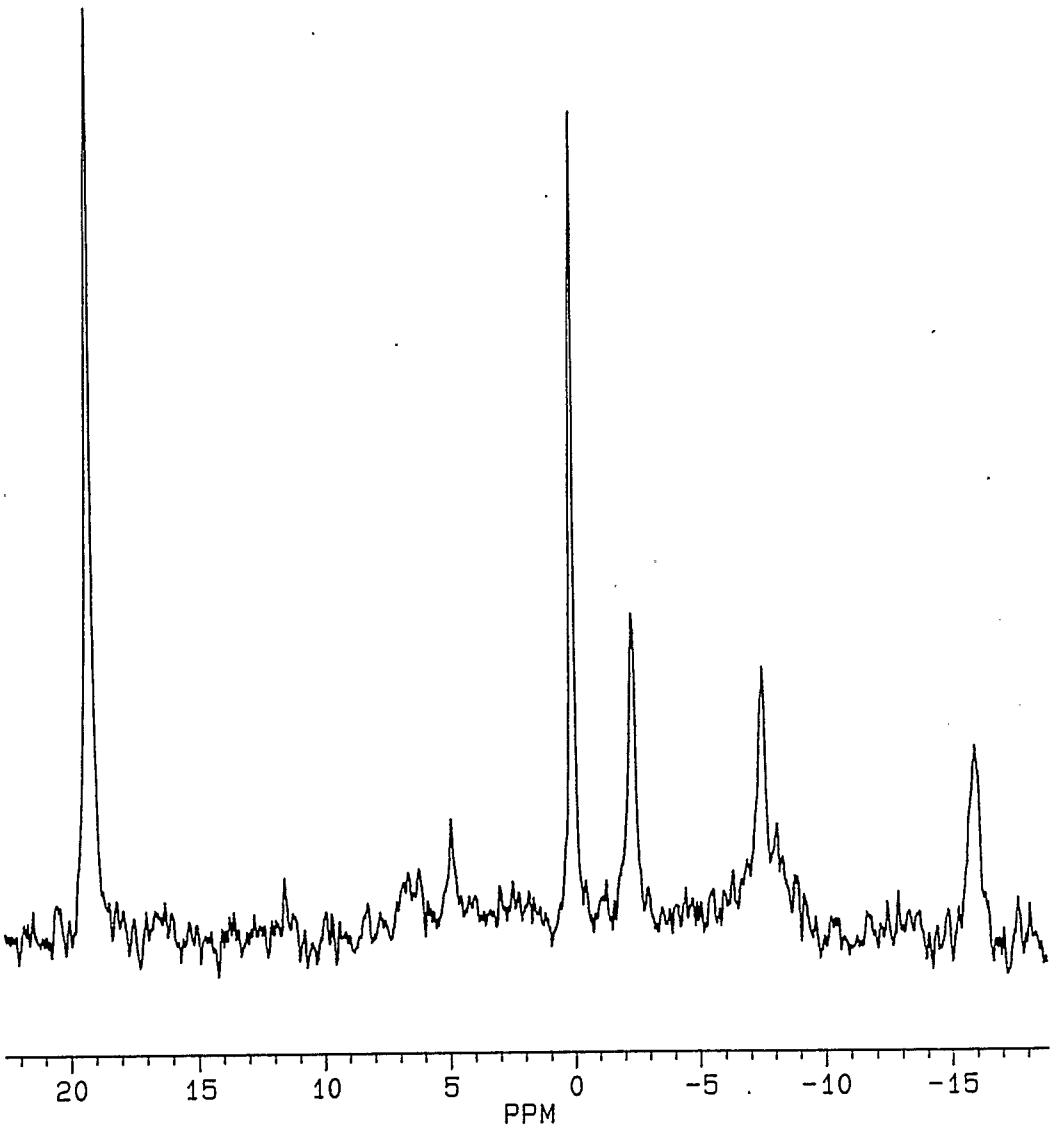

Figure 4.1a: Representative fully relaxed ^{31}P spectrum of the control heart. The peaks are: MDP at 19.2 ppm, phosphomonoesters at 6.5 ppm, Pi at 5 ppm, PCr at 0 ppm, γ-ATP at -3 ppm, α-ATP at -8 ppm, and β-ATP at -16 ppm.

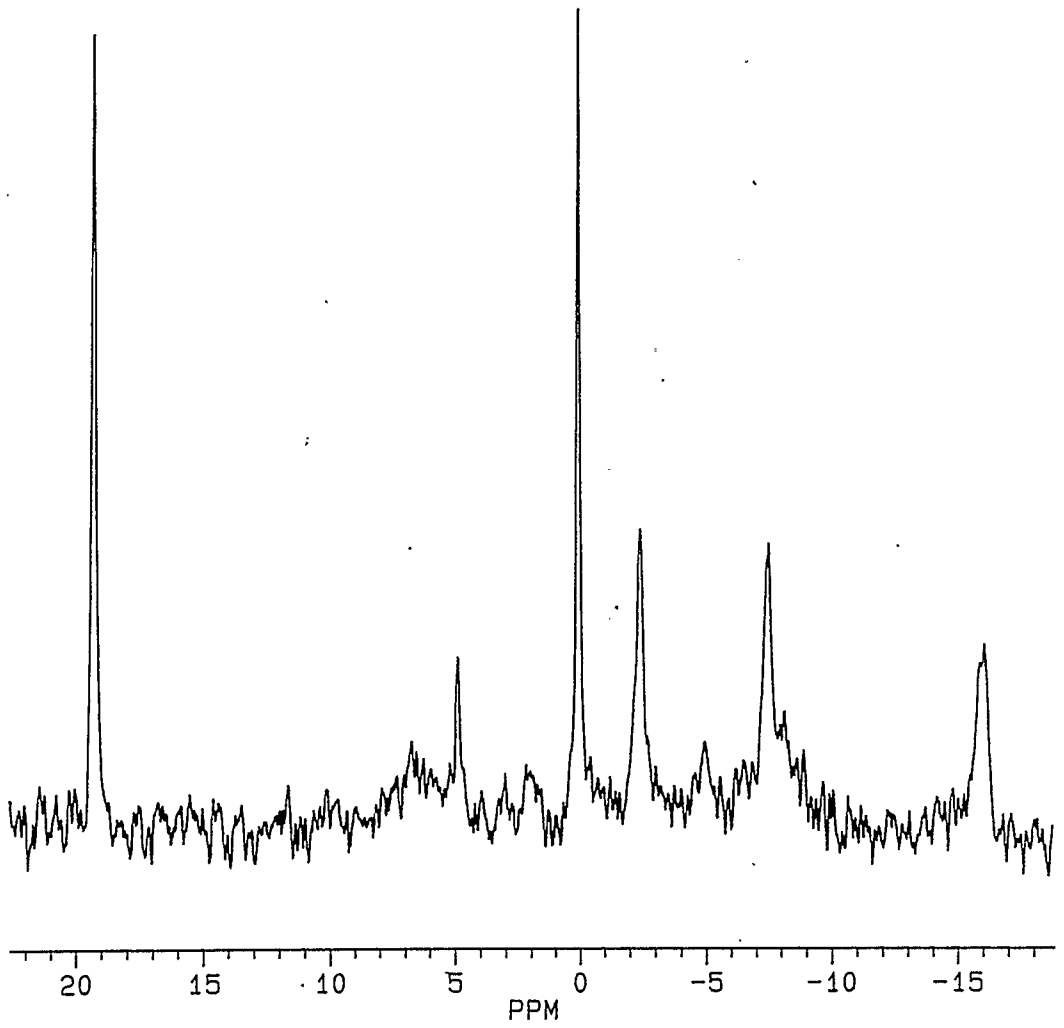

Figure 4.1b: Representative fully relaxed ^{31}P spectrum of CsA treated rat heart. See figure 1a for peak assignments.

Table 4.1: Concentration of phosphorylated metabolites in hearts determined by ^{31}P NMR (umol/gdw, mean±SE).

	Control (n=5)	CsA (n=7)
Sugar-p	7.9±0.59	8.1±1.1
Pi	9.4±1.7	10.6±2.1
PCr	27.4±1.7	26.0±1.6
ATP	20.2±1.9	16.3±1.0*

* $0.05 < p < 0.1$

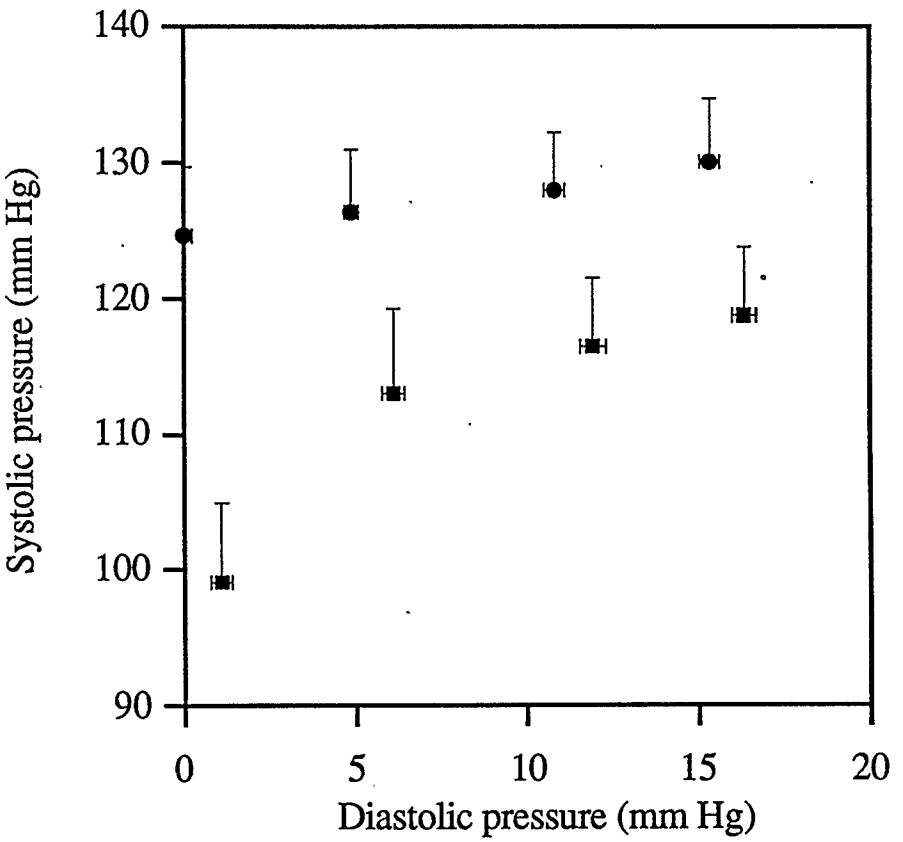

Figure 4.2: Left ventricular systolic pressure of control (●, n=20)and CsA treated (■, n=16) hearts at various diastolic pressures.

Table 4.2a: Functional data of control and CsA treated heart at various preloads.

Diastolic Pressure(mmHg)	0	5	10	15
Control (n=20)				
Systolic(mmHg)	124.6±5.1	126.3±4.7	127.9±4.3	130.0±4.7
Coronary flow (ml/min)	11.1±0.56	10.7±0.55	10.45±0.45	10.6±0.53
Heart rate (bpm)	269±6	272±7	267±7	272±8
CsA (n=16)				
Systolic(mmHg)	99.0±5.9*	113.0±6.2#	116.5±5.0#	118.7±5.0#
Coronary flow (ml/min)	10.3±0.51	10.8±0.49	10.6±0.50	10.6±0.49
Heart rate (bpm)	290±5	289±5	289±5	287±5

(* $p < 0.05$ compared to controls; # $p < 0.1$ compared to controls)

Table 4.2b: ^{31}P NMR data of control and CsA treated heart at various preloads.

Diastolic Pressure(mmHg)	0	5	10	15
Control (n=20)				
pH	7.00±0.004	7.00±0.003	7.00±0.003	7.01±0.004
β-ATP shift(ppm)	-16.02±0.01	-16.03±0.01	-16.03±0.01	-16.02±0.01
PCr/ATP	1.60±0.10	1.47±0.09	1.51±0.05	1.44±0.07
PCr/Pi	1.79±0.14	1.80±0.11	1.76±0.12	1.81±0.13
CsA (n=16)				
pH	7.02±0.004*	7.03±0.006*	7.02±0.005*	7.03±0.006*
β-ATP shift(ppm)	-16.02±0.01	-16.01±0.01	-16.03±0.01	-16.03±0.01
PCr/ATP	1.35±0.06	1.30±0.05	1.36±0.08	1.30±0.05
PCr/Pi	1.69±0.14	1.65±0.11	1.64±0.11	1.63±0.09

(* $p < 0.05$ compared to controls; # $p<0.1$ compared to controls)

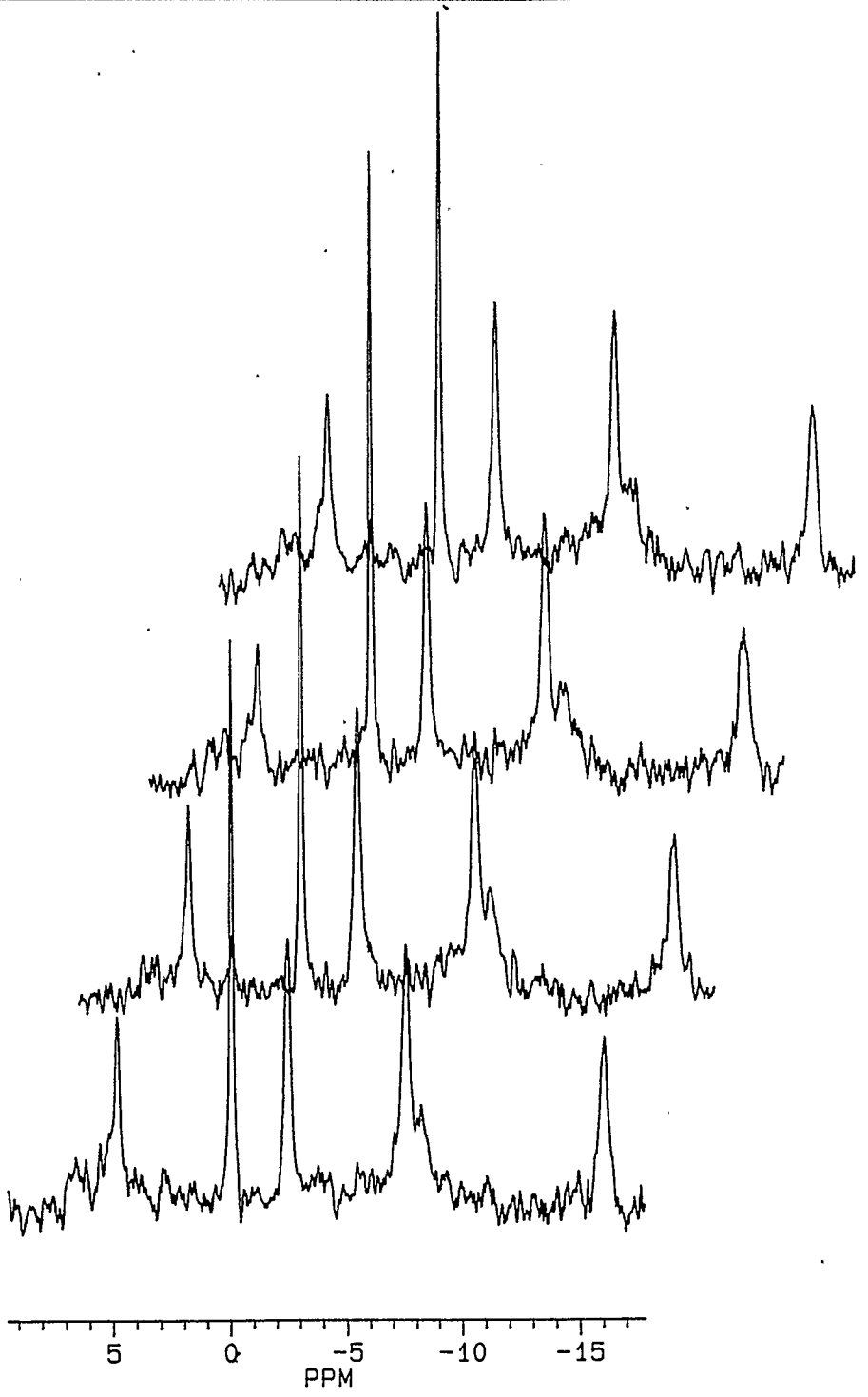

Figure 4.3a: Representative non-fully relaxed ^{31}P NMR spectra of control hearts at various diastolic pressures. See figure 1 for peaks assignment. From bottom to top, the spectra represent 0, 5, 10 and 15 mmHg diastolic pressure.

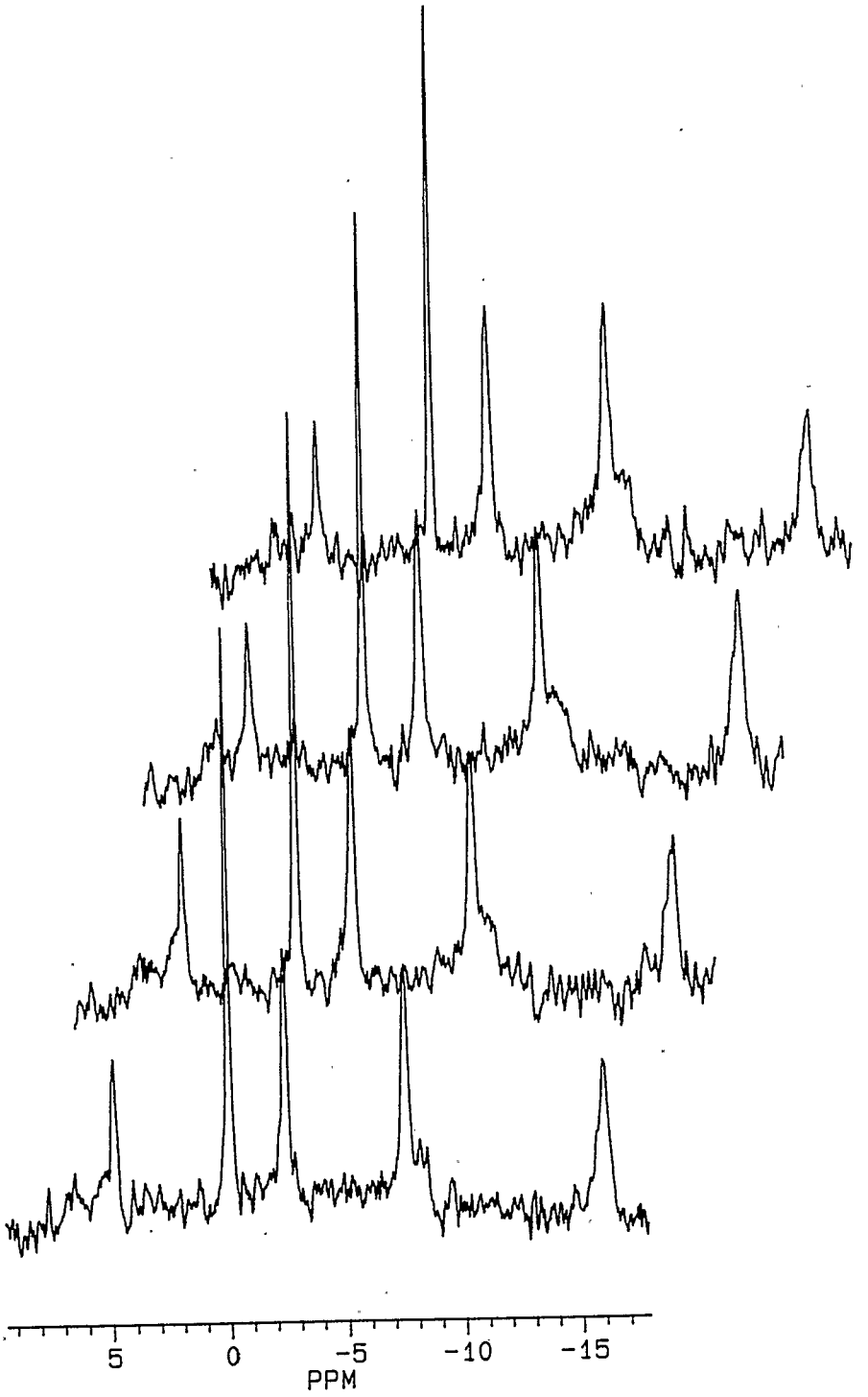

Figure 4.3b: Representative non-fully relaxed ^{31}P NMR spectra of CsA treated hearts at various diastolic pressures. From bottom to top, the spectra represent 0, 5, 10 and 15 mmHg diastolic pressure.

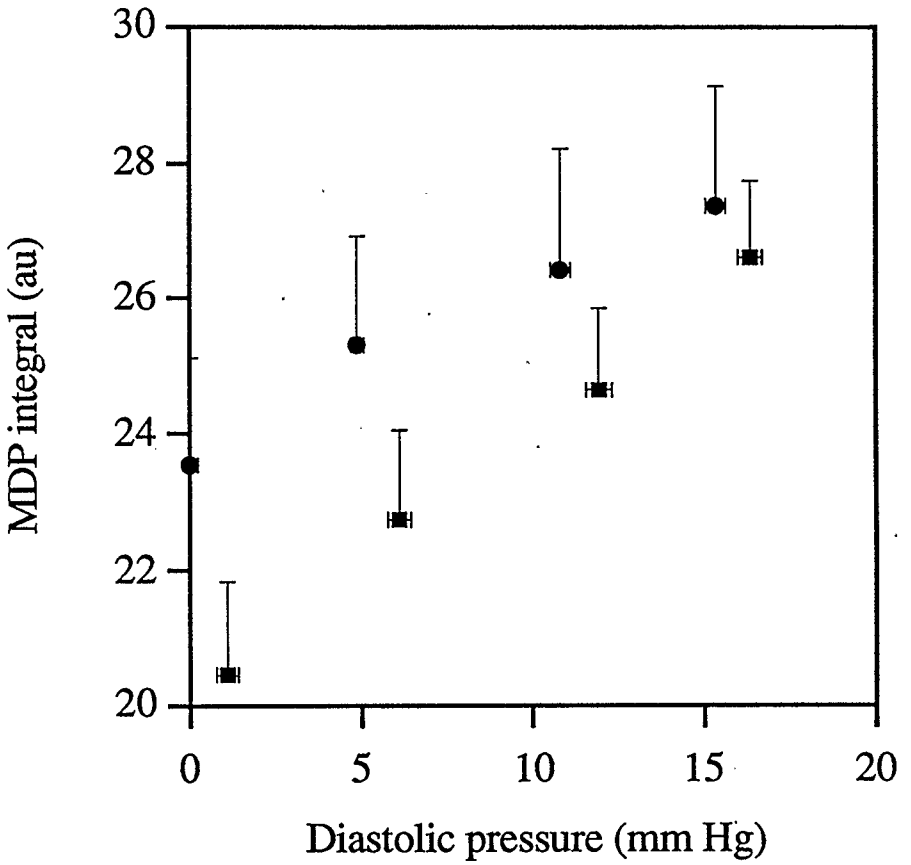

Figure 4.4: MDP integral changes resulting from adjustment of the diastolic pressure of control (●, n=20) and CsA treated hearts (■, n=16).

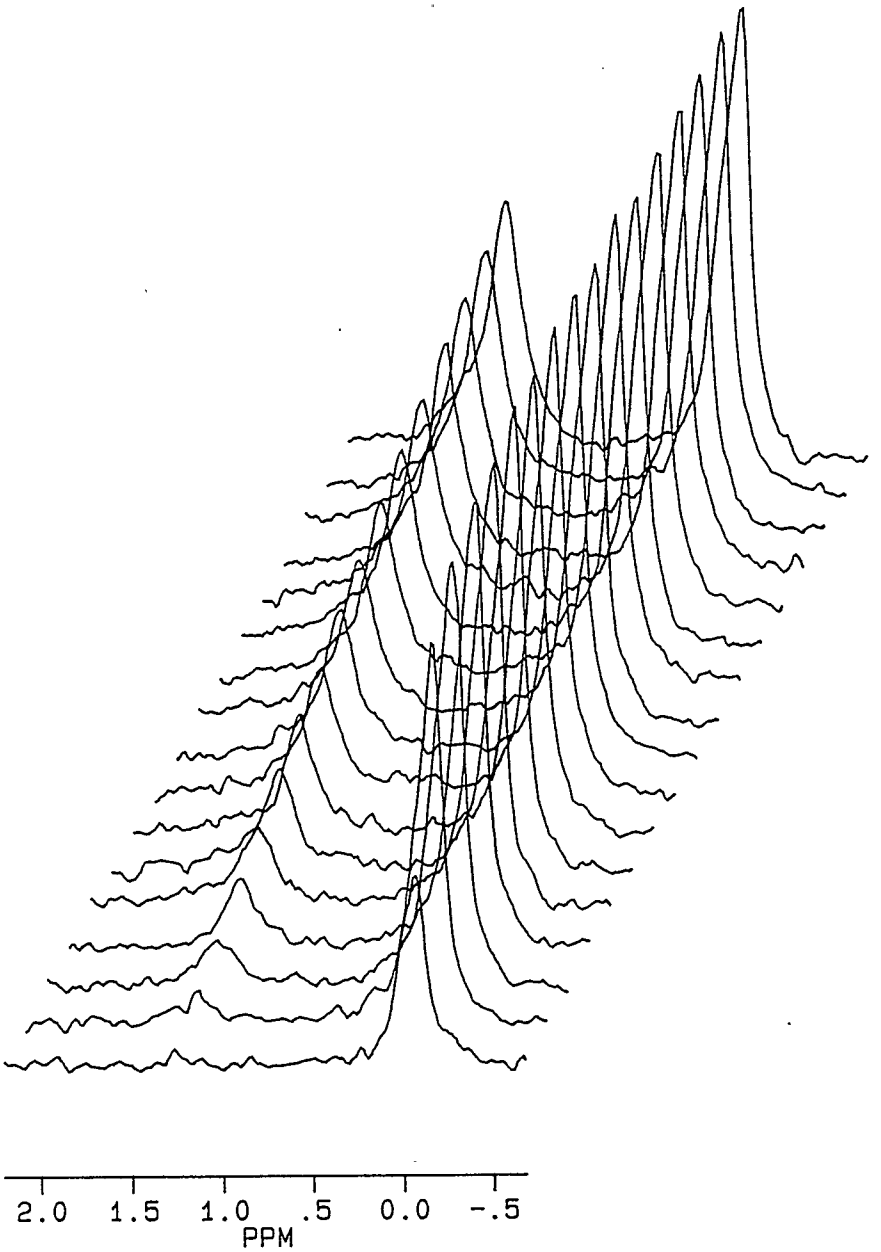

Figure 4.5: Representative ^{133}Cs NMR spectra of Cs^+ uptake by heart. Extracellular and intracellular cesium are assigned as 0 and 1 ppm respectively.

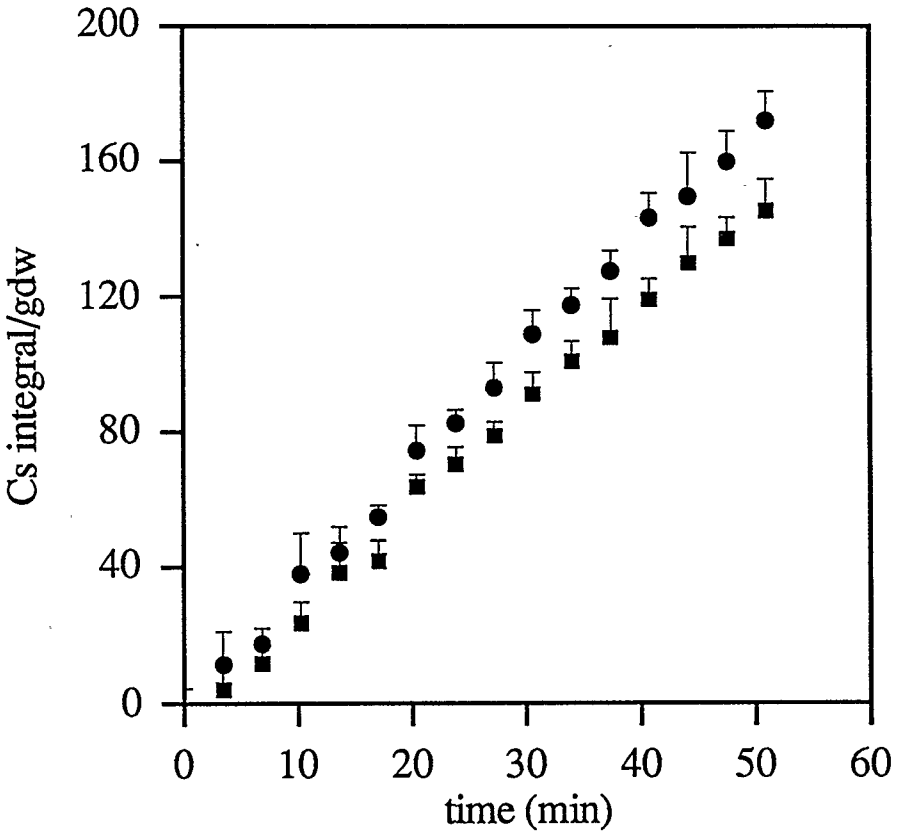

Figure 4.6: Intracellular cesium integrals of control (●, n=3) and CsA treated (■, n=5) hearts with respect to time.

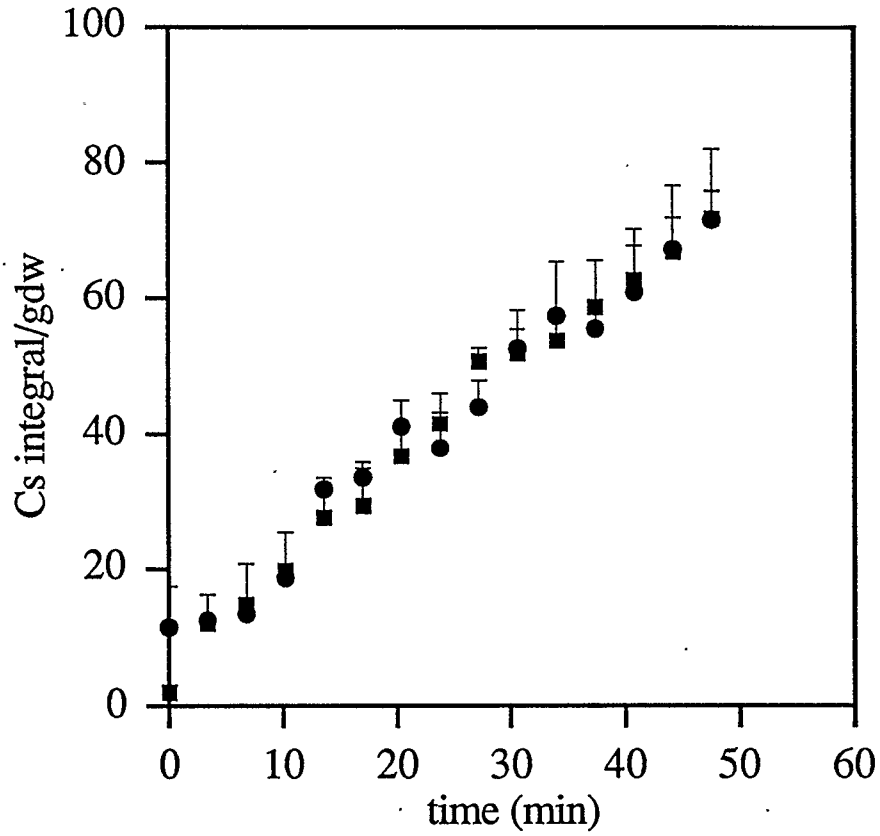

Figure 4.7: Intracellular cesium integrals of K^+-arrested control (●, n=3) and CsA treated (■, n=3) hearts with respect to time.

Chapter 5

Conclusions and suggestions for future work

Conclusions and suggestions for future work

In chapter 1, we have shown that the study of cation metabolism in red blood cells can be achieved through the use of shift reagents. However, because of the inherent difference in the sensitivity of the various cations for shift reagents, optimal conditions for this type of studies needed to be identified through systematic characterization of the shift reagents. In chapter 2, we titrated the various member of the alkali metal family with a number of commonly used shift reagents. A number of nuclei turned out to be suitable for our purpose but for one reason or another they were not optimal. For example, ^{86}Rb is a commonly used K^+-analogue and possesses high NMR-sensitivity but because of its large natural linewidth, quantitative studies would be difficult with this nucleus. ^{41}K is another nucleus that can be used but because of its high cost and low NMR-sensitivity, it proved to be an impractical nucleus. $NH4^+$ equilibrated across the membrane making it less useful. The most attractive nucleus for our type of studies turned out to be ^{133}Cs NMR. The cesium-133 nucleus has high NMR-senstivity, small natural linewidth but most importantly, it does not require the use of a potentially toxic shift reagent to separate intra- and extracellular signals because of its sensitivity to its chemical environment. Consequently, we have used ^{133}Cs-NMR to observe the uptake of Cs^+ by the rat heart. Our results demonstrated that Cs^+ can be used as a K^+-analogue to study the activity of the Na^+/K^+ pump. Furthermore, because NMR is non-invasive, this type of study could be carried out in the intact cell. The uptake of Cs^+ was found to be inhibitable by the cardiac glycoside, ouabain, in a dose-dependent manner. We found that at 150 uM ouabain, the uptake of Cs^+ was inhibited by about 60 % while the cellular energy metabolism was

normal. This showed that the uptake of Cs^+ by the rat heart was mainly carried out by the Na^+/K^+ ATPase. In the washout experiments, the accumulated Cs^+ decreased by only 20 % after 75 minutes; therefore, we can be relatively confident that the observed changes in the intracellular Cs^+ was mainly a reflection of changes in the Na^+/K^+ pump activity.

In the study of the possible functional compartmentation of ATP, our results gave no support to the hypothesis which suggested that glycolytically generated ATP is functionally coupled to membrane functions whereas oxidatively generated ATP is preferentially used by the contractile proteins (142). The uptake rates of Cs^+ by hearts that were designed to give only glycolytically generated ATP (ie glc-CN-Cs and pyr-CN-Cs groups) were lower than that of heart designed to give only oxidatively generated ATP (ie pyr-IAc-Cs group). The low uptake rates in the former group can be due to the inhibition of the Na^+/K^+ pump by the large amount of inorganic phosphate generated as a secondary effect of cyanide poisoning. Likewise, the mechanical function of the hearts cannot be compared directly because of the effects of Pi on the contractile process (143). The uptake rate of Cs^+ in the pyr-IAc-Cs group was in fact higher than that of all the other groups including the ones with both functional glycolysis and oxidative phosphorylation. The reason for this is unclear, but may involve the lower Pi level in the pyr-IAc-Cs group. Although published studies have shown that the non-specific inhibitor iodoacetate has no direct effects on the Na^+/K^+ ATPase activity, it may be worthwhile to repeat the study using deoxy-glucose to specifically block glycolysis and at the same time regulate the Pi level (144). In order to make the present study more quantitative, the visibility of Cs^+ in the various groups will need to be determined since it is well known that the visibility of quadrupolar nuclei can vary in living tissues (145). The easiest way to accomplish this would be to extract the heart at the end of the experiment and determine the Cs^+ content chemically. Alternatively, one can load up the heart with Cs^+ by perfusing with a Cs^+-

containing buffer followed by washing away the extracellular cesium; one can then observe changes in the intra- and extracellular Cs^+ signal by ^{133}Cs NMR as the cell membrane is made leaky by addition of valinomycin.

Upon ischemia, the uptake of Cs^+ was seen to stop immediately in all groups tested. Clearly, there was no correlation with the intracellular ATP level during ischemia. Likewise when pumping activity resumed in the pyruvate hearts, there was a high Pi and a very low NMR-detectable ATP level which was not significantly different from that in the other groups. These data make it unlikely that the ATP level regulated the pump activity. Likewise, high Pi levels do not seem to stop the pump. Consequently, we believe that the inhibition of the Na^+/K^+ pump is due to factors such as changes in membrane fluidity and production of endogeneous inhibitors brought on by ischemia and not to a lack of extracellular Cs^+ as substrate. The fact that only the pyr-Cs group recovered pump function during reperfusion supported our belief that the Na^+/K^+ pump was inactivated during ischemia. One experiment that can be done to shed futher light on this issue would be to subject the hearts to low-flow anoxia. Under these conditions, the extracellular Cs^+ level would be better maintained while the oxygenation condition resemble that of ischemia. Other interesting experiments that can be performed using the present set-up would be to shorten the ischemic period of the glc-Cs group to see whether the non-recovery of pump function is always correlated with the mechanical failure during reperfusion. If recovery of pump and mechanical function are always correlated it is likely that they are regulated in an identical fashion.

In the Cyclosporin A studies, we confirmed that the systolic pressure of the treated rat heart was lower than controls at any diastolic pressures tested. Otherwise we found that the pH and the levels of Pi, PCr, ATP, Mg^{2+} and the activity of the Na^+/K^+ ATPase were not sufficiently different from controls to explain the lower developed pressure. However,

because the hearts were allowed to beat spontaneously, the heart rate was not the same in both groups and this might have some effect on the observed pressure development. Pacing the hearts at a particular heart rate would circumvent this problem.

References

1. Poole-Wilson PA (1987). Reperfusion damage in heart muscle: still unexplained but with new clinical relevance. Clin Physiol 7: 439-453.
2. Downey JM (1990). Free radicals and their involvement during long-term myocardial ischemia and reperfusion. Annu Rev Physiol 52: 487-504.
3. Tani M (1990). Mechanisms of Ca^{2+} overload in reperfused ischemic myocardium. Annu Rev Physiol 52: 543-59.
4. Lucchesi BR (1990). Modulation of leukocyte-mediated myocardial reperfusion injury. Annu Rev Physiol 52: 561-76.
5. Avison MJ, Hetherington HP, Shulman RG (1986). Applications of NMR to studies of tissue metabolism. Annu Rev Biophys Chem 15: 377-402.
6. Hitzig BM, Prichard JW, Kantor HL, Ellington WR, Ingwall JS, Burt CT, Helamn SI, Loutcher J (1987). NMR spectroscopy as an investigative technique in physiology. FASEB J 1: 22-31.
7. Shulman RG (1988). High resolution NMR in vivo. TIBS 13: 37-39.
8. Lundberg P, Harmsen E, Ho C, Vogel HJ (1990). Nuclear magnetic resonance studies of cellular metabolism. Anal Biochem 191: 193-222.
9. Inagaki F, Miyazawa T (1981). NMR analyses of molecular conformations and conformational equilibria with the lanthanide probe method. Prog NMR Spectr 14: 67-111.
10. Berridge MJ, Downes CP, Hanley MR (1989). Neural and developmental actions of lithium: a unifying hypothesis. Cell 59: 411-419.
11. Gache C, Rossi B, Leone FA, Lazdunske M (1979). Pseudo-substrates to analyze the reaction mechanism of the Na, K-ATPase. In: 'Na, K-ATPase

Structure and Kinetics.' ed. Skou JC and Norby JG, publ. Academic Press, London.

12. Gupta RK, Gupta P, Moore RD (1984). NMR studies of intracellular metal ions in intact cells and tissues. Ann Rev Biophys Bioeng 13:221-46.

13. Pike MM, Frazer JC, Dedrick DF, Ingwall JS, Allen PD, Springer CS, Smith TW (1985). ^{23}Na and ^{39}K nuclear magnetic resonance studies of perfused rat hearts. Biophys J 48: 159-173.

14. Springer CS (1987). Measurements of metal cation compartmentalization in tissue by high-resolution metal cation NMR. Ann Rev Biophys Biophys Chem 16: 375-99.

15. Jelicks LA, Gupta RK (1989). Multinuclear NMR studies of the Langendorff perfused rat heart. J Biol Chem 264: 15230-15235.

16. Allis JL, Snaith CD, Seymour AM, Radda GK (1989). ^{87}Rb NMR studies of the perfused rat heart. FEB Letters 242: 215-217.

17. Endre ZH, Allis JL, Ratcliffe PJ, Radda GK (1989). 87-Rubidium NMR: A novel method of measuring cation in intact kidney. Kid Int 35: 1249-1256.

18. Allis JL, Dixon RM, Till AM, Radda GK (1989). ^{87}Rb NMR studies for evaluation of K^+ fluxes in human erythrocytes. J Magn Reson 85: 524-529.

19. Davis DG, Murphy E, London RE (1988). Uptake of cesium ions by human erythrocytes and perfused rat heart: a cesium-133 NMR study. Biochemistry 27: 3547-3551.

20. Pfeffer PE, Rolin DB, Brauer D, Tu SI, Kumosinski TF (1990). In vivo Cs-NMR a probe for studying subcellular compartmentation and ion uptake in maize root tissue. Biochim Biophys Acta 1054: 169-175.

21. Hille B (1984). Ionic channels of excitable membranes. Sinauer Publ. Sunderland, Massachusetts.

22. Meier CF, Katzung BG (1981). Cesium blockage of delayed outward currents and electrically induced pacemaker activity in mammalian ventricular myocardium. J Gen Physiol 77: 531-546.

23. Springer CS (1987). Measurements of metal cation compartmentalization in tissue by high-resolution metal cation NMR. Ann Rev Biophys Biophys Chem 16: 375-99.

24. Lundberg P (1989). PhD thesis, University of Calgary.

25. Robitaille PM, Robitaille PA, Brown GG (1991). An analysis of the pH-dependent chemical-shift behavior of phosphorus containing metabolites. J Magn Reson 92: 73-84.

26. Chu SC, Pike MM, Fossed ET, Smith TW, Balschi JA, Springer Cs (1984). Aqueous shift reagents for high-resolution cationic nuclear magnetic resonance. III. $Dy(TTHA)^{-3}$, $Tm(TTHA)^{-3}$, and $Tm(TPP)_2^{-7}$. J Magn Reson 56: 33-47.

27. Bryden CC, Reilley CN (1981). Multinuclear nuclear magnetic resonance study of three aqueous lanthanide shift reagents: complexes with EDTA and axially symmetric macrocyclic polyamino phlyacetate ligands. Anal Chem 53:1418-1425.

28. Pike MM, Springer CS (1982). Aqueous shift reagents for high-resolution cationic nuclear magnetic resonaces. J Magn Reson 46:348-353.

29. Gupta RK, Gupta P (1982). Direct observation of resolved resonances from intra- and extracellular sodium-23 ions in NMR studies of intact cells and tissues using dysrosium(III)tripolyphosphate as paramagnetic shift reagent. J Magn Reson 47:344-350.

30. Chu SC, Pike MM, Fossel ET, Smith TW, Balshi JA, Springer CS (1984). Aqueous shift reagnets for high-resolution cationic nuclear magnetic resonance. III. $Dy(TTHA)^{-3}$, $Tm(TTHA)^{-3}$, and $Tm(TPP)_2^{-7}$. J Magn Reson 56:33-47.

31. Vogel HJ, Braunlin WH (1985). Shift reagents for calcium-43 NMR studies of calcium-binding proteins. J Magn Reson 62:42-53.

32. Gupta RK, Gupta P, Moore RD (1984). NMR studies of intracellular metal ions in intact cells and tissues. Ann Rev Biophys Bioeng 13:221-46.

33. Springer CS (1987). Measurements of metal cation compartmentalization in tissue by high-resolution metal cation NMR. Ann Rev Biophys Biophys Chem 16: 375-99.

34. Hills BP, Belton PS (1989). NMR studies of membrane transport. Ann Rep NMR Spectr 21:99-159.

35. Post JF (1989). Cation nuclear magnetic resonance (NMR) ^{7}Li- and ^{23}Na-NMR results obtained with human erythrocytes. Scan Microsc 3:877-886.

36. Lundberg P, Harmsen E, Ho C, Vogel HJ (1990). Nuclear magnetic resonance studies of cellular metabolism. Anal Biochem 191: 193-222.

37. Inagaki F, Miyazawa T (1981). NMR analyses of molecular conformations and conformational equilibria with the lanthanide probe method. Prog NMR Spectr 14: 67-111.

38. Chu SC, Xu Y, Balschi JA, Springer CS (1990). Bulk magnetic susecptibility shifts in NMR studies of compartmentalized samples: Use of paramagnetic reagents. Magn Reson Med 13: 239-262.

39. Brophy PJ, Hayer MJ, Riddell FG (1983). Measurement of intracellular potassium ion concentrations by NMR. Biochem J 210:961-963.

40. Hayer M, Riddel FG (1984). Shift reagents for ^{39}K NMR. Inorg Chim Acta 92:L37-L39.

41. Halliday JD, Richards RE, Sharp FRS (1969). Chemical shifts in nuclear resonance of cesium ions in solutions. Proc Roy Soc Lond A 313:45-69.

42. Ramasamy R, Espanol MC, Long KM, Freitas DM, Geraldes CF (1989). Aqueous shift reagents for ^{7}Li NMR transport studies in cells. Inorg Chim Acta 163: 41-52.

43. Pike MM, Fossel ET, Smith TW, Springer CS (1984). High-resolution ^{23}Na-NMR studies of human erythrocytes: use of aqueous shift reagents. Am J Physiol 246:c528-c536.

44. Ogino T, den Hollander JA, Shulman RG (1983). ^{39}K, ^{23}Na and ^{31}P NMR studies of ion transport in Saccharomyces cerevisiae. Proc Natl Acad Sci USA 80: 5185-5189.

45. Pettegrew JW, Post JF, Panchalingam K, Withers G, Woessner DE (1987). ^{7}Li NMR study of normal human erythrocytes. J Magn Reson 71: 504-519.

46. Espanol MC, Freitas DM (1986). ^{7}Li NMR studies of lithium transport in human erythrocytes. Inorg Chem 26:4356-4359.

47. Allis JL, Dixon RM, Till AM, Radda GK (1989). ^{87}Rb NMR studies for evaluation of K^+ fluxes in human erythrocytes. J Magn Reson 85:524-529.

48. Helpern JA, Welch KM, Haluorson JR (1989). Rubidium transport in human erythrocyte suspensions monitored by Rb NMR with aqueous chemical shift reagents. NMR Biomed 2: 47-54.

49. Allis JL, Snaith CD, Seymour AML, Radda GK (1989). ^{87}Rb NMR studies of the perfused rat heart. FEB Lett 242:215-217.

50. Davis DG, Murphy E, London RE (1988). Uptake of cesium ions by human erythrocytes and perfused rat heart: a cesium-133 NMR study. Biochemistry 27: 3547-3551.

51. Pfeffer PE, Rolin DB, Brauer D, Tu SI, Kumisinski TF (1990). In vivo ^{133}Cs-NMR a probe for studying subcellular compartmentation and ion uptake in maize root tissue. Biochem Biophys Acta 1054:169-175.

52. Lundberg P, Vogel HJ (1991). Physiol Plant submitted.

53. Pike MM, Grazer JC, Dedrick DF, Ingwall JS, Allen PD, Springer Cs Smith TW (1985). ^{23}Na and ^{39}K nuclear magnetic resonance studies of perfused rat hearts. Biophys J 48:159-173.

54. Nieuwenhuezen MS, Peters JA, Sinnema A, Kieboom AP, van Bekkum H (1985). Multinuclear NMR study of the complexation of lanthanide (III) cations with sodium triphosphate: induced shifts and relaxation rate enhancements. J Am Chem Soc 107:12-16.

55. Endre ZH, Allis JL, Radda GK (1989). Toxicity of dysprosium shift reagents in the isolated perfused rat kidney. Magn Reson Med 11:267-271.

56. Sze DY, Corbelletta NL, Shochat SJ, Jardetzky O (1990). Inhibition of lymphocyte stimulation by shift reagents. Magn Reson Med 13:14-24.

57. Vogel HJ, Brodelius P, Lilja H, Lohmeier-Vogel EM (1987). Nuclear magnetic resonance studies of immobilized cells. Meth Enzymol 135:512-528.

58. Sorensen TS, Sloth P, Schroder M (1984). Ionic radii from experimental activities and simple statistical-mechanical theories for strong electrolytes with small Bjerrum parameters. Acta Chem Scand A38: 735-756.

59. Hasin Y, Doorey A, Barry WH (1984). Electrophysiologic and mechanical effects of high-energy phosphate production in cultured chick embryo ventricular cells. J Mol Cell Cardiol 16: 1009-1021.

60. Higgins TJ, Bailey PJ (1983). The effects of cyanide and iodoacetate intoxication and ischaemia on enzyme release from the perfused rat heart. Biochem Biophys Acta 762: 67-75.

61. Weiss J, Bradley H (1985). Functional compartmentation of glycolytic versus oxidative metabolism in isolated rabbit heart. J Clin Invest 75:436-447.

62. Weiss JN, Lamp ST (1987). Glycolysis preferentially inhibits ATP-sensitive K^+ channels in isolated guinea pig cardiac myocytes. Science 238: 67-69.

63. Lynch RM, Balaban RS (1987). Coupling of aerobic glycolysis and Na^+-K^+-ATPase in renal cell line MDCK. Am J Physiol 253: C269-C276.

64. Paul RJ, Hardin CD, Raeymaekers L, Wuytack F, Casteels R (1989). Preferential support of Ca^{2+} uptake in smooth muscle plasma membrane vesicles by an endogenous glycolytic cascade. FASEB J 3: 2298-2301.

65. Paul RJ, Hardin C, Campbell J, Raeymaekers L (1989). Compartmentation of metabolism and function in smooth muscle. Prog Clin Biol Res 315: 381-390.

66. Philipson KD, Nishimoto AY (1984). ATP produced by myocardial sarcolemmal-bound creatine kinase is not preferentially used by the Na^+ pump. Biochem Biophys Res Comm 124: 696-702.

67. Soltoff SP, Mandel LJ (1984). Active ion transport in the renal proximal tubule III. The ATP dependence of the Na pump. J Gen Physiol 84: 643-662.

68. Tessitore N, Sakhrani LM, Massry SG (1986). Quantitative requirement for ATP for active transport in isolated renal cells. Am J Physiol 251: C120-C127.

69. Niki I, Ashcroft FM, Ashcroft SJ (1989). The dependence on intracellular ATP concentration of ATP-sensitive K-channels and of Na,K-ATPase in intact HIT-T15β-cells. FEBS Letters 257: 361-364.

70. Halliday JD, Richards RE, Sharp FRS (1969). Chemical shifts in nuclear resonance of cesium ions in solutions. Proc Roy Soc Lond A 313: 45-69.

71. Endre ZH, Allis JL, Radda GK (1989). Toxicity of dysprosium shift reagents in the isolated perfused rat kidney. Magn Reson Med 11:267-271.

72. Springer CS (1987). Measurements of metal cation compartmentalization in tissue by high-resolution metal cation NMR. Ann Rev Biophys Biophys Chem 16: 375-99.

73. Sze DY, Corbelletta NL, Shochat SJ, Jardetzky O (1990). Inhibition of lymphocyte stimulation by shift reagents. Magn Reson Med 13:14-24.

74. Hille B (1984). Ionic channels of excitable membranes. Sinauer Publ. Sunderland, Massachusetts.

75. Meier CF, Katzung BG (1981). Cesium blockage of delayed outward currents and electrically induced pacemaker activity in mammalian ventricular myocardium. J Gen Physiol 77: 531-546.

76. Davis DG, Murphy E, London RE (1988). Uptake of cesium ions by human erythrocytes and perfused rat heart: a cesium-133 NMR study. Biochemistry 27: 3547-3551.

77. Poole-Wilson PA (1987). Reperfusion damage in heart muscle: still unexplained but with new clinical relevance. Clin Physiol 7: 439-453.

78. Tani M, Neely JR (1990). Na^+ accumulation increases Ca^{2+} overload and impairs function in anoxic rat heart. J Mol Cell Cardiol 22: 57-72.

79. Tani M, Neely JR (1990). Intermittent perfusion of ischemic myocardium. Possible mechanisms of protective effects on mechanical function in isolated rat heart. Circ 82: 536-548.

80. Rossier BC, Geering K, Kraehenbuhl JP (1987). Regulation of the sodium pump: how and why? TIBS 12: 483-487.

81. Malloy CR, Buster DC, Castro MM, Geraldes CF, Jeffrey MH, Sherry AD (1990). Influence of global ischemia on intracellular sodium in the perfused rat heart. Magn Reson Med 15: 33-44.

82. Blum H, Osbakker MD, Johnson RG (1991). Sodium flux and bioenergetics in the ischemic rat liver. Magn Reson Med 18: 348-357.

83. Bersohn MM, Philipson KD, Fukushima JY (1982). Sodium-calcium exhange and sacrolemmal enzymes in ischemic rabbit hearts. Am J Physiol 242: C288-C295.

84. Daly MJ, Elz JS, Nayler WG (1984). Sarcolemmal enzymes and Na^{+}-Ca^{2+} exchange in hypoxic, ischemic, and reperfused rat hearts. Am J Phys 247: H237-H243.

85. Shimizu T, Nakanishi T, Uemura S, Jarmakani JM (1983). Effect of hypoxia on ouabain inhibition of sodium pump in newborn rabbit myocardium. Am J Phys 244: h756-h762.

86. Ishida H, Kohmoto O, Bridge JH, Barry WH (1988). Alterations in cation homeostasis in cultured chick ventricular cells during and after recovery from adenosine triphosphate depletion. J Clin Invest 81: 1173-1181.

87. Kim MS, Akera T (1987). O_2 free radicals: cause of ischemia-reperfusion injury to cardiac Na^{+}-K^{+}-ATPase. Am J Phys 252: h252-h257.

88. Chatelain P, Laruel R, Gillard M (1985). Effect of amiodarone on membrane fluidity and Na^+/K^+ ATPase activity in rat-brain synaptic membranes. Biochem Biophys Res Comm 129: 148-154.

89. Mahadik SP, Hawver DB, Hungund BL, Li YS, Karpiak SE (1989). GM1 ganglioside treatment after global ischemia protects changes in membrane fatty acids and properties of Na^+, K^+-ATPase and Mg^{2+}-ATPase. J Neuro Res 24: 402-412.

90. Choong YS, Gavin JB, Armiger LC (1988). Effects of glutamic acid on cardiac function and energy metabolism of rat heart during ischaemia and reperfusion. J Mol Cell Cardiol 20: 1043-1051.

91. Wiesner RJ, Borst AD, Borst M, Schrader J, Grieshaber MK (1989). Glutamate degradation in the ischemic dog heart: contribution to anaerobic energy production. J Mol Cell Cardiol 21: 49-59.

92. Rau EE, Shine KI, Gervais A, Douglas AM, Amos EC (1979). Enhanced mechanical recovery of anoxic and ischemic myocardium by amino acid perfusion. Am J Phys 236: H873-H879.

93. Bunger R, Mallet RT, Hartman DA (1989). Pyruvate-enhanced phosphorylation potential and iontropism in normoxic and postischemic isolated working heart. Eur J Biochem 180: 221-233.

94. Harmsen E, Vogel HJ, ter Keurs HEDJ (1992). Can J Physiol Pharmacol (submitted).

95. Lundberg P, Harmsen E, Ho C, Vogel HJ (1991). Nuclear magnetic resonance studies of cellular metabolism. Anal Biochem 191: 193-222.

96. Kingsley-Hickman PI, Sako EY, Mohanakrishman P, Robitaille PM, From AH, Foker JE, Ugurbil K (1987). ^{31}P NMR studies of ATP synthesis and hydrolysis kinetics in the intact myocardium. Biochemistry 26: 7501-7510.

97. Jeffrey FM, Storey CJ, Nunnally RL, Malloy CR (1989). Effect of ischemia on NMR detection of phosphorylated metabolites in the intact rat heart. Biochemistry 28: 5323-5326.

98. Humphrey SM, Garlick PB (1991). NMR visible ATP and Pi in normoxic and reperfused rat hearts: a quantitative study. Am J Phys 260: H6-H12.

99. Akera T, Ng YC, Hadley R, Katano Y, Brody TM (1986). High affinity and low affinity ouabain binding sites in the rat heart. Eur J Pharm 132: 137-146.

100. Vemuri R, Longoni S, Philipson KD (1989). Ouabain treatment of cardiac cells induces enhanced Na^+-Ca^{2+} exchange activity. Am J Phys 256: C1273-C1276.

101. Apell HJ, Nelson MT, Marcus MM, Lauger P (1986). Effects of ATP, ADP and inorganic phosphate on the transport rate of the Na^+, K^+-pump. Biochim Biophys Acta 857: 105-115.

102. Eisner DA, Richards DE (1982). Inhibition of the sodium pump by inorganic phosphate in resealed red cell ghosts. J Physiol 326: 1-10.

103. Sach JR (1988). Phosphate inhibition of the human red cell sodium pump: simultaneous binding of adenosine triphosphate and phosphate. J Physiol 400: 545-574.

104. Renlund DG, Gerstenblith G, Lakatta EG, Jacobus WE, Kallman CH, Weisfeldt ML (1984). Perfusate sodium during ischemia modifies post-ischemic functional and metabolic recovery in the rabbit heart. J Mol Cell Cardiol 16: 795-801.

105. Vander Elst L, Goudemant JF, Mouton J, Chatelain P, Van Haverbeke Y, Muller RN (1990). Amiodarone pretreatment effects on ischemic isovolumic rat hearts: a

P-31 nuclear magnetic resonance study of intracellular pH and high-energy phosphates contents evolutions. J Cardiol Pharm 15: 377-385.

106. Castro J, Farley RA (1979). Proteolytic fragmentation of the catalytic subunit of the sodium and potassium adenosine triphosphatase. J Biol Chem 254: 2221-2228.

107. Kapakos JG, Steinberg M (1982). Fluorescent labeling of (Na^++K^+)-ATPase by 5-iodoacetamidofluorescein. Biochim Biophys Acta 693: 493-496.

108. Tyson PA, Steinberg M, Wallick ET, Kirley TL (1989). Identification of the 5-iodoacetamidofluorescein reporter site on the Na, K-ATPase. J Biol Chem 264: 726-734.

109. Hoerter JA, Lauer C, Vassort G, Gueron M (1988). Sustained function of normoxic hearts depleted in ATP and phosphocreatine: a ^{31}P-NMR study. Am J Physiol 255: c192-c201.

110. Kentish JC (1986). The effects of inorganic phosphate and creatine phosphate on force production in skinned muscles from rat ventricle. J Physiol 370: 585-604.

111. Pfeffer PE, Rolin DB, Brauer D, Tu SI, Kumosinski TF (1990). In vivo ^{133}Cs-NMR a probe for studying subcellular compartmentation and ion uptake in maise root tissue. Biochim Biophys Acta 1054: 169-175.

112. Masferrer JL, Rios AP, Schwartzman ML (1990). Inhibition of renal, cardiac and corneal (Na-K) ATPase by 12(R)-hydroxyeicosatetraenoic acid. Biochem Pharm 39: 1971-1974.

113. Blum H, Schnall MD, Chance B, Buzby GP (1988). Intracellular sodium flux and high-energy phosphorus metabolites in ischemic skeletal muscle. Am J Physiol 255: C377-C384.

114. McGilvery RW, Goldstein GW (1983). Biochemistry, a functional approach 3rd edition. W B Saunders Co. Philadelphia, USA.

115. Suyatna FD, vanVeldhover PP, Borgers M Mannaerts GP (1988). Phospholipid composition and amphiphile content of isolated sarcolemma from normal and autolytic rat myocardium. J Mol Cell Cardiol 20: 47-62.

116. Paul LC (1989) . Maintenance immunosuppression: Cyclosporine. Contemp Issues in Nephrol19:105-128.

117. Olbrich HG, Dols S, Ver donck L, Kober G, Kalterbach M, Mutschler E (1990). Isolated rat cardiomyocytes as an expermental model for studying acute cardiotoxicity of cyclosporin A. Int J Cardiol 27: 319-325.

118. Paul LC, Kingma I, ter Keurs MHC, ter Keurs HEDJ (1991). Cyclosporine impairs cardiac function in the rat. Transplant Proc 23:475-476.

119. Kingma I, Harmsen E, ter Keurs HEDJ, Benediktsson H, Paul LC (1991). Cyclosporine-Associated Reduction in Systolic Myocardial Function in the Rat. Int J Cardiol (in press).

120. Nicchitta CV, Kamoun M, Williamson JR (1985). Cyclosporin augments receptor-mediated cellular Ca^{2+} fluxes in isolated hepatocytes. J Biol Chem 260: 13613-13618.

121. Hiestand PC (1984). Cyclosporin A modulates the Ca uptake of mitogen-stimulated lymphocytes. Agents Actions 15: 556-561.

122. Pfeilschifter J, Ruegg UT (1987). Cyclosporin A augments angiotensin II-stimulated rise in intracellular free calcium in vascular smooth muscle cells. Biochem J 248: 883-887.

123. Meyer-Lehnert H, Schrier RW (1988). Cyclosporine A enhances vasopressin-induced Ca^{2+} mobilization and contraction in mesangial cells. Kidney Int 34:89-97.

124. Goldbery HJ, Wang PY, Cole EH, Levy GA, Skorecki KL (1989). Dissociation between the immunosuppressive activity of cyclosporine derivatives and their effects on intracellular calcium signalling in mesangial cells. Transplantation 47:731-732.

125. Olbrich HG, Geerts H, Ver donck L, Kober G, Kalterbach M (1991). Cyclosporine A increases the intracellular free calcium concentration in electrically paced isolated rat cardiomyocytes. J Heart Lung Transpl 10: 165.

126. Mottram PL, Mirisklavos A, Mason A, Dumble LJ, Smith JA, Clunie GJA, Panagiotopoulos S, Nayler WG (1989). Immunosuppressive and cardiotoxic effects of cyclosporine in CBA mice. Transplantation 48:720-723.

127. Mirishlavos A, Mottram PL, Smith JA, Mason A, Dumble LJ, Clunie GJA, Panagiotopoulos S, Nayler WG (1987). Cyclosporine A: Graft survival and cardiotoxicity in murine cardiac allografts. Transplant Proc 19: 1259-1261.

128. Barton CH, Vaziri ND, Mina-Araghi S, Crosby S, Seo MI (1989). Effects of cyclosporine on magnesium metabolism in rats. J Lab Clin Med 114:232-236.

129. Suzuki S, Kanashiro M, Amamiya H. Effects of a new immunosuppressant, 15-Deoxyspergualin, on heterotropic rat heart transplantation, in comparison with cyclosporine. Transplantation 1987; 44:483-487.

130. Davis DG, Murphy E, London RE. Uptake of Cesium Ions by Human Erythrocytes and Perfused Rat Heart: A Cesium-133 NMR Study. Biochemistry 1988; 27:3547-3551.

131. Lundberg P, Harmsen E, Ho C, Vogel HJ (1991). Nuclear Magnetic resonance studies of cellular metabolism. Anal Biochem 191: 193-222.

132. Jeffrey FM, Storey CJ, Nunnally RL, Malloy CR (1989). Effect of ischemia on NMR detection of phosphorylated metabolites in the intact rat heart. Biochemistry 28: 5323-5326.

133. Humphrey SM, Garlick PB (1991). NMR-visible ATP and Pi in normoxic and reperfused rat hearts: a quantitative study. Am J Physiol 260: h6-h12.

134. Le Rumeur E, Le Moyec L, Yvin JC, Percehais S, De Certaines JD. Assessment of Intracellular Magnesium Depletion in Rat Striated Muscle by in Vivo ^{31}P NMR. Mag Reson Med 1990; 13:504-506.

135. Adam WR, Craik DJ, Hall JG, Kneen MM, Wellard RM. Problems in the Assessment of Magnesium Depletion in the Rat by in Vivo ^{31}P NMR. Mag Reson in Med 1988; 7:300-310.

136. Hibberd MG (1986). Relationships between chemical and mechanical events during muscular contraction. Ann Rev Biophys Chem 15: 119-61.

137. Kingsley-Hickman P, Sako EY, Mohanakrishman P, Robitaille PML, From AHL, Foker JE, Ugurbil K. ^{31}P NMR Studies of ATP Synthesis and Hydrolysis kinetics in the Intact Myocardium. Biochemistry 1987; 26:7501-7510.

138. Halliday JD, Richards RE, Sharp RR. Chemical shifts in nuclear resonances of cesium. Proc Roy Soc Lond A 1969; 313:45-69.

139. Rossier BC, Geering K, Kraehenbuhl JP (1987). Regulation of the sodium pump: how and why? TIBS 12: 483-487.

140. Fraser CD, Chacko VP, Jacobus WE, Soulen RL, Hutchins GM, Reitz BA, Baumgartner WA (1988). Metabolic changes preceding functional and

morphologic indices of rejection in heterotopic cardiac allografts. Transplant 46: 346-351.

141. Banijamali HS, ter Keurs MHC, Paul LC, ter Keurs HEDJ (summitted). Excitation contraction coupling in rat heart: influence of Cyclosporin-A. Circ Res

142. Weiss J, Bradley H (1985). Functional compartmentation of glycolytic versis oxidative metabolism in isolated rabbit heart. J Clin Invest 75:436-447.

143. Kentish JC (1986). The effects of inorganic phosphate and creatine phosphate on force production in skinned muscles from rat ventricle. J Physiol 370: 585-604.

144. Hoerter JA, Lauer C, Vassort G, Gueron M (1988). Sustained function of normoxic hearts depleted in ATP and phosphocreatine: a ^{31}P-NMR study. Am J Physio 255: c192-c201.

145. Springer CS (1987). Measurements of metal cation compartmentalization in tissue by high-resolution metal cation NMR. Ann Rev Biophys Biophys Chem 16: 375-99.